Environmental Protection Agency
An Ghníomhaireacht um Chaomhnú Comhshaoil

STRIVE
Report Series No.126

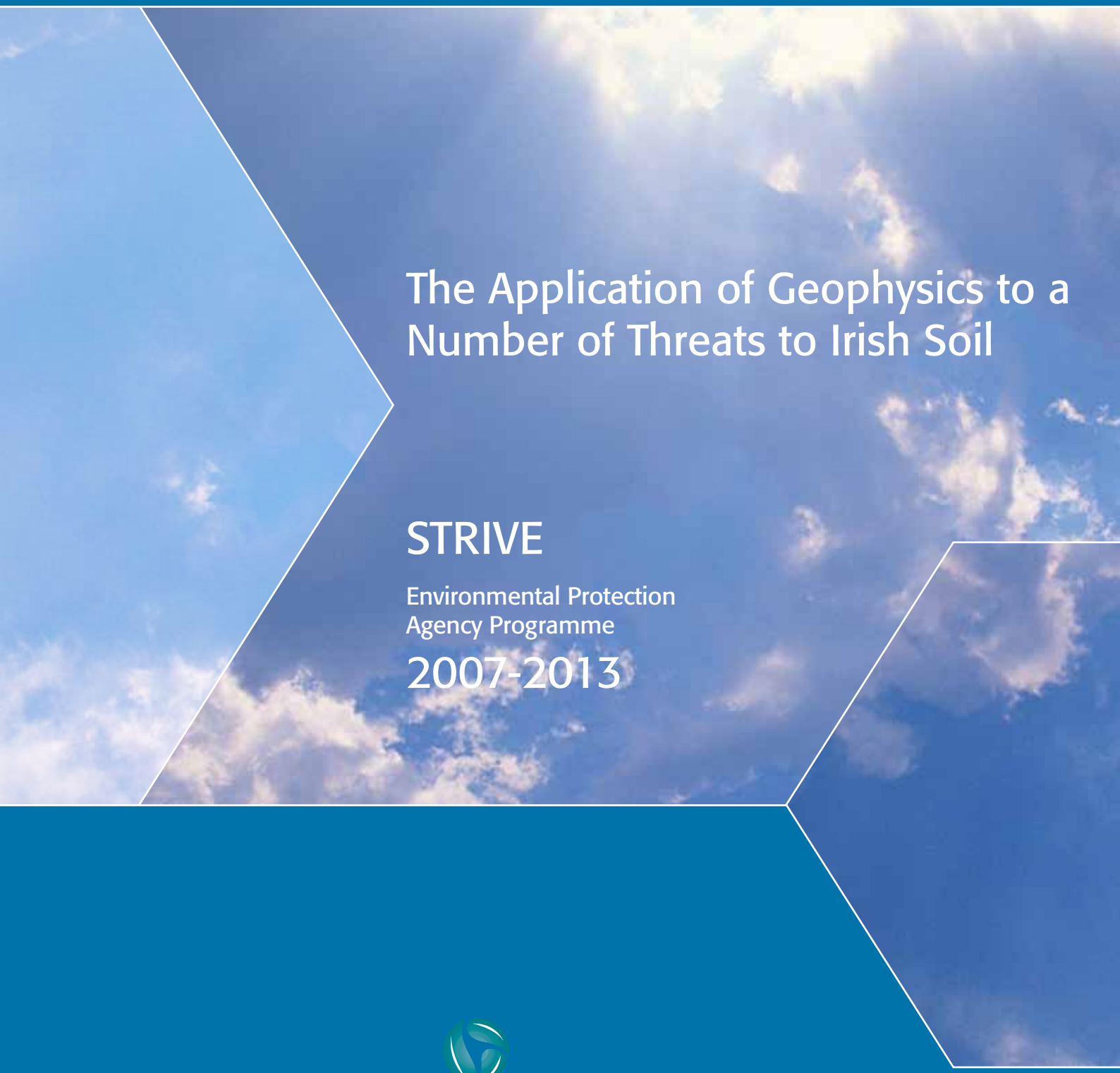

The Application of Geophysics to a Number of Threats to Irish Soil

STRIVE

Environmental Protection Agency Programme

2007-2013

SSTI Strategy for Science, Technology and Innovation

Comhshaol, Pobal agus Rialtas Áitiúil
Environment, Community and Local Government

Environmental Protection Agency

The Environmental Protection Agency (EPA) is a statutory body responsible for protecting the environment in Ireland. We regulate and police activities that might otherwise cause pollution. We ensure there is solid information on environmental trends so that necessary actions are taken. Our priorities are protecting the Irish environment and ensuring that development is sustainable.

The EPA is an independent public body established in July 1993 under the Environmental Protection Agency Act, 1992. Its sponsor in Government is the Department of the Environment, Community and Local Government.

OUR RESPONSIBILITIES

LICENSING

We license the following to ensure that their emissions do not endanger human health or harm the environment:

- waste facilities (e.g., landfills, incinerators, waste transfer stations);
- large scale industrial activities (e.g., pharmaceutical manufacturing, cement manufacturing, power plants);
- intensive agriculture;
- the contained use and controlled release of Genetically Modified Organisms (GMOs);
- large petrol storage facilities;
- waste water discharges;
- dumping at sea.

NATIONAL ENVIRONMENTAL ENFORCEMENT

- Conducting over 1200 audits and inspections of EPA licensed facilities every year.
- Overseeing local authorities' environmental protection responsibilities in the areas of - air, noise, waste, waste-water and water quality.
- Working with local authorities and the Gardaí to stamp out illegal waste activity by co-ordinating a national enforcement network, targeting offenders, conducting investigations and overseeing remediation.
- Prosecuting those who flout environmental law and damage the environment as a result of their actions.

MONITORING, ANALYSING AND REPORTING ON THE ENVIRONMENT

- Monitoring air quality and the quality of rivers, lakes, tidal waters and ground waters; measuring water levels and river flows.
- Independent reporting to inform decision making by national and local government.

REGULATING IRELAND'S GREENHOUSE GAS EMISSIONS

- Quantifying Ireland's emissions of greenhouse gases in the context of our Kyoto commitments
- Implementing the Emissions Trading Directive, involving over 100 companies who are major generators of carbon dioxide in Ireland.

ENVIRONMENTAL RESEARCH AND DEVELOPMENT

- Co-ordinating research on environmental issues (including air and water quality, climate change, biodiversity, environmental technologies).

STRATEGIC ENVIRONMENTAL ASSESSMENT

- Assessing the impact of plans and programmes on the Irish environment (such as waste management and development plans).

ENVIRONMENTAL PLANNING, EDUCATION AND GUIDANCE

- Providing guidance to the public and to industry on various environmental topics (including licence applications, waste prevention and environmental regulations).
- Generating greater environmental awareness (through environmental television programmes and primary and secondary schools' resource packs).

PROACTIVE WASTE MANAGEMENT

- Promoting waste prevention and minimisation projects through the co-ordination of the National Waste Prevention Programme, including input into the implementation of Producer Responsibility Initiatives.
- Enforcing Regulations such as Waste Electrical and Electronic Equipment (WEEE) and Restriction of Hazardous Substances (RoHS) and substances that deplete the ozone layer.
- Developing a National Hazardous Waste Management Plan to prevent and manage hazardous waste.

MANAGEMENT AND STRUCTURE OF THE EPA

The organisation is managed by a full time Board, consisting of a Director General and four Directors.

The work of the EPA is carried out across four offices:

- Office of Climate, Licensing and Resource Use
- Office of Environmental Enforcement
- Office of Environmental Assessment
- Office of Communications and Corporate Services

The EPA is assisted by an Advisory Committee of twelve members who meet several times a year to discuss issues of concern and offer advice to the Board.

EPA STRIVE Programme 2007-2013

The Application of Geophysics to a Number of Threats to Irish Soil

(2008-FS-S-5-S5)

STRIVE Report

Prepared for the Environmental Protection Agency

by

University College Dublin and Queen's University Belfast

Author:

Dr. Shane Donohue

ENVIRONMENTAL PROTECTION AGENCY

An Ghníomhaireacht um Chaomhnú Comhshaoil
PO Box 3000, Johnstown Castle, Co.Wexford, Ireland

Telephone: +353 53 916 0600 Fax: +353 53 916 0699
Email: info@epa.ie Website: www.epa.ie

ACKNOWLEDGEMENTS

This report is published as part of the Science, Technology, Research and Innovation for the Environment (STRIVE) Programme 2007–2013. The programme is financed by the Irish Government under the National Development Plan 2007–2013. It is administered on behalf of the Department of the Environment, Heritage and Local Government by the Environmental Protection Agency which has the statutory function of co-ordinating and promoting environmental research.

DISCLAIMER

 The EPA STRIVE Programme addresses the need for research in Ireland to inform policymakers and other stakeholders on a range of questions in relation to environmental protection. These reports are intended as contributions to the necessary debate on the protection of the environment.

EPA STRIVE PROGRAMME 2007–2013

Published by the Environmental Protection Agency, Ireland

ISBN: 978-1-84095-539-2 **Online version**

Price: Free

Details of Project Partners

Dr Shane Donohue*
School of Architecture, Landscape
and Civil Engineering
University College Dublin
Newstead
Belfield
Dublin 4
Ireland

Dr Michael Long (mentor)
School of Architecture, Landscape
and Civil Engineering
University College Dublin
Newstead
Belfield
Dublin 4
Ireland
Email: Mike.long@ucd.ie

*Current address
School of Planning, Architecture
and Civil Engineering,
Queen's University Belfast
David Keir Building
Belfast
BT9 5AG
Northern Ireland
Tel.: +44 28 90976678
E-mail: s.donohue@qub.ac.uk

Table of Contents

Executive Summary

Recent developments in near-surface geophysical techniques, relating to advances in available computing power, have largely been based on developing systems that generate large, dense datasets efficiently. Some of these geophysical advancements have not previously been reported in the soils and agricultural literature, and this presents an opportunity to explore the novelty of these approaches. This project has applied a number of geophysical techniques in conjunction with conventional approaches to a number of areas of Irish concern to the EU Thematic Strategy (EC, 2006a) for Soil Protection and the proposed Soil Framework Directive (EC, 2006b). Some of this work is also relevant to the European Union (EU) Water Framework Directive (WFD; EC, 2000) and the Habitats Directive (CEC, 1992). Specifically, the areas that were selected for investigation as part of this project included: (i) agricultural soil compaction, (ii) wastewater contamination and (iii) failures in raised bogs.

The EU Thematic Strategy for Soil Protection lists soil compaction as one of eight threats to soil in the EU. In this study, the application of geophysical methods for detecting agricultural compaction in a field environment was investigated at two sites. At both, geophysical methods detected significant differences between compacted and uncompacted ground, and correlated well with conventional field and laboratory assessments. This is also the first study to have reported the use of surface wave methods for assessing agricultural compaction. The geophysical methods tested have a number of advantages over conventional field measures of compaction – their non-intrusive nature and the ability to acquire a large amount of data relatively quickly, particularly if portable systems are employed. The main limitation of the surface wave approach for detection of compaction is the resolution of the technique at very shallow depths. Two alternative systems capable of acquiring high-speed geophysical data were also trialled during this project. Further work is necessary to explore the possibility of using alternative equipment before these methods can be confidently utilised for compaction assessments.

In Ireland, there is limited available information concerning failure rates and required remediation of on-site wastewater treatment systems (OSWTS). This deficit will need to be addressed in order to meet the requirements of the WFD, which aims to restore all surface waters to good ecological status. Also, a 2009 European Court of Justice ruling put pressure on Ireland to implement appropriate inspection procedures for OSWTS, in order to ensure that they do not present an environmental risk and that they comply with regulations. The application of geophysical methods for detecting and mapping effluent discharging from OSWTS to low permeability soils was investigated during this project at a number of sites. This work was performed in collaboration with Dundalk Institute of Technology (DKIT) and Queen's University Belfast (QUB). The extensive DKIT/QUB study, when combined with this work, highlights the need for an appropriate inspection system that is capable of detecting pollution arising from malfunctioning systems. Although some limitations were observed, the geophysical data significantly improved our understanding of the extent of wastewater plumes and helped to identify potential effluent pathways. It was also observed that in a catchment, for example, with a large population of grazing animals, it might be difficult using geophysical techniques to distinguish between OSWTS contamination and that arising from agricultural sources.

Landslides in blanket bogs in Irish upland areas have been relatively well studied and their causal factors are well known. Failures have, however, also occurred in raised bogs in the Irish Midlands which have very shallow slopes. Raised bogs are a rare habitat in the European Union (EU) and a large number of Irish raised bogs have received protection, through designations under European legislation via the EU Habitats Directive (CEC, 1992) and national legislation via the Wildlife (Amendment) Act (2000). Developing an understanding of the underlying causes of these failures is therefore of significant importance. An integrated geophysical and geotechnical approach was used to explore the nature and thickness of peat in order to explain such failures, in particular at two bogs (Aghnamona, Co. Leitrim;

Carn Park, Co. Westmeath). It was found that drainage along the edge of both bogs has caused dewatering of the peat towards the edge of the failure zones and clear thinning and compression of the peat which had led to surface settlement of the bog. The geophysical methods determined that the peat base is relatively flat and does not follow the pronounced variation in surface topography. This suggests that the surface movement has originated within the peat rather than the underlying material. Based on the information obtained from the integrated geophysical and geotechnical investigation, slope stability and seepage analyses have shown that seepage-induced forces were the most likely cause of the failures observed at the sites. Due to the presence of drains/cut faces at the edges of the failed areas, these forces will endure. The existing cracks on the bogs will continue to open and new cracks will develop towards the centre of the bogs, causing further damage. It is recommended that, where infrastructural development is planned in close proximity to peatlands, a significant effort should be made to ensure that drainage of the peat does not occur.

1 Introduction

In its 2002 Communication 'Towards a Thematic Strategy on Soil Protection' (EC, 2002), the European Commission identified the main threats to which soils in the European Union (EU) are confronted. More recently, the EU published a Thematic Strategy for Soil Protection (COM, 2006, 231) as well as a proposal for a Soil Framework Directive (COM, 2006, 232). The proposed directive states that 'Within five years, Member States shall identify the areas in their national territory, at the appropriate level, where there is decisive evidence, or legitimate grounds for suspicion, that one or more of the following soil degradation processes has occurred or is likely to occur in the near future'. The proposed directive includes the 'identification of areas at risk of erosion, organic matter decline, compaction, salinisation and landslides', in addition to identification of contaminated soils and establishment of national programmes of measures. A minority of Member States have, however, blocked further progress to the directive on the grounds of subsidiarity, excessive cost and administrative burden. A policy report published by the European Commission (COM, 2012, 46) has, however, confirmed that the directive remains 'on the Council's table'.

Recent developments in near-surface geophysical techniques, relating to advances in available computing power, have to a large extent been based on the development of systems that efficiently generate large, dense datasets. Continuous galvanic (Sørensen, 1996; Dabas et al., 2000) and capacitive coupled resistivity (CR) systems (Møller, 2001; Kuras et al., 2006) have contributed significantly to the usefulness of electrical and electromagnetic (EM) methods by enabling measurements over large areas to be acquired without sacrificing spatial resolution. Advances in near surface seismic geophysical measurements have also occurred, and, for example, have resulted in the recent development of multichannel surface wave techniques (e.g. Park et al., 1999; Donohue and Long, 2008). Some of these geophysical advancements have not previously been reported in the soils and agricultural literature, and, as such, an opportunity exists to explore the novelty of these approaches.

This EPA STRIVE fellowship ('The Application of Geophysics to a Number of Threats to Irish Soil') applied a number of these recent geophysical developments, in addition to a range of traditional approaches, to a number of areas of Irish concern to the EU Thematic Strategy for Soil Protection (COM, 2006, 231) and the proposed Soil Framework Directive (COM, 2006, 232). Some of this work is also relevant to the EU Water Framework Directive (WFD, 2000/60/EC) and the Habitats Directive (92/43/EEC). Specifically, the areas that were investigated as part of this project included:

- **Agricultural compaction:** The EU Thematic Strategy for Soil Protection lists soil compaction as one of eight threats to soil in the EU. This study explored the possibility of using geophysical measurements as alternatives to conventional methods for detecting agricultural compaction in a field environment. The use of high-speed alternative geophysical measurements was also trialled.
- **Wastewater contamination:** In Ireland, there is limited available information concerning failure rates and required remediation of on-site wastewater treatment systems (OSWTS). This deficit will need to be addressed in order to meet the requirements of the WFD, which aims to restore all surface waters to good ecological status. In addition, a 2009 European Court of Justice ruling put pressure on Ireland to implement appropriate inspection procedures for OSWTS. This study established the effectiveness of a number of geophysical techniques for characterising the three-dimensional (3D) extent of contaminant plumes generated by wastewater treatment system effluent discharging to glacial-till subsoils. This research was performed in collaboration with Dundalk Institute of Technology (DKIT) and Queen's University Belfast (QUB).
- **Failures in raised bogs:** Raised bogs are a rare habitat in the EU and, as such, a large number of Irish raised bogs have received protection under European legislation via the EU Habitats Directive and national legislation via the Wildlife Amendment Act (2000). Ireland has a significant proportion of the total EU resource of raised bogs and developing an

understanding of the underlying causes of failures in raised bogs in the Irish Midlands is therefore of significant importance. This study investigated the causes of Irish raised bog failures using a combination of field geophysical, geotechnical and laboratory geotechnical testing. The information from these investigations was then used in slope stability and seepage analyses to further predict the causes of these failures.

A number of sites were selected for investigation in each of these areas (Fig. 1.1 gives the locations).

Sections 1.1 to 1.3 introduce each of the three areas investigated. Sections 2, 3 and 4 discuss the methodology employed, results obtained and project conclusions respectively. The report concludes with a list of recommendations and project outputs.

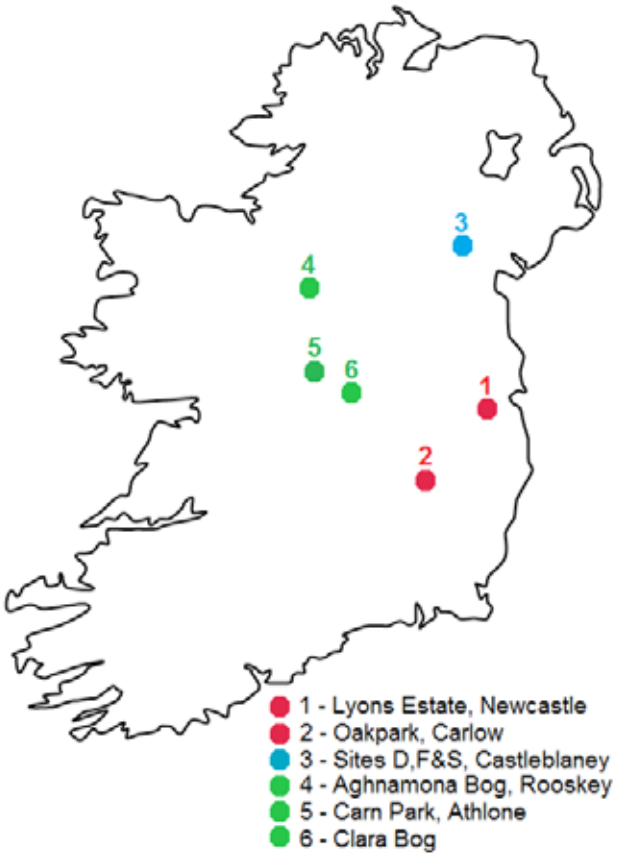

Figure 1.1. Location of all sites discussed in this report. Agricultural compaction sites are shown in red, wastewater contamination in blue and peatland in green.

1.1 Geophysical Assessment of Agricultural Compaction

Soil compaction occurs as a result of loads being applied to the soil surface. Soil particles are pressed together, thereby reducing porosity and permeability, and increasing density and soil strength (Soane and van Ouwerkerk, 1998). Soil compaction caused by machinery or livestock restricts plant growth (Sidhu and Duiker, 2006) and root penetration, and reduces infiltration and drainage of water within the compacted layer. This, in turn, can lead to an increase in run-off, erosion, flooding (Materechera, 2009), transfer of nutrients to surface waters as well as a reduction in agricultural yield. Voorhees et al. (1986) have shown that large farming machinery can cause compaction as deep as 70 cm from the surface. Currently, no comprehensive data is available on the severity or extent of soil compaction in Ireland.

Assessment of agricultural soil compaction is conventionally performed by soil sampling and laboratory testing or by using invasive vertical sensors such as penetrometers (vertical and horizontal) and shear vanes. These approaches may only provide discrete information at individual points on the surface and as such may be inefficient if a dense coverage of data points is required for a complete assessment of compaction.

This study explored the possibility of using a range of non-intrusive geophysical techniques for assessing agricultural compaction. The use of high-speed alternative geophysical measurements was also trialled. Geophysical techniques tested included Multichannel Analysis of Surface Waves (MASW) and Electrical Resistivity Tomography (ERT) using both a stationary and a continuous measurement system. Although the use of ERT and EM methods has occasionally been mentioned in the agricultural literature (e.g. Raper et al., 1990; Freeland et al., 1998; Allred et al., 2008; Besson et al., 2004), to the author's knowledge, seismic field geophysical techniques have rarely been used in precision agriculture. This is predominantly because of the perception that they are slow and results require a complex evaluation (Petersen et al., 2005; Hoefer and Hartge, 2010). Petersen et al. (2005), for example, suggested that seismic methods are not suitable for measuring on a larger scale. Allred et al.

(2008), however, suggested that seismic methods will likely find greater use for agricultural applications in the near future. Although they have rarely been used in field experiments, Lu et al. (2004) have shown a relationship between seismic wave velocity, measured in the laboratory and compaction.

Where seismic methods have been considered in field investigations (e.g. Petersen et al., 2005), most authors have only discussed traditional seismic methods, such as P or S wave seismic refraction. To the author's knowledge, the use of surface wave seismic methods has not been reported thus far in the agricultural literature. In the civil engineering field, however, surface wave methods such as MASW have received considerable attention over recent years, owing to their relatively quick and robust nature and their ability to estimate the shear wave velocity (V_s), and therefore the shear stiffness, at small strain, of near surface materials.

Surface waves, as their name suggests, are seismic waves that propagate along the earth's surface. Their amplitude decreases exponentially with depth and the majority of their energy is contained within one wavelength of the surface. A 'Rayleigh wave' is the particular surface wave most commonly utilised for near surface applications: these travel along the earth–air interface with a retrograde elliptical particle motion. The use of surface waves for determining the elastic properties of the subsurface is based on their dispersive nature, so lower-frequency (longer wavelength) surface waves generally exhibit higher velocities and are more sensitive to the elastic properties of deeper materials. Higher-frequency (shorter wavelength) surface waves are therefore more sensitive to the properties of shallower materials. Therefore, by generating a wide range of frequencies, surface wave surveys use dispersion to produce velocity and frequency (or wavelength) correlations called dispersion curves. For seismic sources located on the earth's surface, surface waves are significantly more energetic than body waves (P and S waves) and are almost always easier to detect and acquire. Surface wave phase velocities are also strongly related (via 'Poisson's ratio') to shear wave velocities and have become the method of choice for measuring V_s, and therefore small strain shear stiffness (Eq. 1.1), in the field of civil engineering over the last number of years. Donohue and Long (2008a), for example, used the technique for measuring the increase in soil stiffness resulting from a combination of lime treatment and machinery compaction.

$$G_{max} = \rho.Vs^2 \qquad \text{(Eq. 1.1)}$$

where G_{max} = small strain shear modulus (Pa), V_s = shear wave velocity (m/s) and ρ = density (kg/m^3). V_s, and therefore G_{max} (Eq. 1) for a particular site is derived by inverting the surface wave dispersion curve (e.g. Aki and Richards, 1980; Xia et al., 1999). The results from part of this study are also published in Donohue et al. (2013).

1.2 Geophysical Assessment of On-site Wastewater Treatment System Contamination

Residential OSWTS, where contaminated wastewater discharges to the subsurface, act as the dominant means of domestic wastewater disposal in rural Ireland. The Central Statistics Office (CSO, 2012) estimates that there are over 480,000 OSWTS in operation in Ireland, which accounts for approximately one-third of all private dwellings. Correctly designed and maintained OSWTS are usually capable of treating and disposing of wastewater effluent. When these systems fail to operate satisfactorily they threaten public health and water quality (EPA, 2010). When domestic wastewater is not absorbed by the soil it can form stagnant pools on the ground surface. In such failures, humans may come in contact with wastewater and be exposed to pathogens. In addition, inadequately treated wastewater systems have the potential to be a source of nutrients to groundwater and surface water (Yates, 1985), which in many areas are also used as drinking water supplies. It is essential that this effluent is treated and disposed of properly (EPA, 2010).

In 2010 the EPA published the 'Code of Practice: Wastewater Treatment Systems for Single Houses' in order to provide guidance on the provision of wastewater treatment and disposal systems for new single houses in Ireland. This code provides guidance on determining site suitability for OSWTS, suitability of different systems, information on the design and installation of a range of OSWTS (e.g. septic tank, filter and packaged treatment systems) and maintenance requirements.

An important role of wastewater treatment systems is the removal of nutrients from wastewater before

it reaches groundwater or surface water. These systems can be broadly divided into two categories (McCarthy et al., 2010): (i) septic tank systems and (ii) secondary treatment systems or proprietary systems (e.g. mechanical aeration systems, filter systems and constructed wetlands). In both system types most treatment is carried out via infiltration and percolation of effluent through soil to achieve purification before recharge to groundwater (Jenssen and Siegrist, 1990; van Cuyk et al., 2001). This process involves a variety of natural, physical, chemical and biological processes, which remove bacteria and other pollutants (van Cuyk et al., 2001).

The success, or otherwise, of the subsoil to treat the wastewater appropriately depends on a number of soil properties – such as the porosity, permeability, texture, organic matter content, ion-exchange capacity, subsoil thickness, water table depth and ground slope (McCarthy et al., 2010). A number of these properties have a significant effect on the length of time that the subsoil is in contact with the wastewater, which is crucial for successful treatment. In coarse soils, for example, wastewater is unlikely to be in contact long enough with the soil particles to provide sufficient treatment (Vinten et al., 1983). Conversely, very fine clay soils are unlikely to be suitable due to their low permeability. This can act as a barrier and limit the mobility of contaminants, possibly leading to 'ponding' of contaminants at the surface (Kaplan, 1991) and the transportation of contaminants to surface water directly via movement along the ground surface (Daly, 2003). Also, as the hydraulic conductivity (K) of the soil varies as a function of water content, wastewater flows more slowly through unsaturated subsoil, thereby providing a greater opportunity for treatment. This, along with the available oxygen in the unsaturated zone, enables decomposition and biodegradation of various organic contaminants (Canter and Knox, 1985).

In order to improve the management of water resources and to meet the requirements of the WFD (2000/60/EC), which aims to restore all surface waters to good ecological status, quantifying the effects of OSWTS on water quality is essential. In addition, as noted above, the European Court of Justice ruling of 2009 has put Ireland under growing pressure to apply appropriate evidence-based inspection procedures for OSWTS (McCarthy et al., 2010) to ensure that they do not present an environmental risk and that they comply with regulations.

Geophysical methods have been used by a number of authors for detecting, characterising and monitoring contaminants resulting from urban residues (domestic and/or industrial). Electrical and EM methods, in particular, have been found to be very suitable as the inorganic pollutants, present in most leachates, increase the fluid conductivity on entering the fluid pathways (thereby reducing the bulk resistivity) due to an increase of the number of ions in the solution. Applications of these techniques, dealing with the detection of landfill boundaries, the detection and monitoring of contaminant plumes, the spread of contamination and predicting future contaminant pathways are described by many authors (e.g. Buselli et al., 1992; Aristodemou and Thomas-Betts, 2000; Orlando and Marchesi, 2001; Martinho and Almeida, 2006; Santos et al., 2006; Lee et al., 2006; Perozzi and Holliger, 2008). A number of authors have also demonstrated reasonable correlations between apparent resistivity/conductivity (EC_a) and a number of chemical constituents. For example, EC_a has been correlated with concentrations of K, Na, Cl, SO_4, NH_4, and $NO3_{-N}$ in soils affected by manure wastes (Eigenberg et al., 1998; Martínez-Pagán et al., 2009; Ranjan and Karthigesu, 1995; Stevens et al., 1995). While some work has been carried out using geophysics to assess contamination from animal wastes, only a limited amount of research has been carried out on the use of geophysics for assessing contaminants resulting from wastewater treatment systems. Lee et al. (2006), for example, successfully used EM induction to identify a failed septic tank system and also used it for detecting the spatial distribution of the resulting effluent plumes in an absorption field.

The objective of this study was to determine the effectiveness of a number of non-invasive geophysical techniques for characterising the 3D extent of contaminant plumes generated by OSWTS effluent discharging to glacial-till subsoils at three test sites within the Lough Muckno catchment, Co. Monaghan, Republic of Ireland. This project was performed in collaboration with a joint DKIT/QUB project entitled 'A Field Study assessing the Impact of On-site Wastewater Treatment Systems on Surface Water in a Co. Monaghan catchment'. The results from that project are discussed in detail by McCarthy et al. (2010).

1.3 Geophysical and Geotechnical Assessment of Failures in Irish Raised Bogs

Landslides in blanket bogs in Irish upland areas have been relatively well studied (Creighton, 2006; Dykes and Kirk, 2001; Long and Jennings, 2006; Long et al., 2011). The predominant triggering mechanism for these slides is heavy rainfall, with historic records usually making a reference to its occurrence just before, or during, a peat failure (Cole, 1897; Colhoun et al., 1965; Alexander, 1985; Warburton et al., 2004; Dykes and Warburton, 2007). While heavy rainfall may trigger the majority of these events, a number of supplementary topographic and hydrological features and anthropogenic effects have been identified that influence peat failures; these are discussed by a number of authors (e.g. Cole, 1897; Warburton et al., 2004; Boylan et al., 2008).

Failures have also occurred in raised bogs in the Irish Midlands which have very shallow slopes, although these have not previously been studied in any detail. Raised bogs are a rare habitat in the EU and, as such, a large number of Irish raised bogs have received protection, through designations under European legislation via the EU Habitats Directive (92/43/EEC) and national legislation via the Wildlife Amendment Act (2000). One hundred and thirty-nine raised bogs have been designated for protection in 53 Raised Bog Special Areas of Conservation (SACs) under the Habitats Directive and 75 Natural Heritage Areas (NHAs) under the Wildlife (Amendment) Act, 2000 (National Parks and Wildlife Service (NPWS), http://www.npws.ie/peatlandsturf-cutting/). Despite significant exploitation over the last few hundred years, Ireland still contains over 50% of the remaining area of uncut raised bog in north-western Europe (Schouten, 2002). Therefore, developing an understanding of the reasons for these failures is of significant importance.

The Geological Survey of Ireland (GSI) holds a database of all known landslide events in Ireland (www.gsi.ie). Most of the GSI data comes from the work of Feehan and O'Donovan (1996), and 14 failures on raised bogs are recorded. These are noted to have occurred throughout the year whereas failures on upland blanket bogs mostly occurred in the wetter autumn and winter months. All except one of the events listed occurred before 1900, and hence due to the lack of information the cause of the failures is not well known. Feehan and O'Donovan (1996) suggest the two main causal factors are: (i) the build-up of water and (ii) gas pressures within the bog or the creation of near vertical faces on the bogs due to turf-cutting for domestic fuel consumption. For example, the failure of Kapanihane bog in Co. Limerick in 1697 was attributed to the accumulation of water either at the base of the bog or in the middle of peat 'sandwich' following a period of heavy rainfall. This caused the bog to swell up and eventually burst. Several other failures are similarly described as 'bursts', 'explosions' or 'eruptions'. The failure of Woodfield bog, near Kilmaleady, Co. Offaly in 1821, was precipitated by the lateral movement of highly decomposed peat from the base of a steep bank. The summer of 1821 was exceptionally dry and it allowed the local turf-cutters to excavate peat to a greater depth than was usual. Some 9 m high faces existed prior to the failure which left in its wake a valley 9 m deep, 2.5 km long and about 0.5 km wide.

As with some of the other areas investigated in this project, there has not been a significant amount of work published on the use of geophysics in peatland investigations. The small amount of work that has been done in relation to raised bogs in Ireland doesn't appear to have made use of modern geophysical data acquisition and inversion methods. Most of the geophysical work published on peat is concerned with mapping the thickness of peat and providing information on the subsurface stratigraphy, predominantly from the perspective of peat exploitation. Ground penetrating radar (GPR) (by far the most frequently used technique in the literature) involves recording two-way travel times of radar waves to produce estimates of the depth-to-subsurface EM reflectors. Usually in peatlands there is a clear reflection of EM waves at the interface between the peat and the underlying material due to the large contrast in material properties. A number of authors have made use of this approach for providing high-resolution and accurate thickness information (Warner et al., 1990; Hanninen, 1992; Theimer et al., 1994; Lapen et al., 1996; Slater and Reeve, 2002; Comas et al., 2004; Rosa et al., 2009; Trafford et al., 2009). A few authors have also taken an integrated geophysical approach to peatland investigations, using a number of geophysical techniques to better characterise the material (e.g. Slater and Reeve, 2002; Parsekian et al., 2008). Slater and Reeve (2002), for example, used a combination of GPR, ERT, IP (Induced Polarisation)

and EM-31 EM methods to provide insight into controls on peatland hydrology and its impact on the distribution of vegetation communities in a peatland.

In order to investigate the causes of raised bog failures, two such failures at Carn Park bog, near Athlone, Co. Westmeath and at Aghnamona bog, near Roosky, Co. Leitrim were studied. The main objective of this work was to highlight the reasons for the failures and to raise awareness of the importance of these areas so future damage can be minimised. Section 3.4 summarises the results of investigations (which included field geophysical, geotechnical and laboratory geotechnical testing of the peat). As will be discussed, the information from these investigations was then used in slope stability and seepage analyses to further predict the causes of these failures. The results from part of this study are also published in Long et al. (2014).

2 Methodology

2.1 Agricultural Compaction

2.1.1 Sites

For this soil compaction study two sites were tested. An initial feasibility study was carried out at a site at the University College Dublin (UCD) Lyons Estate, Newcastle, Co. Dublin. A second study was located at the Teagasc, Oakpark, Crops Research Centre, Co. Carlow. At both sites, compaction was assessed in a conventional manner using cone penetrometers and measurements of bulk density in addition to geophysical measurements incorporating traditional stationary receivers. At Oakpark, high-speed geophysical measurements were also employed in order to assess the potential large-scale application of these methods for rapidly assessing compaction.

2.1.1.1 Lyons Estate

The trial site was located at the the UCD Lyons Estate in Newcastle. The soils from this site are poorly drained of limestone origin (glacial limestone drift). They are described in detail by Lalor (2004) and O'Flynn (2013). The 'A' horizon is 25–28 cm thick and described as a dark brown silty clay loam. The underlying 'B' horizon is approximately 12–20 cm thick and is described as a yellowish brown sandy loam to loam. This work was part of a collaboration with researchers from UCD and Teagasc (Mr Michael O'Flynn and Dr John Finnan) who are studying the influence of harvest traffic and soil conditions on soil compaction and crop response in establishing an Miscanthus crop. From this project's perspective, the Lyons Estate site provided an excellent feasibility study to determine the influence of controlled harvest trafficking on the results of two geophysical methods, MASW and ERT.

Although the UCD/Teagasc project focuses more specifically on the influence of harvest traffic before and after shoot emergence and in wet and dry soil conditions on soil compaction and crop response, O'Flynn (2013) has concluded that on this occasion the time of trafficking and moisture condition of the soil had no significant impact on the results. Athough all treatments significantly compacted the soil, the individual treatments could not be distinguished from one another in terms of compaction using a number of conventional methods. For the current study the individual treatments are not discussed and a direct comparison between trafficked and untrafficked/control treatments is provided.

Bulk density was determined on 98 cm^3 cores: in total, 20 cylinders were sampled. Cores were sampled from four locations in each area, to a maximum depth of 45 cm. Measurements of gravimetric soil water content were also carried out at each location.

2.1.1.2 Oakpark

The soils at this site are derived from compact but non-tenacious, calcareous glacial till, predominantly of limestone origin and of Weichsel Age. The soils of this series consist mainly of well-drained podzolics, of loam texture and high base status, and vary in depth from 0.5–0.75 m. The soil profile consists of a brown to dark brown surface 'A' horizon, approximately 0.25 m deep, overlying a yellowish-brown textural 'B' horizon. The specific site under investigation in this study contained a headland ('Area 1'), where a general decrease in yield had been observed during the previous year's harvest. Another area of the site ('Area 2'), located 30 m to the north-east of the headland, was also selected for testing. This area had been subjected to minimal trafficking over the previous number of years and, as it was expected to be largely uncompacted, was also selected for comparison. The basic physical characteristics of the soils at both locations, which are summarised in Table 2.1, are very similar.

Bulk density was determined on 98 cm^3 cores sampled immediately after the field experiments discussed in Section 2.12. In total, 30 cylinders were sampled, 15 in each area. Cores were sampled from three locations in each area, to a maximum depth of 50 cm. Measurements of gravimetric soil water content were also carried out at each location. These cores were not acquired at specific depths within the A (0–25 cm) and B (25–50 cm) horizons initially so a direct comparison between the density of the compacted and uncompacted areas may only be done between the A and B horizons rather than at specific depths. It was intended to return to the site two days later to acquire more detailed and sequential bulk density data, but

Table 2.1. Basic soil physical characteristics for Areas 1 and 2.

		Clay (%)	Silt (%)	Sand (%)	Total organic C (%)
Area 1 (Headland)	Horiz. A (0–25 cm)	18	46	35	2.3
	Horiz. B (25–50cm)	25	44	31	0.9
Area 2	Horiz. A (0–25 cm)	17	45	38	2.3
	Horiz. B (25–50 cm)	30	46	24	0.9

the field had been ploughed in the intervening period, removing any chance of obtaining a more detailed bulk density profile. (The farmer had, unfortunately, assumed our work was complete and was eager to plough the field.) Although this was obviously unfortunate, the number of density measurements acquired previously was not insignificant and clearly enabled the distinguishing between compacted and uncompacted ground and the verification of the extent of compaction, providing a basis for which the MASW, resistivity and penetration resistance measurements could be compared.

2.1.2 Techniques

2.1.2.1 Conventional assessment of compaction

In addition to the measurements of bulk density, described above, profiles of cone penetrometer resistance were also measured at both the Lyons and Oakpark sites, in order to provide a comparison with the geophysical approaches for detecting soil compaction. Shear vanes were also used at the Oakpark site.

An ASAE standard (S313.3) 30-degree cone with a base diameter of 12.8 mm and a base area of 130 mm^2 was used for these experiments.

For the Lyons site, 50 profiles were acquired in total, and the results were averaged for both the control and the trafficked treatments. The average depth of the penetrometer profiles was 45 cm with measurements acquired at 1-cm intervals.

For the Oakpark site, 27 profiles were acquired in both Areas 1 and 2, and the results were averaged for each area. All profiles were taken to a depth of 42 cm at intervals of 4 cm. In order to provide a comparison with the two-dimensional (2D) geophysical measurements discussed in the next section, 9 of the profiles were acquired at 1-m spacing in a linear profile in Area 1 and a further 9 were acquired in an identical setup in Area 2. In total, 12 measurements of undrained shear strength were made using shear vanes at Oakpark, 6 in each area. All of these measurements were focused in the A horizon (0–25 cm depth).

2.1.2.2 MASW data acquisition and inversion parameters

As the MASW geophysical technique has not previously been discussed in the agricultural literature, this approach will be introduced in more detail in this report. In order to produce a V_s profile from an MASW survey the following procedure must be followed (see Fig. 2.2):

1 Generate vertical ground motions using a vertical impulsive source – for example, a hammer hitting a metal plate placed on the ground surface;

2 Measure these ground motions using 12–60 low-frequency geophones. The geophones should usually be arranged along a straight line and the impulsive source position located at a certain offset from one of the end geophones. An appropriate source offset should be determined during an initial trial and should be selected in order to limit the occurrence of near field effects (non-horizontal propagation of surface waves near the source) on the seismic data. Park et al. (1999) discuss the avoidance of near-field effects in detail and Park et al. (2002) suggest optimum field-acquisition parameters for MASW surveys used in engineering applications. For shallow-soils applications, the acquisition parameters (e.g. geophone spacing, geophone frequency, source type, source location) used in this paper should serve as an initial guide, although it is strongly recommended that a quick field trial is carried out in order to determine the site-specific optimum parameters;

(a) (b)

Figure 2.1. Oakpark test site with (a) Electrical Resistivity Tomography (ERT) and (b) Multichannel Analysis of Surface Waves (MASW) profile receiver arrangements.

3 Record the seismic data (Fig. 2.2a) using a conventional seismograph;

4 Pick a dispersion curve from the peak amplitude of a phase velocity-frequency spectra of the seismic data (Fig. 2.2b). In this paper, this spectrum was generated using a wavefield transformation method (McMechan and Yedlin, 1981; Park et al., 1998);

5 Invert the picked dispersion curve to produce a one-dimensional (1D) subsurface profile of the variation of shear wave velocity with depth (Fig. 2.2c and 2.2d). Socco et al. (2010) provide an in-depth review of the different ways in which surface wave data can be processed and inverted. If necessary, Steps 4 and 5 may be carried out using a number of readily available commercial software packages;

6 Combination of the 1D inverted profiles to produce a 2D V_s profile (see Fig. 2.2e).

The MASW data for both the Lyons and Oakpark test sites was recorded using a Geometrics Geode seismograph (with 24 geophones, see Fig. 2.1b). As recommended by Donohue and Long (2008b), an initial test profile was conducted at each site. This involved varying the source type and the source/receiver locations in order to determine the optimum acquisition parameters. From this initial test it was found that good-quality data could be acquired on both sites using a 500 g carpentry hammer to generate the surface waves, which were in turn detected by 14 Hz geophones at 0.12 m intervals.

For the Lyons test site, 10 individual 1D profiles were acquired, 5 in each of the control and trafficked treatments respectively. For the Oakpark test site, 26 MASW profiles were acquired, 16 of which were located in Area 1 (where soil compaction was assumed to have its greatest effect) and the further 10 profiles were located in Area 2. Four geophones along each profile line were spatially referenced using a Trimble PRO-XR dGPS, which provides sub-meter accuracy.

Processing of all MASW data was performed by selecting dispersion curves from a phase velocity-frequency spectra, which had been generated using a wavefield transformation method, as in Fig. 2.2b. A normally dispersive phase velocity–frequency relationship was observed for both areas, dominated by the fundamental mode Rayleigh wave.

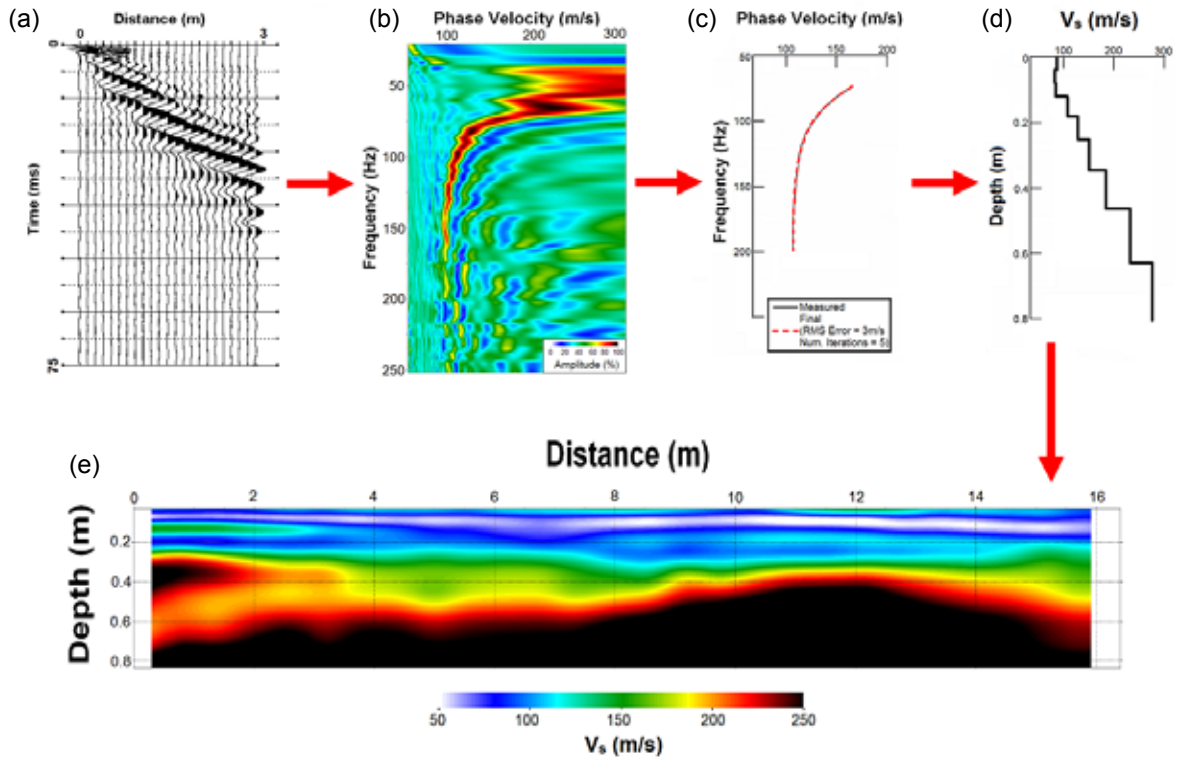

Figure 2.2. Various stages involved in producing 2D Multichannel Analysis of Surface Waves (MASW) profile: (a) raw seismic data, (b) dispersion image, (c,d) inversion and production of a 1D V_s-depth profile and (e) 2D V_s image combining inverted 1D V_s profiles.

One-dimensional shear wave velocity models were estimated using the least-squares approach of Xia et al. (1999). A number of different initial models with different numbers of layers were selected in the initial model in order to test the robustness of the inversion and to determine the model with the lowest misfit. Following the recommendations of Luke and Calderón-Macías (2007) and Cercato (2009), the layer thickness in the model was increased exponentially with depth. This reflects the fact that the resolving power of MASW data decreases with depth. Each inversion was allowed a sufficient number of iterations to converge and was stopped after the overall Root Mean Square (RMS) error was less than 4 m/s. All of the inversions performed converged rapidly, usually within four iterations. It was consistently found that a nine-layer initial model produced the lowest RMS error. Additional layers produced similar errors: however, these resulted in over-parameterised inversions, as evidenced by artefact low-velocity layers, not supported by evidence from the local geology.

2.1.2.3 Resistivity data acquisition and inversion parameters

For the Lyons site 2D galvanic ERT profiles were acquired in each of the control and trafficked treatments respectively.

For the Oakpark test site, galvanic measurements (Fig. 2.1a) were acquired in both Areas 1 and 2. At this site capacitive measurements were also acquired to assess the feasibility of using this approach for high-speed ERT assessment of compaction. For this approach, a two-receiver Geometrics ohmmapper (TR-2) was used, consisting of two transmitting dipole cables and associated receiver cables. A range of dipole spacings was used in order to construct a 2D subsurface plot of apparent resistivity. A number of marks relating to specific points along the profile lines were applied to the continuously recorded data. These specific points were previously surveyed using a Trimble PRO-XR dGPS, which enabled spatial referencing of all ohmmapper profiles to be carried out.

Galvanically coupled ERT measurements for both sites were acquired using a multi-electrode Campus Tigre resistivity meter with a 32-takeout multicore cable and 32 conventional stainless steel electrodes at 0.1-m spacing. A Wenner alpha array was used since subsurface layers were not expected to deviate significantly from the horizontal and it generally provides a good signal-to-noise ratio. This array has also been used successfully in similar studies (Besson et al., 2004). Four electrodes along each of these profile lines were spatially referenced using a Trimble PRO-XR dGPS, which provided sub-meter accuracy.

Inversion of all of the apparent resistivity data was carried out with Res2Dinv software (Loke, 2004) using the L_2 norm inversion optimisation method. Due to the large subsurface resistivity contrast present at the site, the quasi-Newton least squares method (Loke and Barker, 1996) was not deemed appropriate: instead, the Gauss-Newton method (Sasaki, 1989; deGroot-Hedlin and Constable, 1990) was selected for the first two or three iterations, after which the quasi-Newton method was used. In many cases, this provides the best compromise between computational time and accuracy even at sites with large resistivity contrasts (Loke and Dahlin, 2002). For this study all inversions performed converged to a normalised RMS error of less than 7% within five iterations.

2.1.3 Data Analysis

For the Lyons test site, an analysis of variance (ANOVA) was used on the bulk density and moisture content data to test for differences between the trafficked and control treatments. Analysis of variance was also used on the cone-penetration resistance, electrical resistivity and shear-wave velocity data to test for differences between treatments at each depth level. All variables were checked for normality before analysis.

For the Oakpark test site, an ANOVA was used on the bulk density and moisture content data to test for differences between Area 1 (expected to be heavily compacted) and Area 2 (expected to be relatively uncompacted) for the soil A (0–25 cm) and B horizons (25–50 cm). ANOVA was also used on the cone-penetration resistance and shear wave velocity data to test for differences between Areas 1 and 2 at each depth level. All variables were checked for normality before analysis.

2.2 Wastewater Contamination

2.2.1 Sites

Three sampling sites ('D', 'F' and 'S') located within the Lough Muckno catchment, Castleblaney (Fig. 1.1) were selected for the DKIT/QUB project. This is situated in a drumlin landscape consisting primarily of agricultural pasture. These sites were chosen based on a number of factors – including consent from the homeowner, distance to the nearest watercourse, the presence of likely interfering or confounding features such as roads or pathways, or the presence of obvious sources of alternative organic pollution (e.g. nearby slatted house or slurry pit). A drinking water abstraction point is located downstream of Lough Muckno, which services three towns in neighbouring counties. Gley soils overlay glacial till of variable thickness across most of the catchment, with alluvium located adjacent to rivers and streams. Owing to community concern regarding the deterioration of the raw water quality, this catchment has been the subject of an intensive monitoring programme carried out in collaboration with the Local Churchill and Oram Scheme group water scheme (GWS), a co-operative which sources its water from Milltown Lake, a subcatchment of the Lough Muckno catchment. The GWS services approximately 431 households in addition to 157 land only and businesses and 26 social facilities, with approximately 731 m^3 of water abstracted from Milltown Lake on a daily basis. The principal water quality pressures identified within the catchment were poor farmyard practices, cattle access to streams and runoff from slurry and fertiliser spreading. However, the impact of diffuse contamination on water quality within this poorly drained sub-catchment has warranted more detailed investigation of wastewater delivery mechanisms to surface water bodies (McCarthy et al., 2010).

The sites (Fig. 2.3) were all located in areas that were underlain by clayey glacial till, resting on a poorly productive sequence of Lower Palaeozoic shales and greywackes (highly compacted/lithified sandstones). In the vicinity of Site D the shale is described as dark, fissile with occasional pyrite being recorded. A GSI subsoil permeability map of the area records the subsoil as of 'low' permeability, suggesting that runoff usually dominates over infiltration. However, as the aquifer vulnerability in the area is mapped as being of 'extreme'

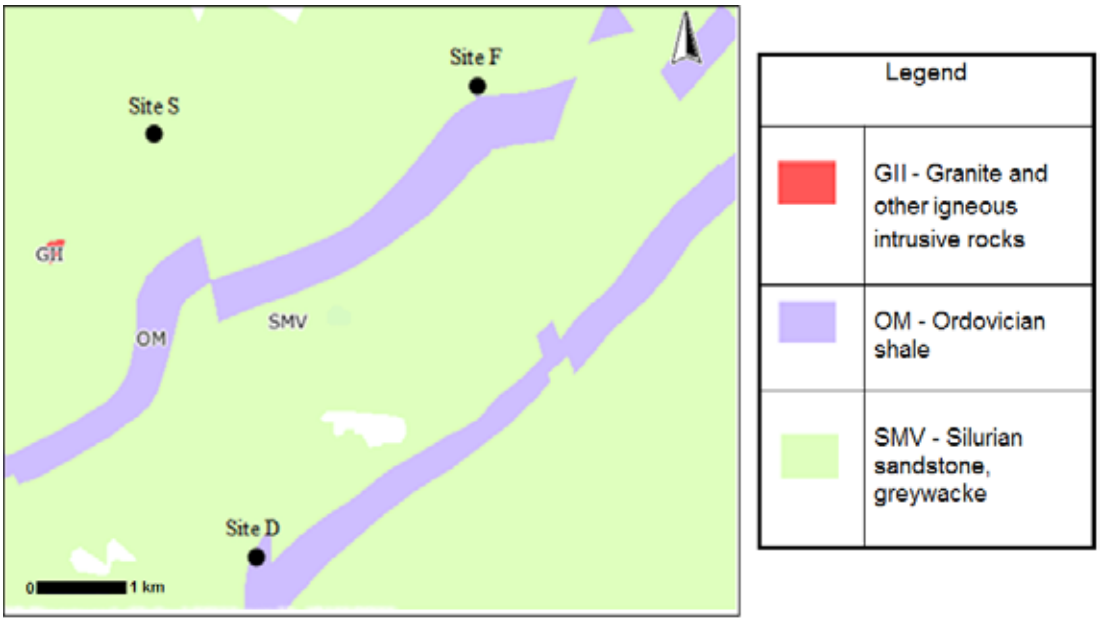

Figure 2.3. Geological map of area, indicating location of the three sites.

vulnerability, the soil at the sites may, therefore, be relatively well drained as the depth to bedrock is quite shallow. Consequently, groundwater may be at risk if the minimum depths required are not achieved or if the percolation rate is too rapid. A minimum thickness of 1.2 m of unsaturated subsoil below the base of the percolation trenches is recommended for septic tanks by the EPA Code of Practice on Wastewater Treatment and Disposal Systems Serving Single Houses, and 0.9 m for secondary systems (EPA, 2010). A site characterisation, which is detailed in McCarthy et al. (2010) was carried out at each site in November 2008, and this incorporated percolation tests to ascertain the assimilation capacity of the subsoil. A percolation test was also carried out at each site (Table 2.2), the details of which can be found in McCarthy et al. (2010). This is a measurement of the length of time it takes for the water level in the percolation hole to fall from a height of 300 mm to 200 mm above the base of the test hole in a percolation area. The percolation values of the subsoils were determined by a modified version of the on-site standardised Irish falling head percolation test, the 'T-test'. The 'T-value' is the average time in minutes it takes for the water level to fall 25 mm in each of two percolation test holes dug at depths at least greater than 400 mm below ground level. A low T-value (<3) denotes a coarse-grained soil that is highly permeable (generally sand or gravel) and is, therefore, not suitable for the installation of a septic tank, while a high T-value (>50) is more indicative of a less permeable, often clayey soil, which is again not suitable for a conventional septic tank (EPA, 2010). The percolation test at these sites involved the excavation of two percolation test holes which were dug in an area adjacent to the current percolation area. In addition to the 'T-value', the 'P-value' was obtained. The P-test is generally carried out at ground level to establish a percolation value for soils with 'T-values' ≥75 and ≤90 that are being considered for an alternative treatment system. Each of the sites investigated during this study is described in detail by McCarthy et al. (2010) and summarised below.

Table 2.2. Average percolation T- and P-values for each site (adapted from McCarthy et al., 2010).

Site	T-value min/25 cm	P-value min/25 cm
D	38	23
F	98	25
S	>100	63

Table 2.3. Mean hydraulic conductivity (K) measurements from rising head tests carried out at the three sites (adapted from Orr, 2009).

Site		Mean K (cm/s)
D	n=5	3.23×10^{-4}
F	n=10	5.42×10^{-5}
S	n=14	5.58×10^{-5}

In order to calculate hydraulic conductivity (*K*) rising head tests were carried out at each of the piezometers. Details of these tests are provided by Orr (2009) and McCarthy et al. (2010). The subsoil's receiving septic tank effluent were found to have moderate to low hydraulic conductivities (*K*) (Table 2.3), which are typical of silt, sandy silts, clayey sands and till (Fetter, 2001). No statistically significant differences in (*K*) were observed between sites (Orr, 2009).

2.2.1.1 Site D

Site D is located on the south-eastern shoulder of a low ridge, within a hummocky area of an otherwise higher drumlin landscape adjacent to a relatively dense cluster of houses. A map of the site is shown in Fig. 2.4 along with the various testing locations. Figure 2.5 displays a picture of the site during geophysical testing. The majority of land on and around the site is on a gradient. A fast-flowing, meandering stream flows from east to west 105 m south-south-east of the site with Lough Muckno located 460 m south-south-west. A drain occurs along the hedgerow, approximately 100 m down-gradient of the site. This channels surface water into the stream along a 65-m long stretch of land. The on-site system and percolation area are located in the garden to the north-east of the house (Fig. 2.4). The system in use is a relatively modern secondary treatment system with an associated percolation area. Some slight ponding was observed across the hedge from the site to the north-east, and some saturated ground also occurred in the flat, narrow floodplain of the stream located 130 m south-east of the site.

Following borehole drilling, trial pitting and a visual inspection of the site, the overall area was observed to be dominated by bedrock within 3 m of the surface and would therefore be considered to be of 'extreme' groundwater vulnerability. Infiltration to the groundwater table and lateral flow across and through a relatively permeable uppermost bedrock surface dominates over overland flow at this site (McCarthy et al., 2010). Highly weathered fissile shale was observed in the central and the south-east parts of the site during trial pitting. The soils from this site consist of a 10–15 cm thick A horizon described as a dark brown, variable compact to very soft loam. The underlying B horizon is approximately 30–45 cm thick and is described as dark brown, very soft to soft sandy silt with common gravels.

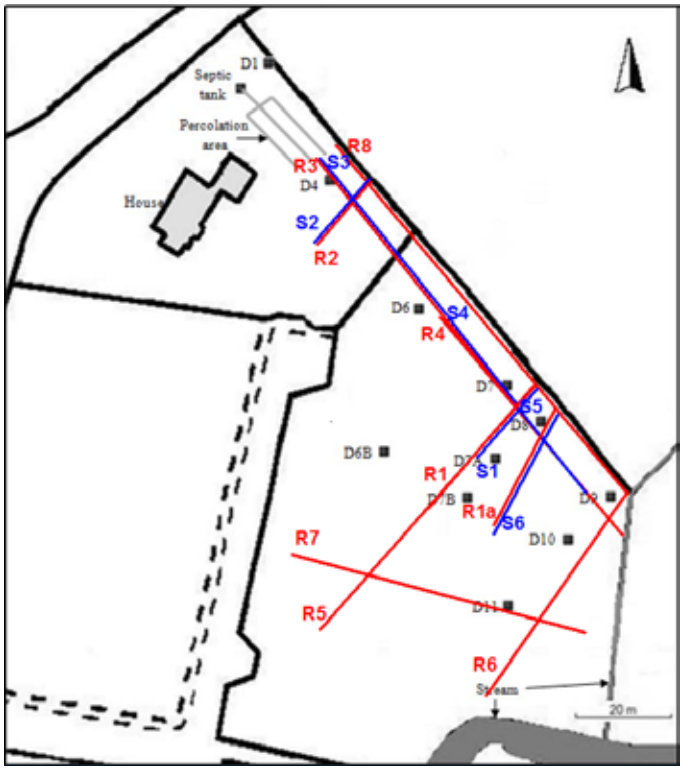

Figure 2.4. Map of Site D, showing locations of piezometers (black squares), Electrical Resistivity Tomography (ERT) profiles (red lines) and seismic refraction profiles (blue lines).

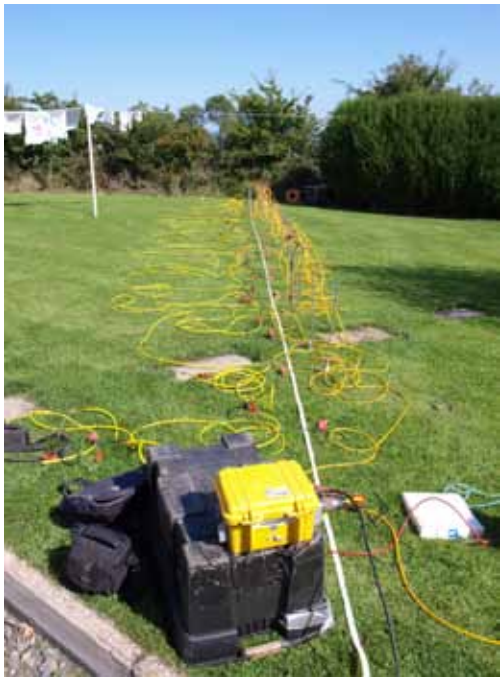

Figure 2.5. Geophysical testing at Site D.

A cone penetration test (CPT) survey of Site D was also performed in order to confirm the depth to bedrock and to help characterise the soils (Fig. 2.5). In total, 28 profiles were acquired in the area surrounding the septic tank. In addition to the standard CPT, an electrical resistivity array was incorporated into the sleeve behind the cone which allowed measurements of resistivity to be taken. The intention was to use this data to help calibrate the surficial measurements acquired from the ERT surveys. A problem arose, however, when the CPT was unable to penetrate deeply into the subsoil. This was likely due to: (i) the presence of cobbles and boulders in the soil; (ii) the small size of the rig that was used; and (iii) the limited reaction force available. The use of a larger rig would not have been feasible due to the potential damage to the landowner's garden. This data is not discussed further in this report.

Two sets of 'T-test' holes were dug at this site (McCarthy et al., 2010). One of these was located down-gradient of the percolation area at the OSWTS. The T-value at this site was >50 min/25 mm: however, seepage was entering this test hole during excavation arising from effluent originating from the OSWTS, suggesting that the test may have overestimated the subsoil percolation value. The second set of test holes was located up-gradient of the OSWTS and indicated average percolation characteristics of the subsoil material (Table 2.2). The average P-value recorded at the site indicated good percolation characteristics of the topsoil material (Table 2.2). During site assessment subsurface water was first encountered in the trial pit at a depth of 0.99 m below ground level and, in the trail pit, bedrock was encountered at a depth of between 1.21 and 1.29 m below ground level.

It should be pointed out that at this site a pipe entering the water course, adjacent to D9 (Fig. 2.4), was also observed during this study. It is very likely that this pipe originated from the percolation area of the OSWTS and this suggests the possibility of an alternative effluent plume pathway facilitated by its presence. The use of discharge pipes such as this to provide additional drainage is common throughout the catchment and, based on anecdotal evidence, often used as a 'back-up' for percolation areas located in poorly draining land.

2.2.1.2 Site F

Site F is located on the southern shoulder of a high-ribbed moraine ridge located in a drumlinised ribbed moraine landscape. A map of the site is shown in Fig. 2.6, along with the various testing locations. The on-site septic tank system and soakaway are located in a field 25 m southwest of the house and farmyard. Figure 2.7 displays a picture of the site during geophysical testing. A fast-flowing stream flows from north to south, 53 m south-east of the tank, with the bedrock exposed at the base of the channel. Two smaller streams flow into this from the east, 110 m north-east of the tank. Drainage ditches occur along most of the hedgerows surrounding the site, and these channel water down slope during heavy rain. Agricultural pasture occurs in the surrounding fields, with some scrub also occurring alongside the stream, 50 m east of the tank. An extensive area of bedrock outcrop is seen from 50 m east of the tank at the sides of the steep gully flanking the stream channel, and extending northwards on each side of the gully for a distance of over 200 m. The field immediately surrounding the tank is relatively firm and even, although directly up-gradient of the tank the land is completely saturated, suggesting that the inlet pipe is broken.

A series of boreholes and a trial pit indicated that the soils from this site consist of a 20–30 cm thick 'A' horizon described as a dark brown, compact sandy loam with occasional gravels. The underlying 'B' horizon is approximately 30–35 cm thick and is described as dark yellowish brown, stiff silty sand with common gravels.

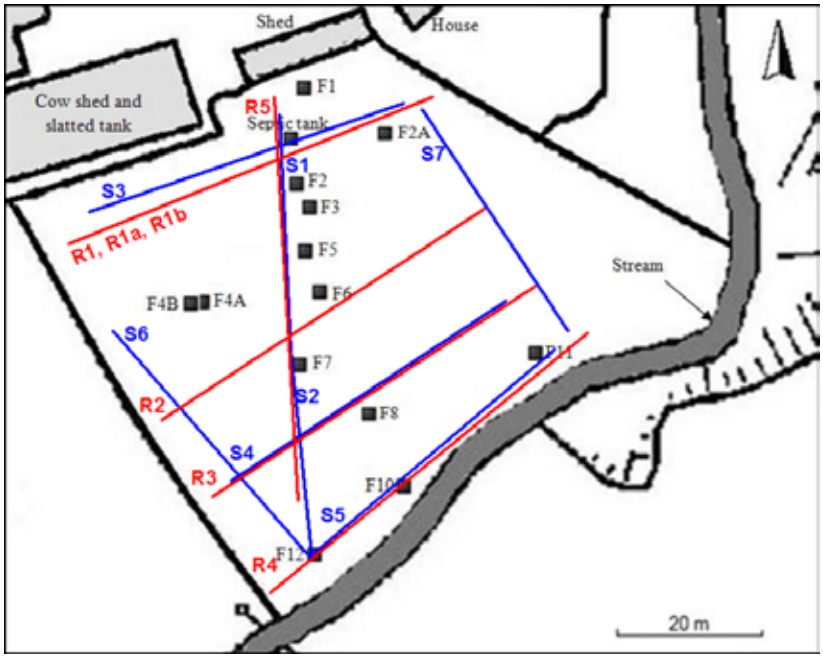

Figure 2.6. Map of Site F, showing locations of piezometers (black squares), Electrical Resistivity Tomography (ERT) profiles (red lines) and seismic refraction profiles (blue lines).

The underlying 'C' horizon is a mottled brownish grey, stiff, slightly sandy silt/clay. The area around the site is dominated by bedrock within 3 m of the surface and is therefore classified as having 'extreme' groundwater vulnerability. Infiltration to the saturated layer and lateral flow across and through a relatively permeable uppermost bedrock surface dominates over overland flow in the area of bedrock outcrop/subcrop. A trial pit which was dug at this site was outside this area, adjacent to the tank itself, and was well drained owing more to the texture of the uppermost subsurface layers and the slope on the site than to the actual permeability of the subsoil. As the subsoil gets deeper away from the tank, and the area of bedrock outcrop and subcrop, the subsoil is likely to be less permeable. Percolation tests (Table 2.2) showed high T-values, indicating poor percolation characteristics of the subsoil material and a P-value less than 50, suggesting good percolation characteristics of the topsoil material.

Figure 2.7. Geophysical testing at Site F.

It should be pointed out that a slatted tank and an outhouse used to house animals at this site are located up-gradient of the tank on its western side, which was approximately five years old at the start of the study. In addition, a portion of the site's greywater (perhaps arising from the washing machine or relatively recently installed dishwasher) was being piped separately to a nearby ditch running along the eastern side of the site. As such, this site had potential alternative sources of contamination that may confound data relating to the effluent plume.

2.2.1.3 Site S

The site is located on a slope of a high drumlin ridge, within a drumlin landscape. The tank is situated in a field 25 m south of the house. A map of the site is shown in Fig. 2.8, along with the various testing locations. A fast-flowing stream has been channelled under and alongside the laneway flanking the site. Figure 2.9 displays a picture of the site during geophysical testing. Agricultural pasture around the site and the fields to the south and east are relatively firm and even. The fields to the north, north-west and west are softer and are commonly used by cattle.

A series of boreholes and a trial pit indicated that the soils from this site consist of a 10–15 cm thick A horizon described as a dark yellowish brown, variable soft to soft clay loam. The underlying B horizon is approximately 25–35 cm thick and is described as mottled dark brown, variable soft to firm clay with occasional gravels. This site is in an area dominated by relatively deep subsoils, and the majority of rainfall is likely to run off the site. As shown, percolation testing has resulted in high T- and P-values, indicating the unsuitability of the subsoil at this site for the majority of OSWTS, according to the EPA's Code of Practice (EPA, 2010). Contaminant distribution at this site may be complicated by the presence of high levels of a salt tracer (NaCl), injected prior to the start of this project.

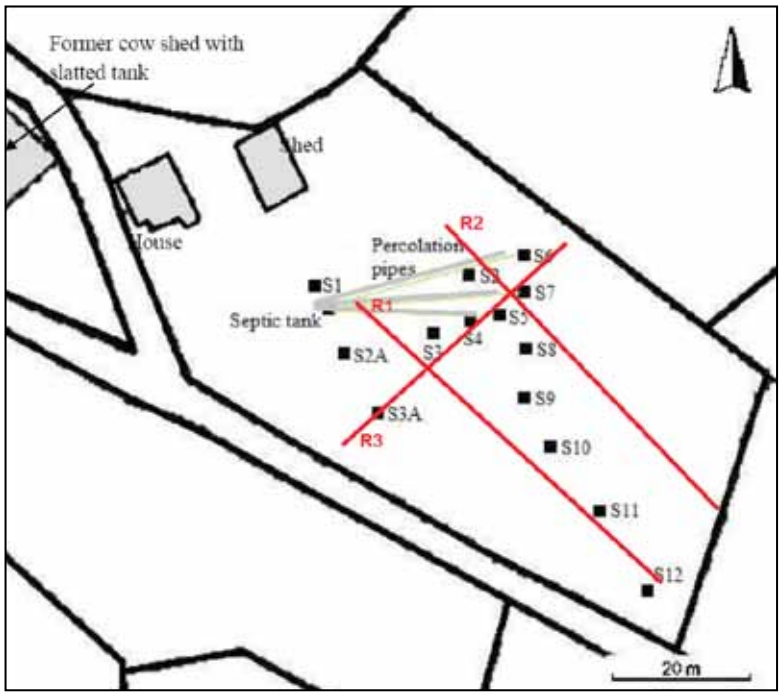

Figure 2.8. Map of Site S, showing locations of piezometers (black squares) and Electrical Resistivity Tomography (ERT) profiles (red lines).

Figure 2.9. Geophysical testing at Site S.

2.2.2 Subsurface Contaminant Measurements

At each site a number of piezometers were installed between March and July 2008, down-gradient of each OSWTS depending on its proximity to the nearest water course. The installation of piezometers at the sites under investigation is described in detail by McCarthy et al. (2010). Subsurface water samples from the piezometers were collected twice a month between August 2008 and June 2009, and monthly until August 2009. Laboratory analysis carried out on these samples by McCarthy et al. (2010) involved determining the concentration of a range of possible contaminants, for example, sulphate, chloride, sodium, potassium, phosphorus and nitrogen analyses, total coliforms and *E. coli*, as well as a number of other contaminant indicators. Electrical conductivity (EC), pH and dissolved oxygen were also measured on site during sampling.

For this study, comparisons with the surface geophysical data will be made with chloride and EC, which were used as conservative natural tracers at these sites.

2.2.3 Geophysical Techniques

2.2.3.1 Electromagnetic ground conductivity mapping: data acquisition parameters

An EM ground conductivity survey, using a Geonics EM-31 EM induction meter, was carried out at Sites F and S. This approach was shown to be successful in a similar study by Lee et al. (2006) for determining the extent of septic tank-derived contamination in glacial till. These surveys operate by transmitting an EM field using a transmitter coil which is located a fixed distance of 3.66 m from a receiver coil (Geonics 1984). Both coils are housed in a 4-m long boom, which is carried horizontally above the ground. The EM radiation from the transmitter coil propagates into the subsurface where a secondary magnetic field, which is dependent on the conductivity of the ground, is generated in response. Both the primary and secondary transmitted fields are then detected by the receiver coil, which enables measurement of the secondary field, as the instrument compensates for the primary field. The ratio of the field strengths is a function of the apparent conductivity of the ground through which the EM energy has passed. The EM-31 instrument can be deployed in two different modes, as a horizontal magnetic dipole (HMD), which provides a bulk measure of conductivity for the upper 3 m, and as a vertical magnetic dipole (VMD), which provides a measure of the upper 6 m (approximately). Both the quadrature and the in-phase components of the EM field can be measured using this instrument. All EM data was spatially referenced using a continuously recording handheld GPS. The spatial data was automatically coupled to the EM data during acquisition.

Due to the presence of overhead cables and a significant amount of fencing in the vicinity of Site D, which would have resulted in considerable electrical noise, this approach was not deemed suitable for testing at this location. The surveys of both sites were carried out at walking pace using both the the VMD and HMD modes and data from the quadrature and in-phase components of the EM field was recorded at 2 second (s) intervals, corresponding to a sampling interval of approximately 1 m. This enabled a qualitative map of the distribution of apparent electrical conductivity (EC_a) for approximately the upper 3 m and 6 m of the subsurface be obtained. This approach was also used as a quick reconnaissance tool in order to assist selection of appropriate locations for ERT and seismic profiles.

2.2.3.2 Resistivity data acquisition and inversion parameters

Galvanically coupled ERT measurements for all sites were acquired using a multi-electrode Campus Tigre resistivity meter with a 32 takeout multicore cable and 32 conventional stainless steel electrodes. A number of different array geometries was used, depending on the depth requirements of the survey and the available space at each site. All ERT profiles acquired are listed on Table 2.4, along with the relevant data-acquisition parameters. It was also attempted to acquire two three-dimensional (3D) profiles at Site D, with the aim of mapping the effluent plume in the immediate vicinity of the treatment system. Electrical noise caused by a number of sources, including a buried electrical cable which provided power to the OSWTS, resulted in poor data quality and these profiles are not included in this report. A Wenner alpha array was used for the majority in order to provide a greater signal-to-noise ratio. Although some issues were encountered with the instrument and cables, these were resolved and all subsequent data recorded was of good quality. Electrical Resistivity Tomography electrodes were spatially referenced using a Trimble PRO-XR dGPS, which provides submeter accuracy.

Table 2.4. Electrical Resistivity Tomography (ERT) data acquisition parameters.

Site	Profile	Array type	Profile length (m)	Electrode spacing (m)	Comments
D	R 1a	Wenner α	61	1	Large error recorded, issues with cables
D	R 1	Wenner α	31	1	
D	R 2	Wenner α	32	0.5	
D	R 3	Wenner α	62	2	
D	R 4	Wenner α	62	2	
D	R 5	Wenner α	62	2	
D	R 6	Wenner α	52	2	
D	R 7	Wenner α	62	2	
D	R 8	Wenner α	94	3	Excessive noise
D	3D 1	DD	25 x 10m	2.5	
D	3D 2	DD	25 x 10m	2.5	
F	R 1a	Wenner α	62	2	Issues with instrument
F	R 1b	DD	62	2	
F	R 1	Wenner α	62	2	
F	R 2	Wenner α	62	2	
F	R 3	Wenner α	31	1	Issues with instrument
F	R 4	Wenner α	62	2	
F	R 5	Wenner α	62	2	
S	R 1	Wenner α	62	2	Large error recorded
S	R 2	Wenner α	62	2	Large error recorded
S	R 3	Wenner α	46.5	1.5	Large error recorded

DD = Dipole Dipole.

Inversion of all of the apparent resistivity data was carried out with the software Res2Dinv (Loke, 2004) using the L_2 norm inversion optimisation method. Due to the large subsurface resistivity contrast at the site, the quasi-Newton least-squares method (Loke and Barker, 1996) was not deemed appropriate. Instead, the Gauss-Newton method (Sasaki, 1989; deGroot-Hedlin and Constable, 1990) was selected for the first three iterations, after which the quasi-Newton method was used. In many cases, this provides the best compromise between computational time and accuracy even at sites with large resistivity contrasts (Loke and Dahlin, 2002). For this study the majority of inversions performed converged to a normalised RMS error of less than 6% within five iterations. Exceptions to this include Profile R1a from Site D (RMS error of 32.4%), Profile R1b from Site F (RMS error of 12.4%) and all three profiles acquired from Site S (RMS error >13% for all). This issue with Profile R1a from Site D was related to a faulty cable, which was subsequently replaced. The higher error recorded on Profile R1b, acquired using a Dipole Dipole (DD) array, confirmed that the Wenner α array resulted in lower RMS inversion errors. The Wenner α array was subsequently used for the remainder of the profiles. Finally, a large amount of electrical noise was recorded on all profiles acquired at Site S, which resulted in large inversion RMS errors (>25%). The reasons for this are not clear and could be related to electrical noise present on site or more likely to an issue with the geophysical hardware such as a faulty cable.

2.2.3.3 Seismic refraction data-acquisition parameters

Seismic refraction data was recorded at Sites D and F only using a Geometrics Geode seismograph. A 10 kg sledgehammer was used to generate the seismic waves which were in turn detected by 10 Hz vertical geophones. Acquisition parameters are reported in Table 2.5. The majority of profiles were acquired using 24 geophones at a spacing of 2 m, although this was altered on a number of occasions to take into account site-specific limitations. In general, for seismic refraction testing, shots (hammer blows) were recorded at every sixth geophone, with offshots recorded off each end of the profile. As with the ERT data, geophones were spatially referenced using a Trimble PRO-XR dGPS, which provides sub-meter accuracy.

In most cases, clear and unambiguous first arrivals were observed on the acquired profiles. The refraction data was interpreted using GREMIX, which incorporates the slope-intercept method, parts of the Plus-Minus Method of Hagedoorn (1959), Time-Delay Method (see Wyrobek, 1956), and features the generalised reciprocal method (GRM) of Palmer (1980).

Table 2.5. Seismic data acquisition parameters.

Site	Profile	Num. geophones	Geophone spacing (m)	Source locations
D	S 1	24	1	G1+2 m (o), G1, G6, G12, G18, G24, G24+10 m (o)
D	S 2	24	0.75	
D	S 3	24	2	G1+10 m (o), G1, G6, G12, G18, G24, G24+10 m (o)
D	S 4	24	1	G1+10 m (o), G1, G6, G12, G18, G24, G24+10 m (o)
D	S 5	24	1	G1+4 m (o), G1, G6, G12, G18, G24, G24+10 m (o)
D	S 6	12	3	G1+21 m (o), G1, G6, G12
F	S 1	12	3	G1+15 m (o), G1, G3, G6, G9, G12, G12+7 m(o)
F	S 2	12	3	G1+15 m (o), G1, G3, G6, G9, G12
F	S 3	24	2	G1+4 m (o), G1, G3, G6, G9, G12, G15, G18, G21, G24, G24+10 m
F	S 4	24	2	G1+10 m (o), G1, G3, G6, G9, G12, G15, G18, G21, G24, G24+4 m
F	S 5	24	2	G1+10 m (o), G1, G3, G6, G9, G12, G15, G18, G21, G24, G24+7 m
F	S 6	24	2	G1+10 m (o), G1, G3, G6, G9, G12, G15, G18, G21, G24, G24+4 m
F	S 7	24	2	G1+6 m (o), G1, G3, G6, G9, G12, G15, G18, G21, G24, G24+6 m

Note: (o) refers to seismic refraction offshots.

2.3 Failures in Irish Raised Bogs

2.3.1 Sites

2.3.1.1 Carn Park

Carn Park bog is situated 8 km east of Athlone, Co. Westmeath, in the Irish Midlands. The site is a candidate Special Area of Conservation (cSAC) for raised bogs as listed in Annex I of the EU Habitats Directive. Due to its ecological importance it was selected for restoration as part of Coillte's EU 'LIFE' funded project entitled 'Demonstrating Best Practice in Raised Bog Restoration in Ireland'. A survey of the site prior to restoration in 2003 (Conaghan, 2003) showed much of the bog had been planted with conifer trees up to 25 years old. Aerial photographs taken pre-restoration in 1995 and 2000 showed no evidence of failure in the southern area of the bog adjacent to a plantation. However, some small failed areas were evident in the northern part of the bog (see Fig. 2.10). These were adjacent to some vertical faces which had been created by turf cutting for fuel. The failures manifested themselves as a series of concentric vertical cracks, approximately 100 m in diameter, radiating back from the face.

Similarly, aerial photographs from 2003 showed no evidence of cracking in the southern area. This failure was first noticed on a site visit by the EU LIFE project steering group in September 2006 and was later shown to be present in photographs from 2005 which were taken prior to restoration (see Fig. 2.11a). The southern failure also occurred just behind an area where peat was being harvested for domestic purposes. Another important feature of this area is a drain which runs approximately east-west, just south of the failed area. Again, the failure comprised a series of concentric cracks radiating from the southern edge of the bog. At that time it was estimated that the failed area extended over a width of some 250 m and extended 400 m into the bog (Derwin, 2006). The zone of cracking appears to be confined to the east by the main forestry drain. Originally, the northern limit of the cracking coincided with a townland boundary drain.

Restoration of the site took place in 2005 and comprised removing the plantation and blocking the drain network (Derwin, 2008). Subsequent aerial photographs of the area from 2007, 2009, 2010 and 2011 (see Fig. 2.11b) show no change in the lateral extent of the failed area but some small growth in the area of the cracking towards the former northern extent of the forestry.

Figure 2.10. Section of 2005 aerial photograph of Carn Park bog showing northern failed area (courtesy Charise Mc Keown, Geological Survey of Ireland).

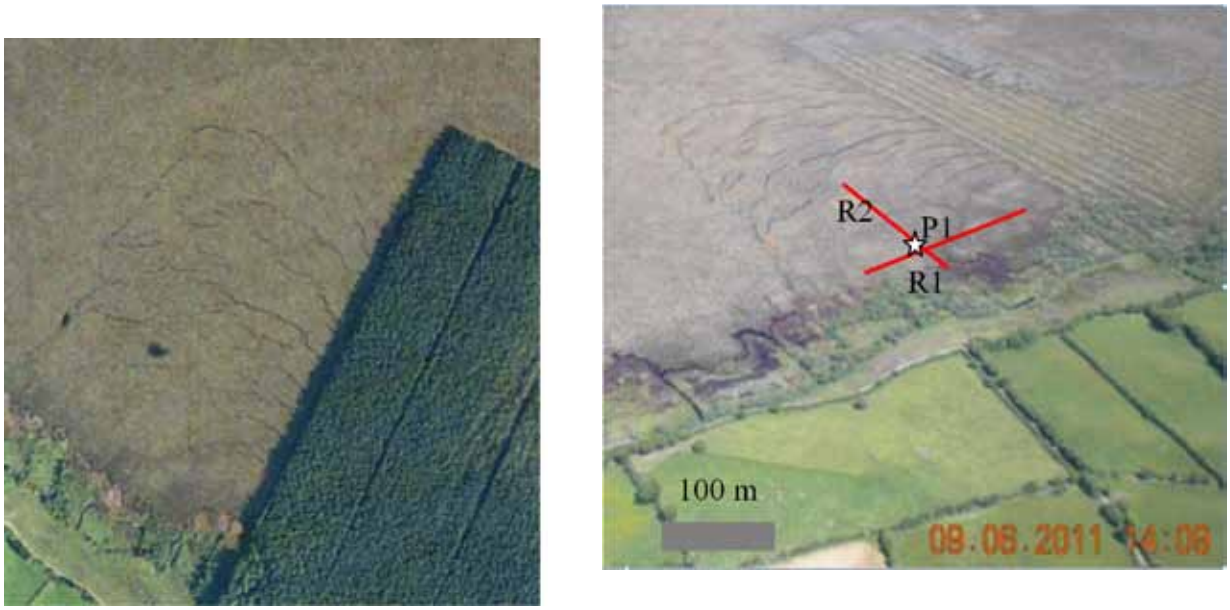

(a) (b)

Figure 2.11. Southern failed area at Carn Park bog: (a) from 2005 aerial photograph (courtesy Charise McKeown, Geological Survey of Ireland) and (b) section of 2011 ortho-rectified photograph of Carn Park bog (courtesy Andrea Webb, National Parks and Wildlife Services).

(a) (b)

Figure 2.12. Photographs of southern failed area of Carn Park bog: (a) new pool in south-west corner of failed area thought to be origin of the failure (photo from December 2006) and (b) photograph of crack from February 2011.

Some photographs of the cracks in the southern area are shown on Fig. 2.12. Figure 2.12a shows a newly formed pool at the south-west corner of the cracking from 2006. The flora present in the pool suggests it was newly formed at that time. It was thought to be the origin of the cracking and occurs at the top of an old peat-cutting drain. There was an obvious bulge in the face bank where the peat has slid southwards. A photograph of one of the cracks, taken in February 2011, is shown on Fig. 2.13b. It can be seen that they are up to 1 m wide and are of significant depth.

2.3.1.2 Aghnamona

Aghnamona Bog is classified as a National Heritage Area (NHA) and is situated 2 km east of the village of Roosky, close to the border between Cos Leitrim and Longford. The site under investigation here is located in Co. Longford. It is located some 45 km north of Carn Park (see Fig. 1.1). The Roosky Bypass (N4 Primary Road) was constructed between July 2006 and December 2007. The main impact of the works on Aghnamona Bog involved cuts of up to 5 m to facilitate the construction of two link roads and a large roundabout on the south-west corner of the bog as well as some realignment

Figure 2.13. Image showing failed section of Aghnamona Bog, Roosky. Imagery © DigitalGlobe, Map data © Google.

Figure 2.14. Photographs of cracking on Aghnamona bog, Roosky (April, 2011).

and deepening of the surface drains by up to 1.5 m (Minerex Environmental Ltd., 2004). The failure was first noticed in 2008, after completion of the road works, and the nature of the failure is illustrated on Fig. 2.13. Similar to Carn Park it has manifested itself as a series of concentric cracks, about 70 m in diameter, radiating about 100 m into the bog away from the roadway/ drainage works associated with the roundabout on the Roosky Bypass. Some photographs of the cracks are shown on Fig. 2.14. It can be seen that they are up to 1 m wide and are of significant depth.

2.3.2 Previous Monitoring

A series of timber stakes was installed in October 2006 across cracks at Carn Park to enable monitoring of the crack movement and to mark the extent of the failed area. These stakes were resurveyed in August 2008 and showed additional movements of up to 0.2 m between the stakes.

In May 2005 a series of standpipes was installed to record any changes in water level due to bog-restoration activities, for example, drain blocking or tree removal. Initially, water levels were found to be up to 0.6 m below the surface of the mature conifer plantations and close to the surface of the open bog. With the removal of the conifers (summer 2005) and the blocking of drains (summer 2006), there was a significant rise in the water level. Extensive areas of open water were created in the open bog and the water level was found to remain close to the bog surface throughout most of the year, a crucial requirement for bog restoration.

2.3.3 Field Testing

A series of peat sampling and geophysical testing exercises were carried out at both bogs. At Carn Park, peat probing and Ground Penetrating Radar (GPR) and ERT was carried out in October 2011. Subsequently, block sampling of the peat was carried out on the southern failed area in November 2011 and on the northern failed area in February 2012. At Aghnamona, peat probing, block sampling and a similar set of geophysical tests were carried out in June 2011. Details of these testing exercises follow.

2.3.3.1 Peat probing and sampling

The peat probing was carried out using a 'Russian' sampler, which produces a 0.5 m long, hemispherical core (Fig. 2.15). The depth limit with the particular probes used is 4.1 m. At Carn Park one peat probe to 3.0 m was carried out at the junction of the two ERT lines (see Fig. 2.11b). Penetration beyond 3.0 m was not possible due to resistance from roots and wood fragments. Small (»50 g) samples were taken from the Russian sampler for laboratory water content determination. Additional samples were taken by the Russian sampler along the line of ERT profile R2, at depths of 1.0 m and 1.5 m. Block samples (» 200 mm x 200 mm x 50 mm high) were also extracted by hand from the walls of the cut face at both the southern and northern failed areas.

At Aghnamona two peat probes, including sampling, to the full depth of the equipment were carried out at the eastern extremity of the failed area and in the centre of the failed area (see Fig. 2.16). Additional samples were taken with the Russian sampler along the line of ERT

Figure 2.15. Russian peat sampling at Carn Park.

profile R2 at depths of 0.5 m and 1.5 m. Block samples (» 200 mm x 100 mm x 50 mm high) were also extracted by hand from the walls of the drains located along the western boundary of the failed area.

2.3.3.2 Electrical resistivity tomography

Two-dimensional (2D) ERT surveys were performed at both sites as shown on Figs 2.11b and 2.16 respectively. Galvanically coupled ERT measurements for all but one profile for both sites were acquired using a multi-electrode Campus Tigre resistivity meter with two 32 takeout multicore cables and 64 conventional stainless steel electrodes. Profile R3 at Aghnamona was acquired using a single cable with 32 conventional stainless steel electrodes. An electrode spacing of 2 m was chosen for all profiles in order to provide an adequate trade-off between depth and resolution. A four-electrode Wenner array configuration was used to acquire multiple readings for each 2D ERT profile. The Wenner array was used here as it was found to provide a good signal-to-noise ratio. ERT electrodes were spatially referenced using a Trimble PRO-XR dGPS, which provides sub-meter accuracy.

Inversion of all of the apparent resistivity data was carried out with the software Res2Dinv (Loke, 2004) using the L_2 norm inversion optimisation method. The Gauss-Newton method (Sasaki, 1989; deGroot-Hedlin and Constable, 1990) was selected for the first three iterations, after which the quasi-Newton method was used. For this study all inversions performed converged to a normalised RMS error of less than 5% within five iterations.

2.3.3.3 Ground penetrating radar

The GPR work was carried out using a 100 MHz antenna with a 0.2 m trace interval. The GPR is linked to an accurate RTK dGPS (centimetre accuracy) which enables rapid coverage, spatial relocation to GPS co-ordinates as well as providing topographic information. A similar system was used by Trafford (2009), where it was shown that GPR has proven to be the most effective geophysical technique for accurate assessment of peat thickness. A number of processing steps were applied to the data, including a time-zero adjustment, a Butterworth bandpass filter, a running average and an energy decay compensation (time variant gain). The time-zero adjustment was done by correction for maximum positive phase due to the transmitter, receiver offset.

In order to convert two-way travel time to depth a GPR velocity of 0.035 m/ns was used following depth calibration with the peat probes performed directly along

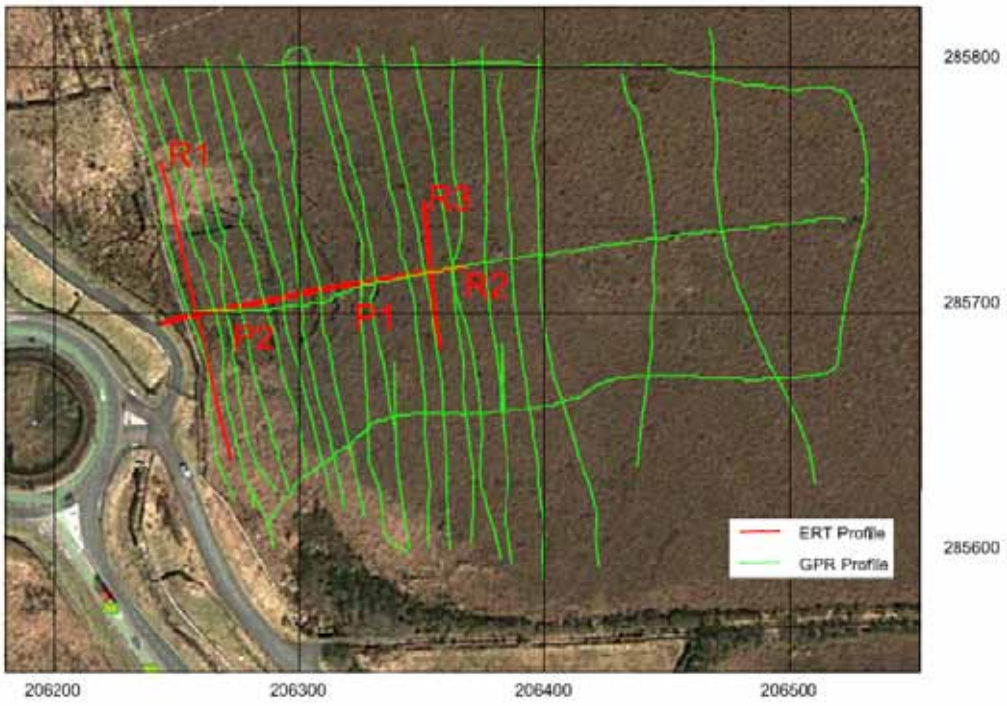

Figure 2.16. Test locations at Aghnamona site (east and north co-ordinates are given in m). Location of ERT test lines and deep probes are designated R1, R2 and R3 and P1 and P2 respectively. Adapted from the following sources: Imagery © DigitalGlobe, Map data © Google.

(a) (b)

Figure 2.17. Acquisition of (a) Ground Penetrating Radar (GPR) data at Aghnamona using a 100 MHz antenna and (b) Electrical Resistivity Tomography (ERT) data at Carn Park.

the GPR profiles. Trafford (2009) also used this velocity for depth calibration at other raised bogs in Ireland. A topographic correction was also applied to the data using the elevation data acquired using the RTK dGPS.

For the Aghnamona site the GPR lines are shown in Fig. 2.16. At both sites, the GPR equipment was person-hauled across the bog surface as shown in Fig. 2.17. Profiles were acquired in a north-south direction (approximately). Around the failure zone profiles were closely spaced (around 10 m apart), whereas profiles that were acquired away from the failure zone, further to the east were separated by greater distances (approximately 50 m), as shown in Fig. 2.16.

At Carn Park, data was collected from across, as well as around, the perimeter of the failure, in order to assess the distribution of peat throughout the survey area. An issue arose with the RTK dGPS, which failed during data acquisition. As a result, it was not possible to acquire all of the intended data at this site. The acquisition of spatially referenced data in conjunction with the GPR data is deemed crucial, particularly during a survey such as this, which is person-hauled across rough terrain, where it is not difficult to veer off intended profile lines.

2.3.4 Laboratory Testing

2.3.4.1 Oedometer tests

Conventional maintained load oedometer tests were carried out according to BSI (1990). Generally, the initial load was 5 kPa and the load increment ratio 2.0. Each increment was maintained for 24 hours. A slightly larger sample than normal (37.5 mm high as opposed to the standard 19 mm) was used in order to try to capture the mass behaviour of the naturally variable fibrous peat. The specimen diameter was 76 mm.

2.3.4.2 Direct simple shear tests

For the direct simple shear tests (DSS) tests, a Geonor H12 DSS apparatus was used. Bjerrum and Landva (1966) provide a full description of the apparatus. Undrained tests are conducted as constant volume tests, where the height of the specimen is held constant throughout the shearing stage of the test. Test specimens have a diameter of 79.5 mm and a height of 19 mm. In general, the test procedures were those typically used at the Norwegian Geotechnical Institute (NGI), as reported by Andresen et al. (1979). Samples were consolidated in a single step to the estimated in-situ effective stress (σ_{v0}') of 10 kPa and were left to consolidate overnight. On the following day, samples

were sheared at a constant linear displacement which gave a shear strain rate of approximately 4% shear strain per hour. The undrained shear strength (s_u) is either taken to be equal to the peak horizontal shear stress ($\tau_{h\text{-}max}$) attained during shearing or alternatively the shear stress measured at 15% shear strain, whichever occurs first.

2.3.4.3 Von Post classification

The peat material has been classified according to the scheme described originally by von Post and Granlund (1926), and extended by Hobbs (1986).

2.3.4.4 Loss on ignition

Loss on ignition testing was carried out by igniting approximately 10 g peat samples in a muffle furnace at 440°C for 5 hours (Arman, 1971). The resulting value is often considered to be equivalent to the organic content of the peat.

3 Results and Discussion

3.1 Agricultural Compaction

3.1.1 Lyons Estate

3.1.1.1 Conventional measures of compaction

Plots of bulk density and gravimetric water content are shown in Fig. 3.1a and 3.1b respectively. Significant differences in bulk density are observed between the trafficked area and the control at depths of 15 and 30 cm, indicating compaction of the soils in the treatment subjected to machinery trafficking. Little difference in gravimetric water content was observed at these depths.

The mean results for the penetrometer data measured on both areas are illustrated in Fig. 3.2. A significant difference in penetrometer resistance between the two treatments was measured for all data points between 6 cm and 28 cm depth ($p < 0.01$ for all). As expected, the trafficked area exhibited a significantly greater penetrometer resistance for this depth interval, confirming compaction of the soils in this area.

3.1.1.2 Multichannel Analysis of Surface Waves

For both treatments the mean values and standard deviations (SDs) were calculated for each of the layers in the upper 0.6 m, distinguished in the shear wave velocity inversion process (Fig. 3.3). A significant difference ($p < 0.01$) in the shear wave velocity distribution was measured for layers between 12 and 28 cm depth, with mean velocities between 17 and 30 m/s higher for the trafficked treatment compared to the control. This zone of elevated shear wave velocities also corresponds quite closely to the peak penetrometer resistance and the relatively high bulk density measurements discussed above. Below this depth, the velocity profiles from the two treatments converge and there is an increase in the SD for both profiles in the deeper layers, representing a reduction in resolution of the MASW measurements.

It should be pointed out that, for these experiments, the maximum frequency picked for construction of the surface wave dispersion curves was between

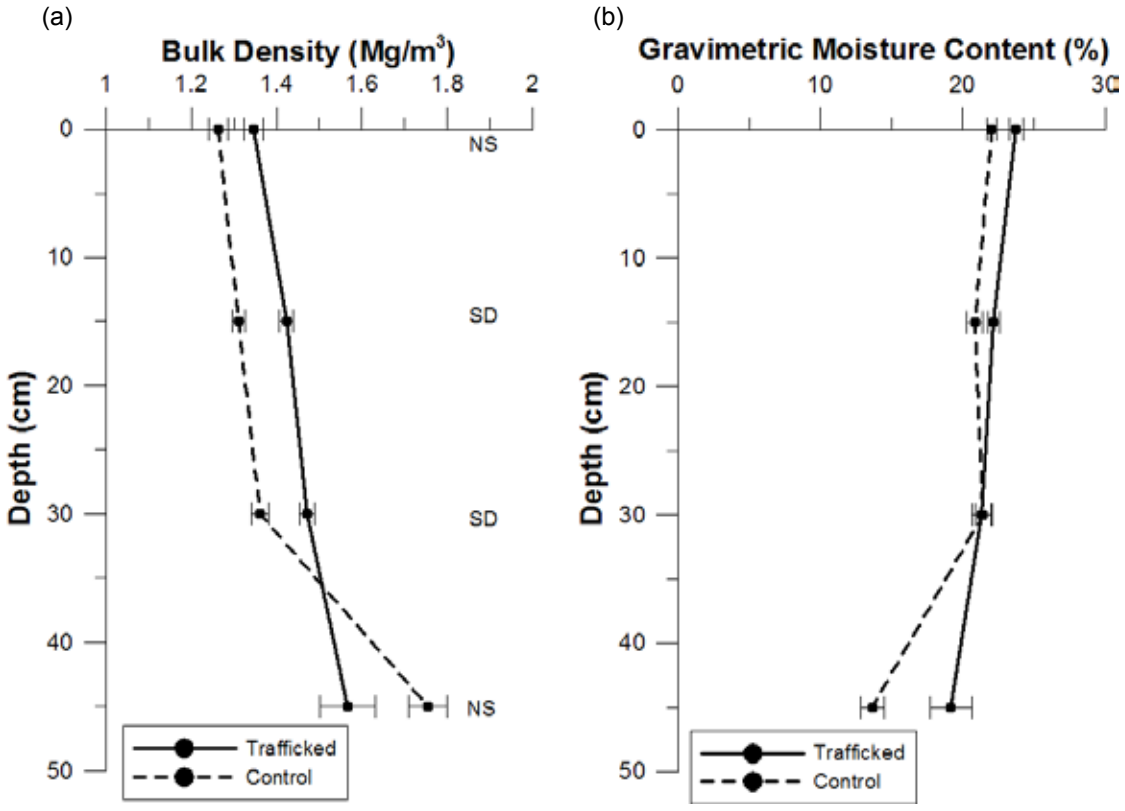

Figure 3.1. (a) Mean bulk density and (b) gravimetric moisture content for trafficked and control treatments, with associated standard deviation (error bars). Note: SD = significant difference (P < 0.01); NS = not significant.

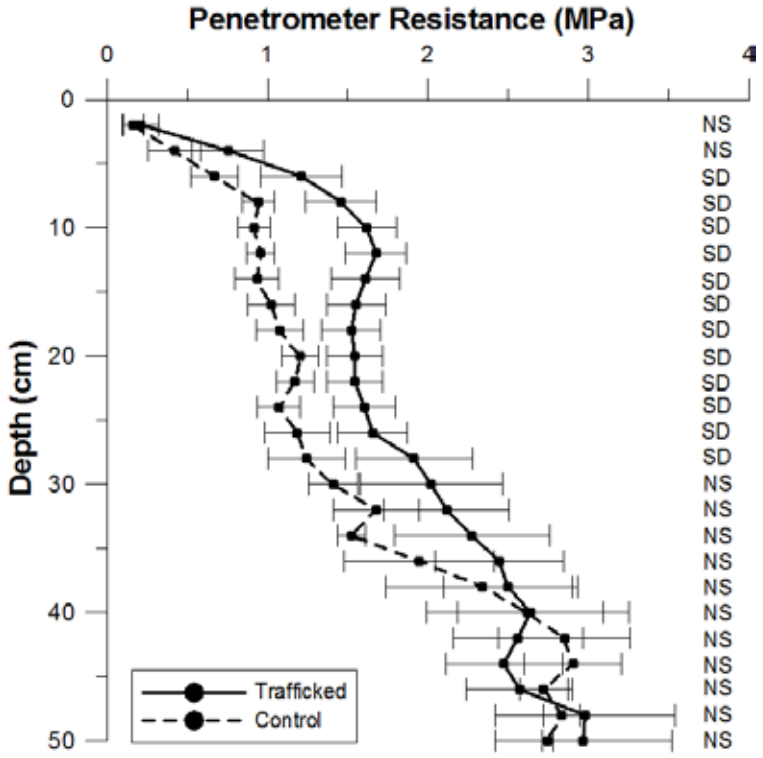

Figure 3.2. Mean penetrometer resistances for trafficked and control treatments, with associated standard deviation (error bars) for each data point. Note: SD = significant difference (P < 0.01); NS = not significant.

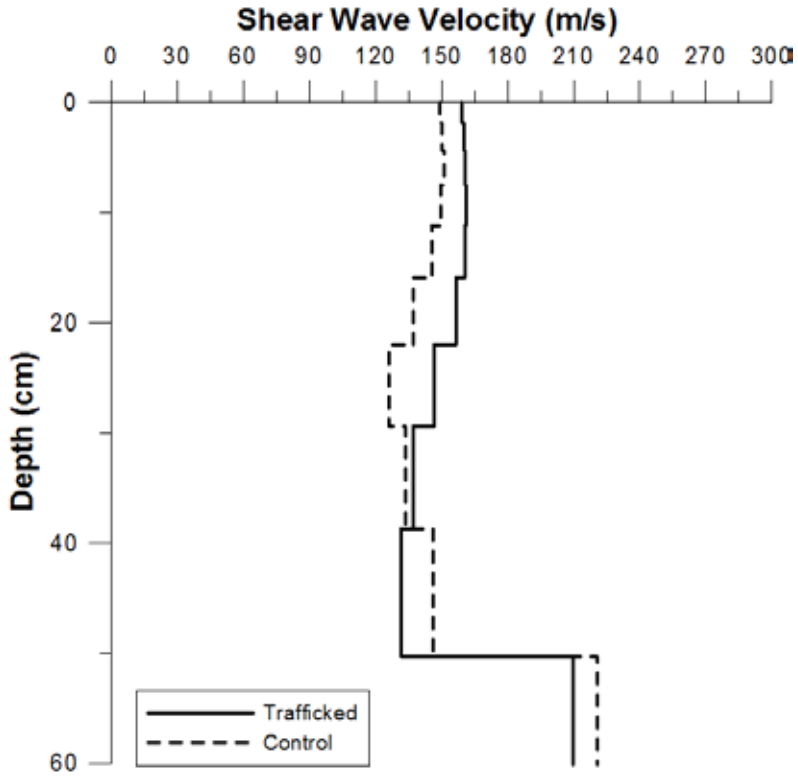

Figure 3.3. Mean shear wave velocities for trafficked and control treatments, with associated standard deviation (error bars) for each data point. Note: SD = significant difference (P < 0.01); NS = not significant.

230 Hz and 300 Hz, which, given the phase velocities measured, would correspond to a minimum resolvable upper inverted layer of approximately 12–15 cm. Although the inversion process provides velocities for layers shallower than this, the results for these layers are unlikely to have been accurately resolved. This lack of resolution can be seen when the V_s results (Fig. 3.3) from this depth range are compared to the equivalent penetrometer resistances. As shown in Fig. 3.2, the penetrometer resistances measured for the upper 6 cm depth are very low relative to deeper measurements. This is in contrast to the V_s measurements for this depth range, where the velocities are similar to those measured below 10 cm depth. If accurate, higher-resolution information is required for the upper 10 cm, higher-frequency surface waves will need to be generated, possibly by using an alternative source to that used in this study.

3.1.1.3 Resistivity

Figure 3.4 provides mean inverted resistivity data from the trafficked and control treatments. The data from the treatment subjected to trafficking exhibits a significantly lower resistivity than the control to a depth of 34 cm. Below this depth the differences are not statistically different. It should also be pointed out that there is significant variation in the inverted resistivity data close to the surface, as evidenced by large standard deviations. The reduction in resistivity detected in the trafficked treatment is almost certainly caused by the reduction in the density/volume of voids in the soil caused during the compaction process. This reduction corresponds well to the reduction in bulk density (Fig. 3.1a) and penetrometer resistance (Fig. 3.2), discussed above. Similar findings have been reported by Seladji et al. (2010) and Besson et al. (2004), although the magnitude of the reduction in resistivity observed in this study appears to be nearly twice that observed by Besson for a similar change of bulk density.

Examples of inverted 2D ERT profiles acquired in the trafficked and control treatments are shown in Fig. 3.5a and 3.5b respectively. For these examples, the resistivity of the upper 30 cm (approx.) is clearly different, with the trafficked treatment displaying lower resistivities than the control. Below this depth, however, the inverted resistivities are similar for both sites and, if anything, slightly higher for the trafficked treatment.

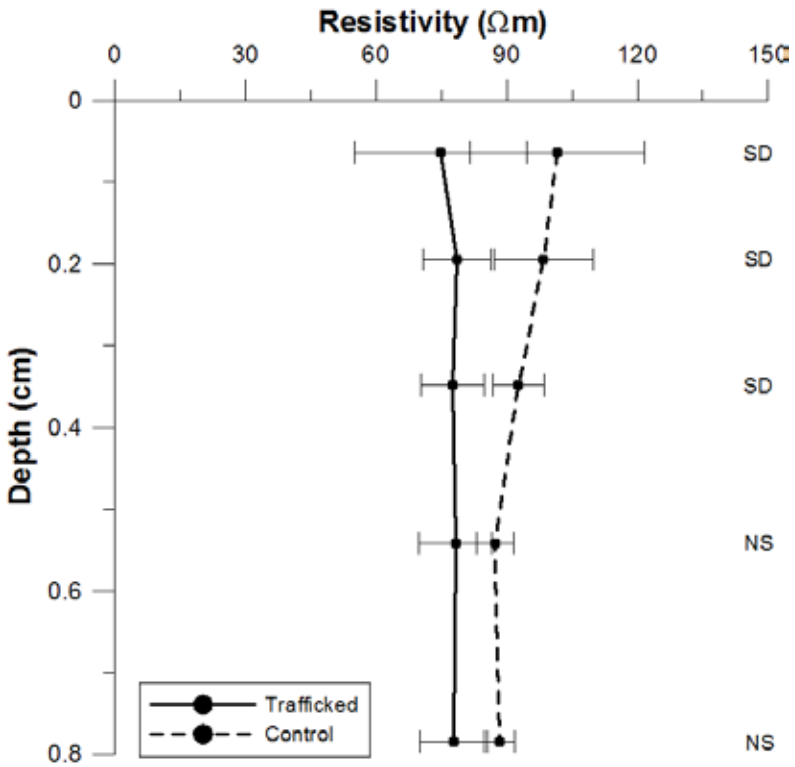

Figure 3.4. Mean resistivity for trafficked and control treatments, with associated SD (error bars). Note: SD = significant difference (P < 0.01); NS = not significant.

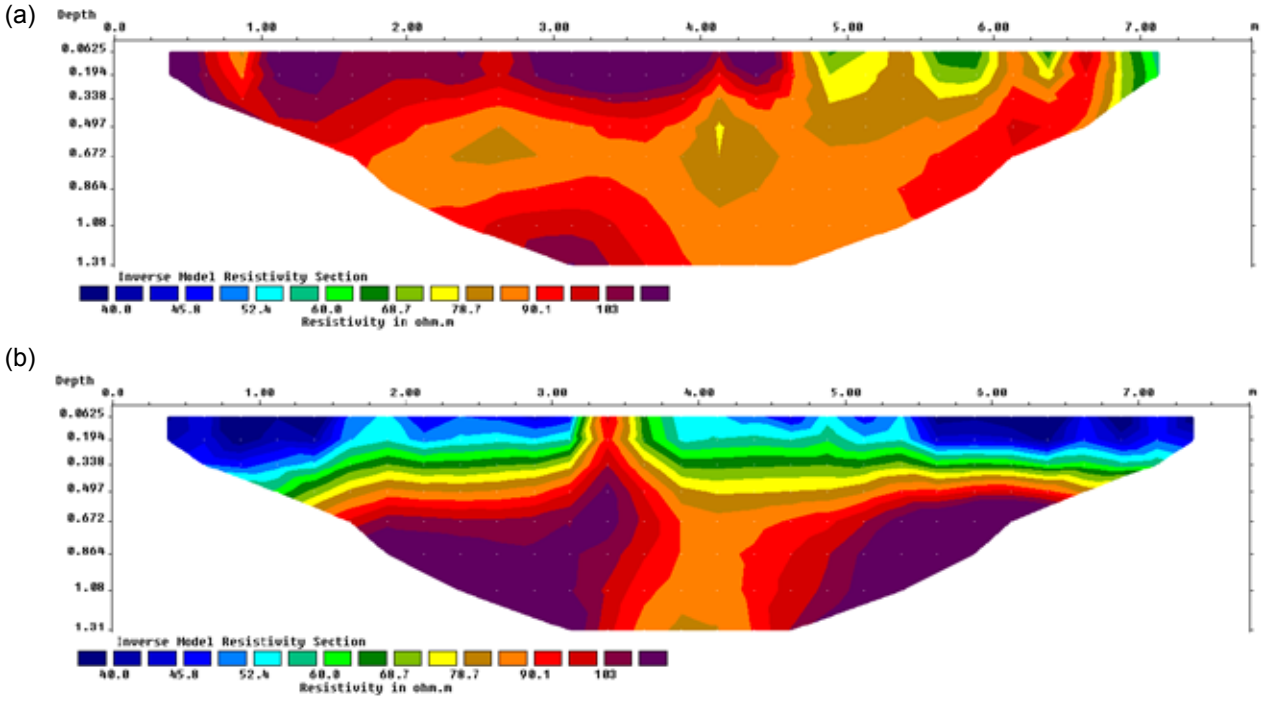

Figure 3.5. Examples of inverted 2D electrical resistivity tomography (ERT) profiles acquired in the (a) trafficked and (b) control treatments.

3.1.2 Oakpark

3.1.2.1 Conventional measures of compaction

Gravimetric water content and bulk density data for the A and B horizons of the two study areas is provided in Table 3.1. Area 1 (headland) exhibited a significantly greater bulk density than Area 2, for the A horizon ($p<0.01$), which suggests that it has been compacted quite heavily. For the B horizon, Area 1 exhibited a higher mean bulk density than Area 2, although the difference is not statistically significant. In addition, the gravimetric water contents measured for both horizons in Area 1 were lower than in Area 2, although not significantly so. Undrained shear strength, c_u, was also measured using shear vanes in both areas for the soil A horizon only (Table 3.1). The measured c_u values were found to be significantly greater for Area 1 than for Area 2, with the c_u value of the compacted headland being more than double that of the uncompacted Area 2.

Table 3.1. Gravimetric soil water content and bulk density data for Areas 1 and 2.

		Gravimetric soil water content (%)	Bulk density (Mg/m^{-3})	Undrained shear strength (kPa)
Area 1 (Headland)	Horiz. A (0–25 cm)	16.6 (2.03)	1.59 (0.04)	75 (15)
	Horiz. B (25–50 cm)	20.5 (1.15)	1.66 (0.08)	
Area 2	Horiz. A (0–25 cm)	18.2 (1.65)	1.41 (0.03)	34.7 (9.5)
	Horiz. B (25—50 cm)	21.2 (1.77)	1.59 (0.07)	

Note: The numbers presented are mean values and the numbers in brackets are standard deviations.

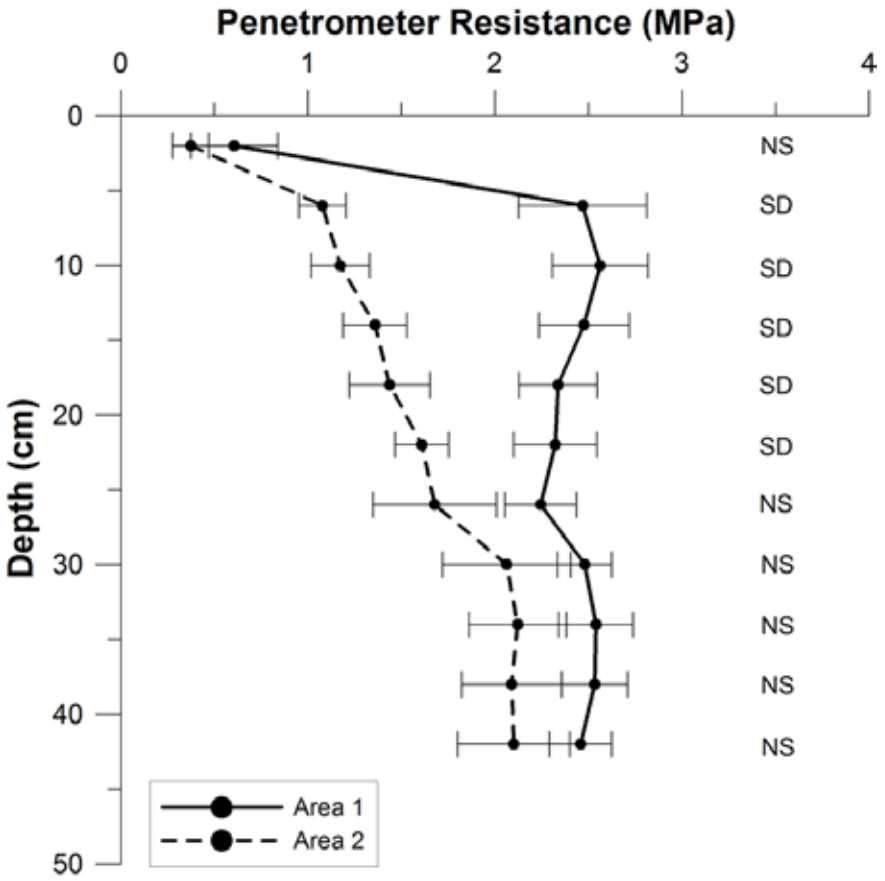

Figure 3.6. Mean penetrometer resistances for Area 1 and Area 2, with associated standard deviation (SD) (error bars) for each data point. Note: SD = significant difference (P < 0.01); NS = not significant.

The mean results for the penetrometer data measured on both areas are illustrated in Fig. 3.6. A significant difference in penetrometer resistance between the two areas was measured for all data points in the A horizon from 6 cm to 22 cm depth ($p < 0.01$ for all), with the headland exhibiting a significantly greater penetrometer resistance for this depth interval. Penetrometer resistances measured for the A horizon in Area 1 are on average 45% greater than those measured for Area 2. Peak penetrometer resistance was measured between 5 and 15 cm depth. Below 22 cm depth (B horizon) a difference between the two areas exists, although it is not statistically significant. As discussed above, for comparative purposes nine profiles were acquired at 1 m spacing in a linear profile on both areas. The results of these individual profiles are illustrated in Fig. 3.7a and 3.7b for Areas 1 and 2 respectively. As shown in Fig. 3.7a, higher penetrometer resistances were generally measured between 0 and 5 m along the linear profile between 6 and 18 cm depth.

3.1.2.2 Multichannel Analysis of Surface Waves

Each of the individual 1D profiles has been incorporated into 2D depth sections of V_s in Fig. 3.8a and 2.10b for Areas 1 and 2 respectively. As illustrated, the inverted shear wave velocities vary both vertically and horizontally. For both locations the mean values and standard deviations weres calculated along horizontal lines for each of the layers in the upper 0.5 m, distinguished in the shear wave velocity inversion process (Fig. 3.9). A significant difference ($p < 0.01$) in the shear wave velocity distribution was measured for all of the inverted layers. The velocities measured for the A horizon in Area 1 were on average 21% greater than those measured for Area 2. At the headland, the MASW method clearly detected the previously observed compaction in the A horizon, which was indicated by mean shear wave velocities in excess of 120 m/s. The zone of elevated shear wave velocities observed in Fig. 3.8a, at a distance of 2–5 m, and a depth of 7–21 cm also corresponds quite closely with the peak penetrometer resistance indicated in Fig.

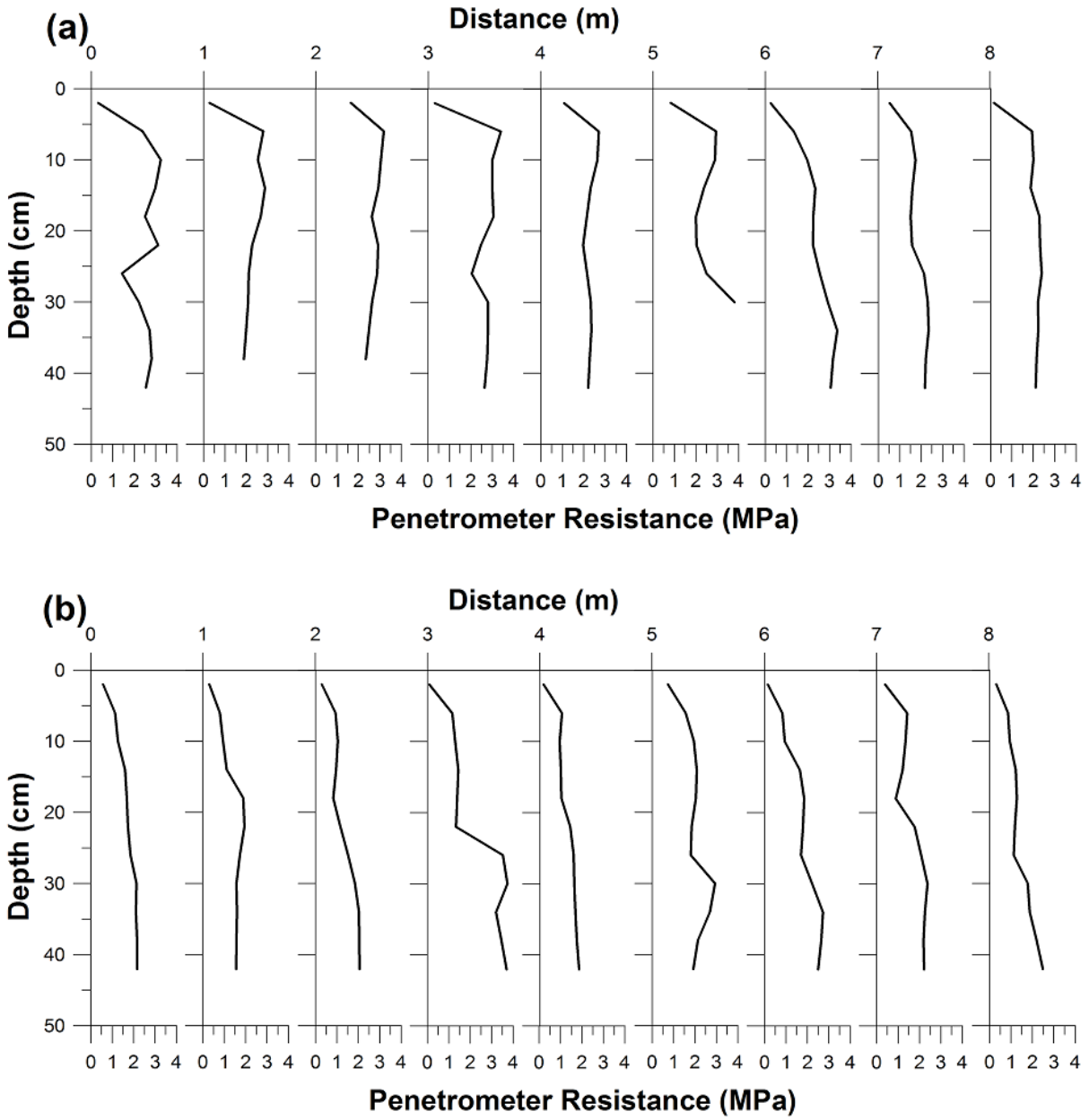

Figure 3.7. Linear profile of cone penetrometer soundings for: (a) Area 1 and (b) Area 2.

3.7a. A peak V_s of 137 m/s was detected for the soil A horizon, at 0.18 m depth (Fig. 3.8a), 3.5 m from the start of the profile, which again compares well to the cone penetrometer data, where the highest measured resistances were detected on the profile at 3 m distance. At distances greater than 6 m along the 2D profile, V_s decreases slightly, reflecting what appears to be a reduction in compaction. A similar reduction in compaction is also apparent in the cone penetrometer results, between 5 and 8 m (Fig. 3.7a).

As observed previously for the Lyons site, for these experiments the maximum frequency picked for construction of the surface wave dispersion curves was between 250 Hz and 300 Hz, which, given the phase velocities measured, would correspond to a minimum resolvable upper inverted layer of approximately 10 cm. Although the inversion process provides velocities for layers shallower than this (0.03 cm and 0.07 cm in this study), the results for these layers are unlikely to have been accurately resolved. This lack of

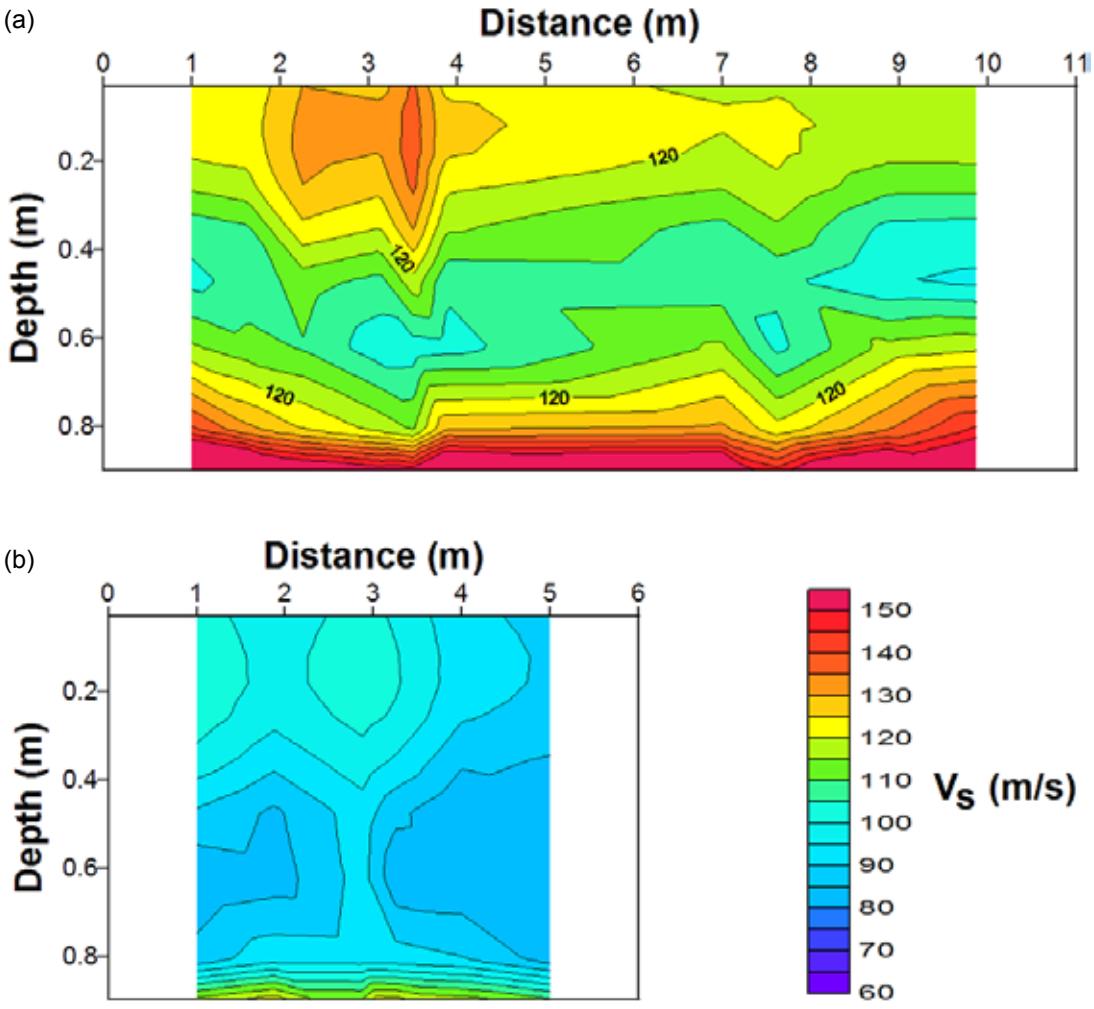

Figure 3.8. 2D inverted shear wave velocity (V_s) profile for (a) Area 1 and (b) Area 2.

resolution, in this instance, can be seen when the V_s results (Fig. 3.9) from this depth range are compared to the equivalent penetrometer resistances. As shown in Fig. 3.6, the penetrometer resistances measured at 2 cm depth for Area 1 are very low relative to deeper measurements. This is in contrast to the V_s measurements for this depth, where the velocities are similar to those measured below 10 cm depth. If accurate higher-resolution information is required for the upper 10 cm, higher-frequency surface waves will need to be generated, possibly by using an alternative source to that used in this study.

Shear wave velocities measured in Area 1 for the B horizon (0.25 m to 0.5 m depth) are also significantly different to those measured for Area 2 – indicating compaction of this layer. As discussed above, a marginally higher (although not statistically significant) bulk density and penetrometer resistance were also detected at the headland for this layer. With increasing depth in the B horizon, the difference in inverted V_s decreases considerably, suggesting a reduction in compaction with depth.

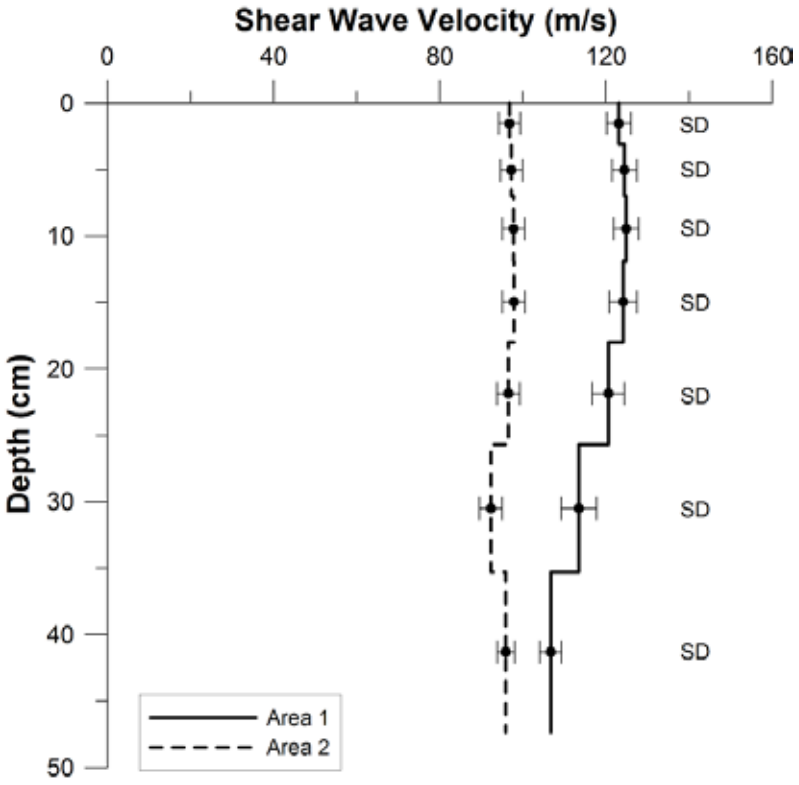

Figure 3.9. Mean shear wave velocities for Area 1 and Area 2, with associated standard deviation (error bars). Note: SD = significant difference (P < 0.01); NS = not significant.

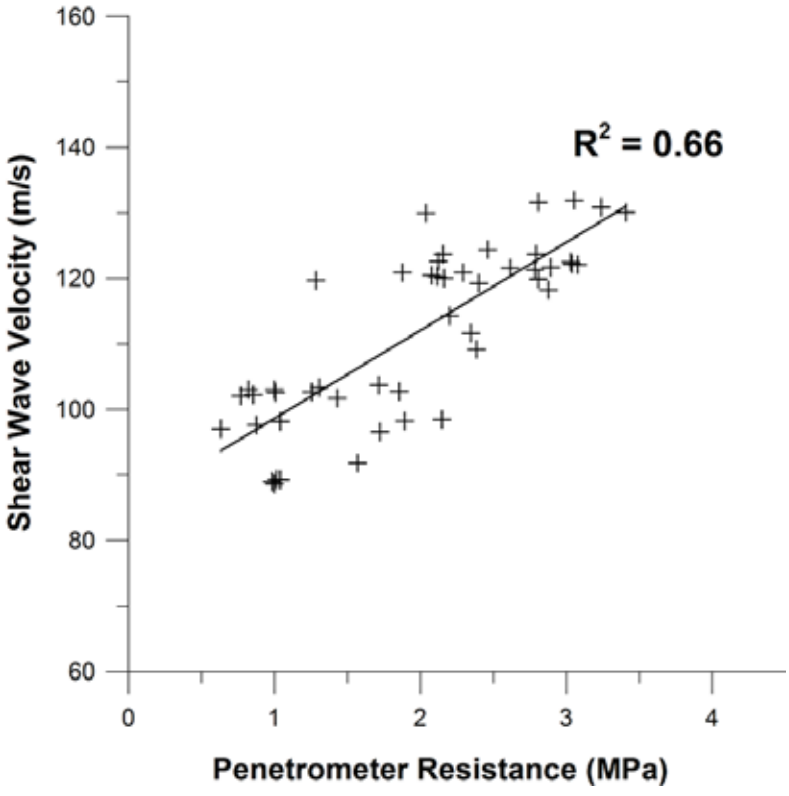

Figure 3.10. Relationship between V_s and penetrometer resistance.

The relationship between V_s and penetrometer resistance is illustrated in Fig. 3.10. The data presented in this plot is taken from the linear profiles of V_s and penetrometer resistance, which provides a direct comparison between the two sets of data. Data was only used at the depth levels where data exists for both sets. Although there is some scatter in the data, a linear relationship provides a best fit between the two parameters (R^2 =0.66, P<0.001, n=48), with high V_s generally corresponding to high penetrometer resistances. Similar relationships have been observed between V_s and penetration resistance from civil engineering cone penetration tests for a range of subsoils (e.g. Mayne and Rix, 1993; Mayne and Rix, 1995; Schnaid et al., 2004; Long and Donohue, 2010), although a number of these relationships are best fit to a power function. Also, based on these relationships (for subsoil only), V_s would generally be expected to be higher than that measured here, particularly for the higher penetration resistances measured.

3.1.2.3 Resistivity

Mean inverted resistivity data for Areas 1 and 2 are provided in Fig. 3.11. As was observed at the Lyons test site, soil compaction has had a significant effect on inverted resistivities measured at the Oakpark site. Similarly to the MASW data, the inverted resistivity data for Area 1 exhibits a significantly lower resistivity than Area 2 to a depth of 54 cm. Below this depth the differences are not statistically different. As with the data from the Lyons test site significant variation in the inverted resistivity data close to the surface was observed, as evidenced by large standard deviations. The reduction in resistivity detected in the trafficked treatment is almost certainly due to the reduction in the density/volume of voids in the soil caused during the compaction process. The reduction in resistivity relating to compaction corresponds well to the reduction in bulk density (Table 3.1), penetrometer resistance (Fig. 3.6), and shear wave velocity (Fig. 3.9) discussed above.

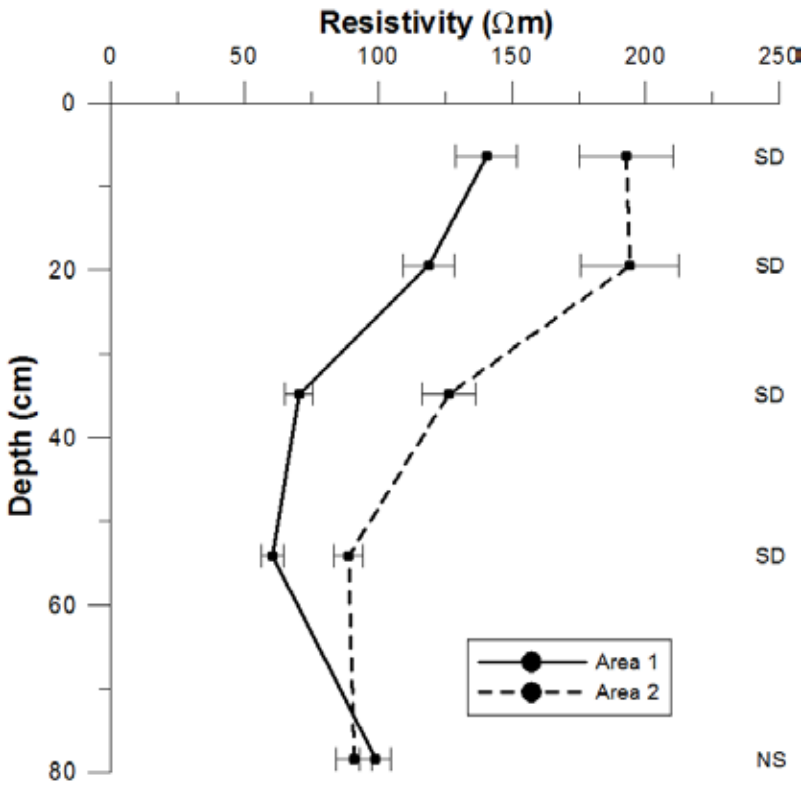

Figure 3.11. Mean resistivity for Areas 1 and 2, with associated standard deviation (error bars). Note: SD = significant difference (P < 0.01); NS = not significant.

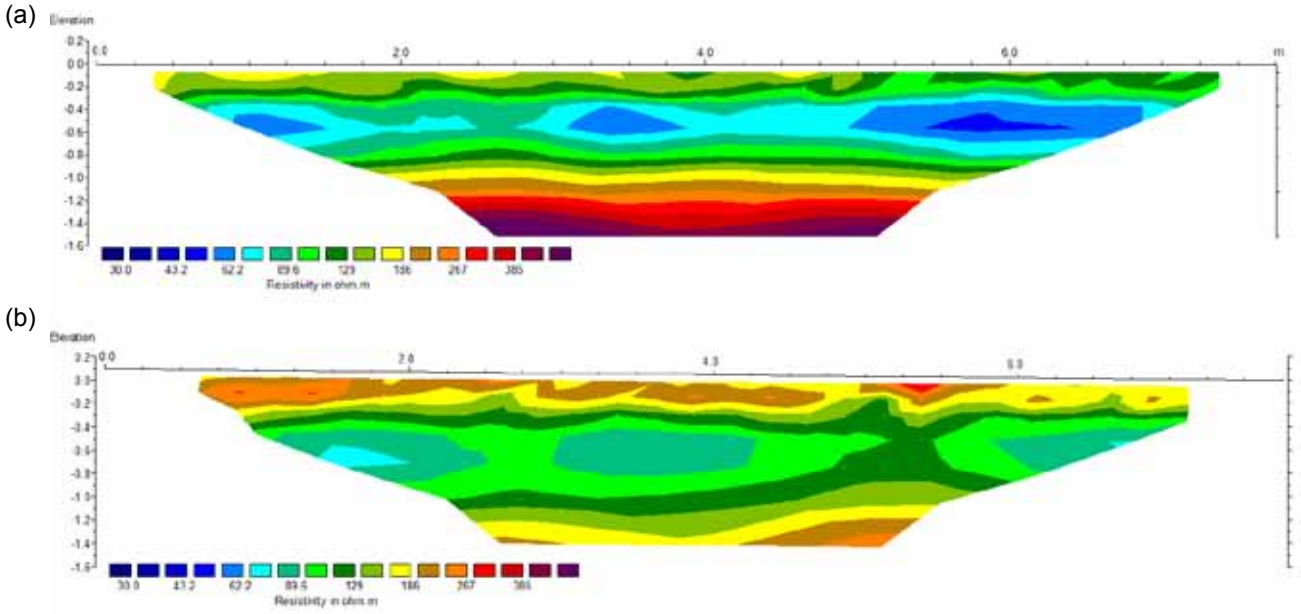

Figure 3.12. Examples of inverted 2D Electrical Resistivity Tomography (ERT) profiles acquired in (a) Area 1 and (b) Area 2.

Examples of inverted 2D ERT profiles acquired in both areas are illustrated in Figs 3.12a and 3.12b respectively. As shown, the resistivity of the upper 30 cm (approx.) is consistently lower for the compacted headland (Area 1) than for Area 2.

3.1.3 Assessment of High-speed Geophysical Measurements for Assessment of Compaction: Multichannel Analysis of Surface Wave Landstreamer

A high-speed system for acquiring MASW data was tested at the Oakpark site. This system involved a landstreamer with 24 14-Hz geophones. The geophones were spaced at 20 cm and were coupled to small metal plates to enable easy movement of the system which was towed behind a vehicle. As with the stationary MASW measurements, an initial test profile was conducted at the site, which involved varying the source type and the source/receiver locations, in order to determine the optimum acquisition parameters. From this initial test it was again found that the 500-g carpentry hammer was the most suitable available source for surface waves generation. It was found that this system considerably increased the efficiency of data acquisition as the system did not have to be disassembled and reassembled after each individual 1D survey.

Figure 3.13 shows a direct comparison between the dispersion images produced by the stationary, spike-coupled geophones and the landstreamer with plate-coupled geophones. Both dispersion images were acquired for 1D profiles located at the exact same location. The spike-coupled geophones in this case were significantly more sensitive to higher frequency surface wave data than the plate coupled geophones. The spike-coupled data has enabled both fundamental and 1st order higher-mode surface waves to be resolved to frequencies in excess of 200 Hz. When using plate-coupled geophones, the spectral coherence is significantly poorer at frequencies above 130 Hz and the higher mode surface wave is barely evident. The use of plate-coupled geophones on this occasion would therefore only likely result in a minimum resolvable depth of approximately 25–30 cm, which is not satisfactory for assessments of agricultural compaction.

(a)

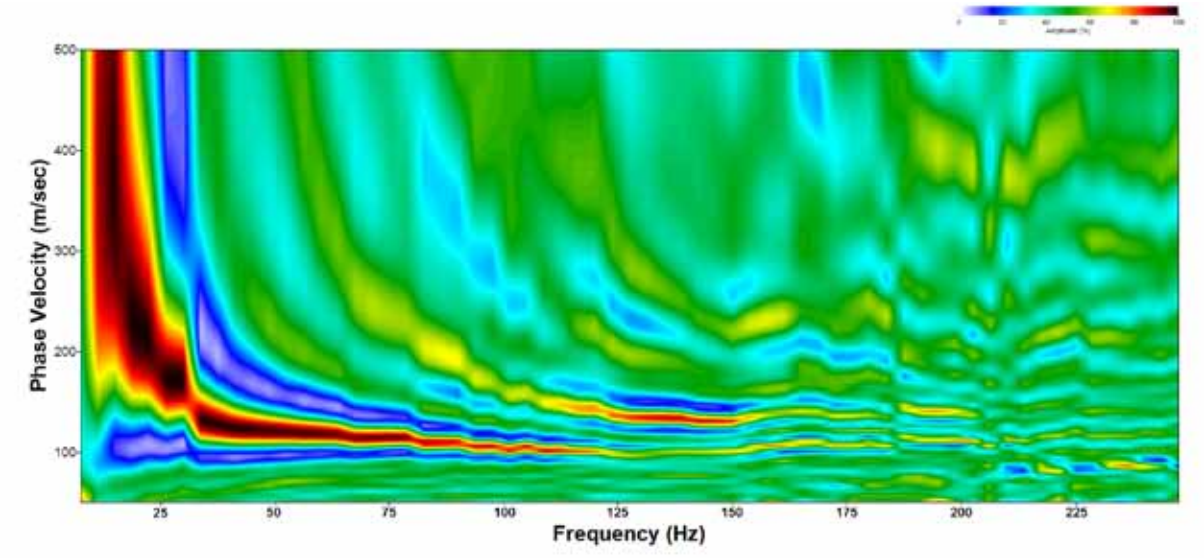

(b)

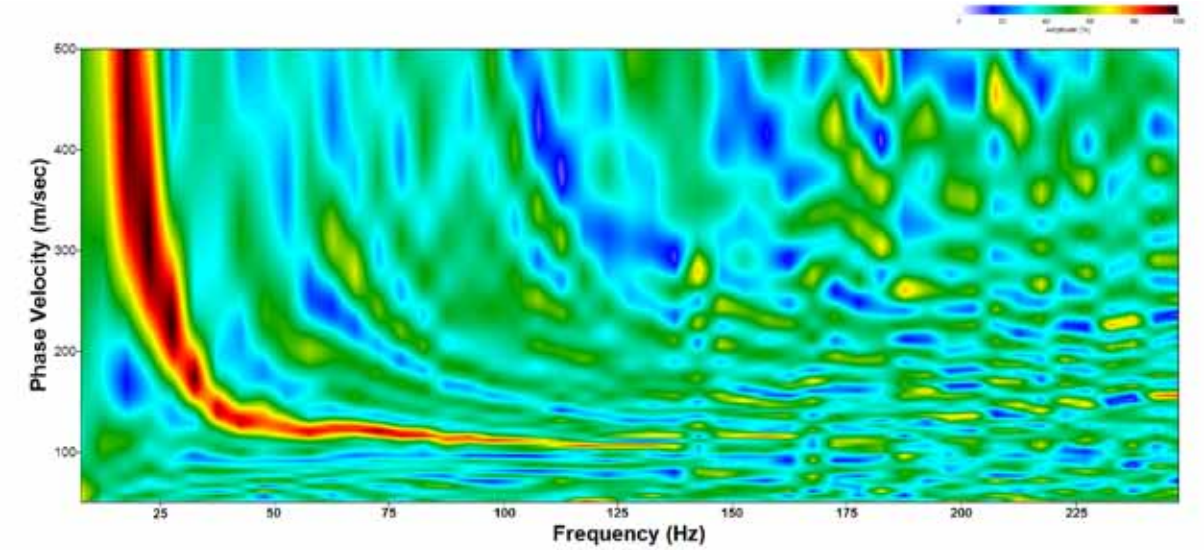

Figure 3.13. Dispersion images following wavefield transformation of surface wave seismic data produced from seismic data acquired using: (a) stationary, spike-coupled 14 Hz geophones and (b) a landstreamer with plate-coupled 14 Hz geophones.

3.1.4 Assessment of High-speed Geophysical Measurements for Assessment of Compaction: Capacitively Coupled Resistivity

Capacitively CR systems (Kuras et al., 2007), such as the Geometrics Ohmmapper that was used by Pellerin et al. (2003), have a number of advantages over traditional stationary galvanic resistivity systems, where electrodes are generally planted in the ground. For example, (i) they enable high-speed high-resolution continuous data acquisition with spatial sampling at the centimetre scale, and (ii) they are not affected by contact resistance and can therefore be used in high-resistivity environments. Coupled resistivity systems are a recent geophysical development and as such there is not a great deal of work making use of these systems in the published literature, despite their many benefits.

The capacitively coupled Geometrics Ohmmapper system was trialled at the Oakpark test site. Figure 3.14 gives the mean inverted resistivity resulting from this CR data for Areas 1 and 2. As observed for the galvanically coupled electrodes, soil compaction had a

significant effect on inverted resistivities measured at the Oakpark site. The inverted resistivity data for Area 1 exhibits a significantly lower resistivity than Area 2 to a depth of 54 cm. Below this depth the differences are not statistically significant. It should be pointed out, however, that the resistivity values measured here are considerably greater than those measured for the galvanically coupled data (Fig. 3.11), particularly for the relatively uncompacted Area 2 where the measured resistivity values from the inverted CR data are nearly twice that calculated for the galvanic data at a depth of 32 cm. The electrode array used with the CR system is DD compared to the Wenner array used for the galvanic system. However, this is unlikely to explain the large difference in calculated resistivities. One possible explanation for the large differences could be the considerable range of apparent resistivities observed near the surface, which could have affected convergence of the inverted models. On average, the ERT models using the CR data converged to a RMS error of around 6%–9% within five to six iterations. Although this does not indicate that the data is of poor quality, it should also be noted that a number of outlier points had to be removed from the dataset before processing. Previous inversions without removing the outliers resulted in larger inversion RMS errors (10–15%). In the author's experience, where significant variations in the measured apparent resistivity exist, artefact high and low resistivities can be introduced into inverted models, particularly at higher iterations.

Finally, despite the computation issues involved in processing the CR datasets, as with the other conventional and geophysical datasets discussed above, they clearly detected the reduction in resistivity

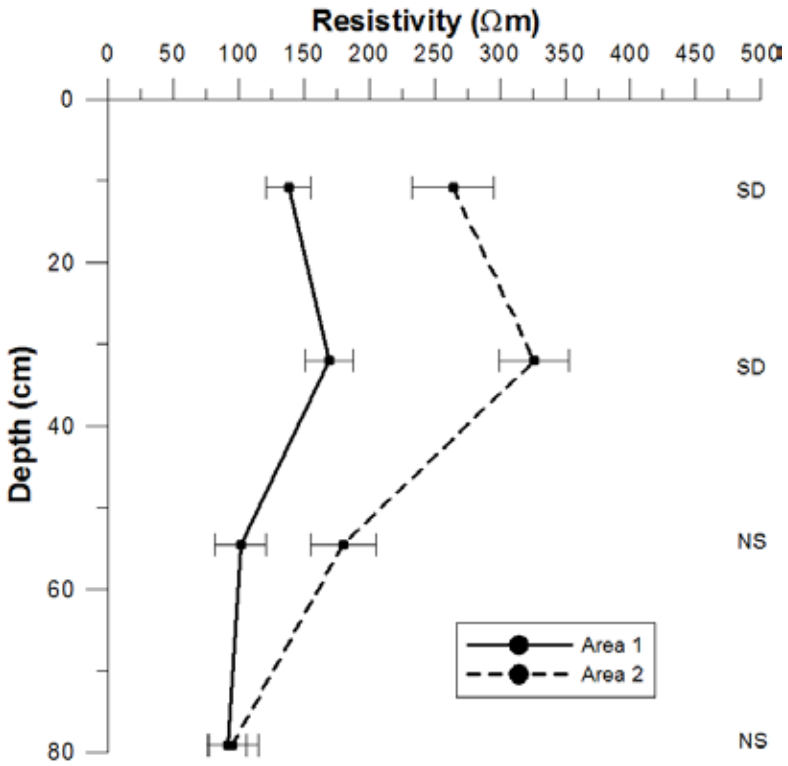

Figure 3.14. Mean resistivity for Area 1 and 2, acquired using a capacitively coupled Geometrics Ohmmapper, with associated standard deviation (error bars). Note: SD = significant difference (P < 0.01); NS = not significant.

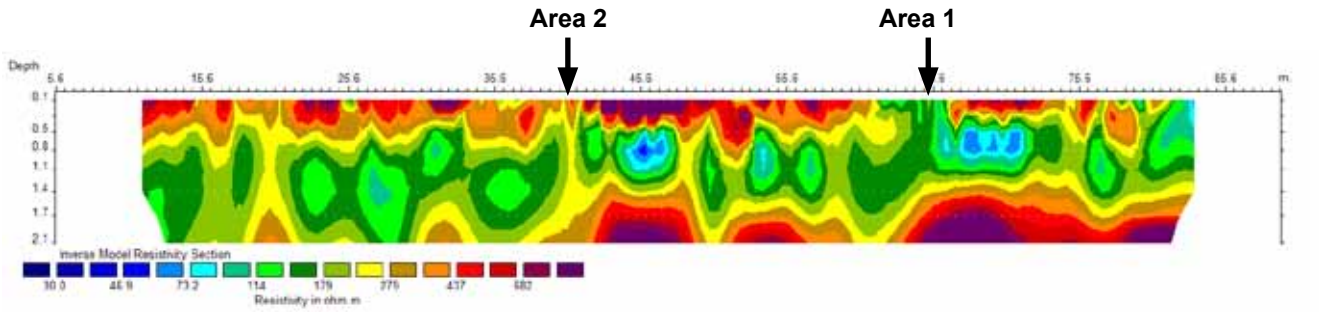

Figure 3.15. Example 2D electrical resistivity tomography (ERT) profile acquired using a Geometrics Ohmmapper, a capacitively coupled resistivity (CR) system.

of the compacted headland (Area 1). An example of an inverted 2D Electrical Resistivity Tomography (ERT) profile acquired using the capacitively coupled Geometrics Ohmmapper is shown in Fig. 3.15 with the location of Area 1 and Area 2 highlighted.

3.2 Wastewater Contamination

3.2.1 Site D

3.2.1.1 Subsurface contaminant concentrations at Site D

For this site, high concentrations of both EC and Cl^- were recorded at Sites D and F in monitoring wells D3 and D4 (Figs 3.16 and 3.17), nearest to the treatment system (22 m south-east) and adjacent to the percolation area (McCarthy et al., 2010). Samples taken from the other monitoring wells at the site, which were located at least 56 m from the system, with the exception of D9, resulted in significantly lower concentrations of these parameters. At D9, elevated concentrations of indicator parameters, including Cl^- were consistently recorded relative to the piezometers directly up-gradient (D7 and D8, Fig. 3.17), indicating the possibility of an alternative effluent plume pathway, facilitated by the presence of the drainage pipe, as discussed above. The existence of this pipe possibly provides an alternative route for effluent to flow, and may divert the subsurface flow around D7 and D8 towards D9 and consequently could account for the observed patters of contaminant movement at this site. Based on this scenario, interactions between the soil surface and contaminants may be limited in the vicinity of this drain, consequently reducing the capacity for effluent attenuation. It should be pointed out that background concentrations of indicator contaminants of effluent pollution showed low levels of most indicator parameters at all sites (McCarthy et al., 2010).

Solute flux calculations for Cl^- suggest a loss of Cl^- from the plume with increasing distance from the source, suggesting that this loss of contamination occurred to the underlying material. Consistent concentrations observed from subsurface water samples extracted from piezometers down-gradient of the system at these sites suggest that effluent had been entering groundwater at a constant rate over the duration of the monitoring period and had reached an invariant or steady-state configuration (McCarthy et al., 2010).

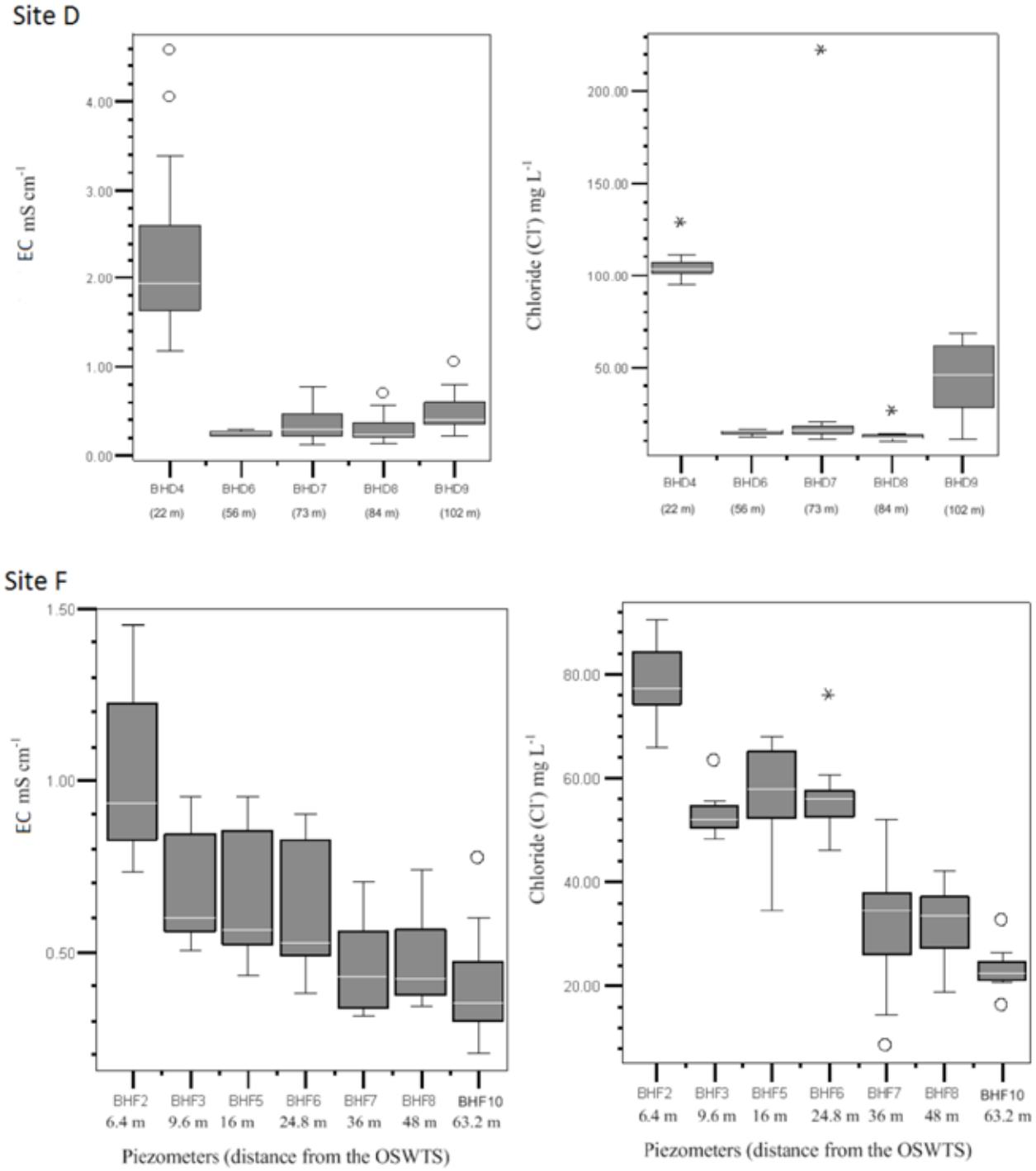

Figure 3.16. Distribution of conductivity and chloride (Cl-) concentrations, Site D August 2008–August 2009, showing the median, 75th and 25th percentile, whiskers delineate the data value less than or equal to 1.5 times the inter-quartile range outside the quartile. * = extreme value, o = outlier data value less than or equal to 3 times and greater than 1.5 times the inter-quartile range outside the quartile (from McCarthy et al., 2010).

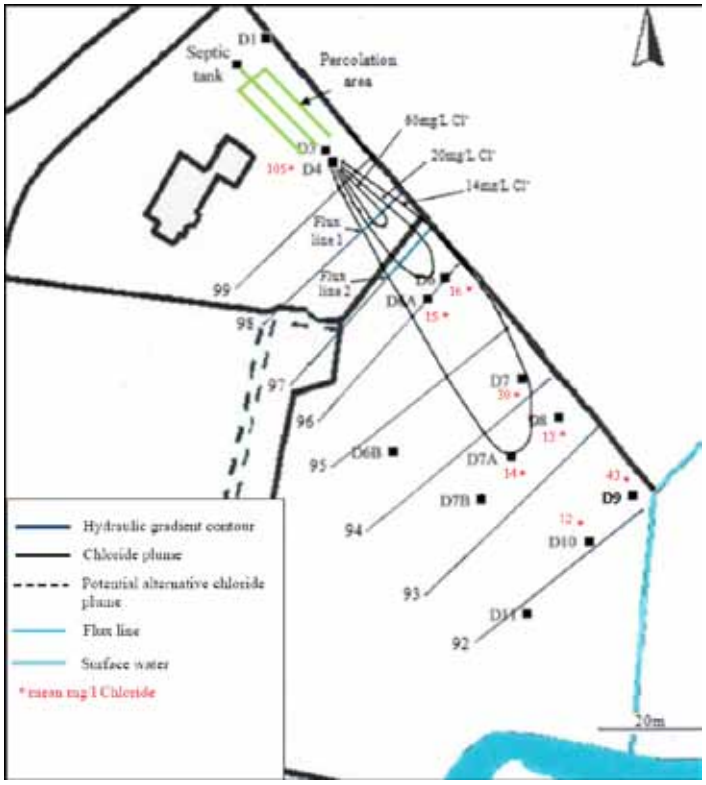

Figure 3.17. Site D chloride (Cl-) concentration distribution map showing the Cl- plume in subsurface water in glacial till and subsoil and flux lines. Mean Cl- concentrations calculated from the sampling period August 2008–August 2009 (from McCarthy et al., 2010).

3.2.1.2 Electrical resistivity tomography

Each of the 2D inverted ERT profiles has been combined into a quasi-3D fence diagram in Fig. 3.18, in order to provide an indication of the 3D distribution of resistivity for the site. For orientation purposes, each of the monitoring well locations, in addition to the treatment system location, are highlighted on this figure.

A large contrast in resistivity may be observed, at depths greater than 2 m depth between the north-west and south-east areas of the site. Geological maps suggest a contact between two rock units, Ordovician shale and Silurian sandstone and greywacke in the vicinity of the site, which could explain this electrical contrast. As mentioned in Section 3.2.1 above, the shales are recorded as being occasionally pyritic, which could explain the extremely low resistivities (<10 Ωm) measured throughout most of the site. It is likely that the overlying high resistivity material relates to the highly weathered fissile shale, observed during pits dug at the site. In the north-western part of the site, significantly higher resistivities were measured at depths greater than 2 m (>400 Ωm), confirming the location of the geological contact between the Ordovician shales and the Silurian sandstone/greywacke. The high resistivity values measured are typical for these materials.

The effluent plume was detected in the vicinity of piezometers D3 and D4 and is indicated on Fig. 3.18 as a zone of lower resistivity relative to the surrounding material (40–110 Ωm). As is to be expected, with increasing distance from the treatment system the resistivity increases considerably, with no sign of the plume present at piezometer D6. This is consistent with the direct measurements of contaminants in water samples, discussed above and illustrated in Figs 3.16 and 3.17, where high concentrations of both EC and Cl^- were detected at piezometers D3 and D4 and significantly lower concentrations were measured in piezometers D6, D7 and D8. Interestingly, the inverted resistivity in the vicinity of D9, between 0 and 2 m depth, is again low relative to the surrounding material. This compares favourably with the measurements of EC and Cl^- on water samples from this piezometer, which, as discussed above, were high relative to measurements of these parameters in the piezometers up gradient.

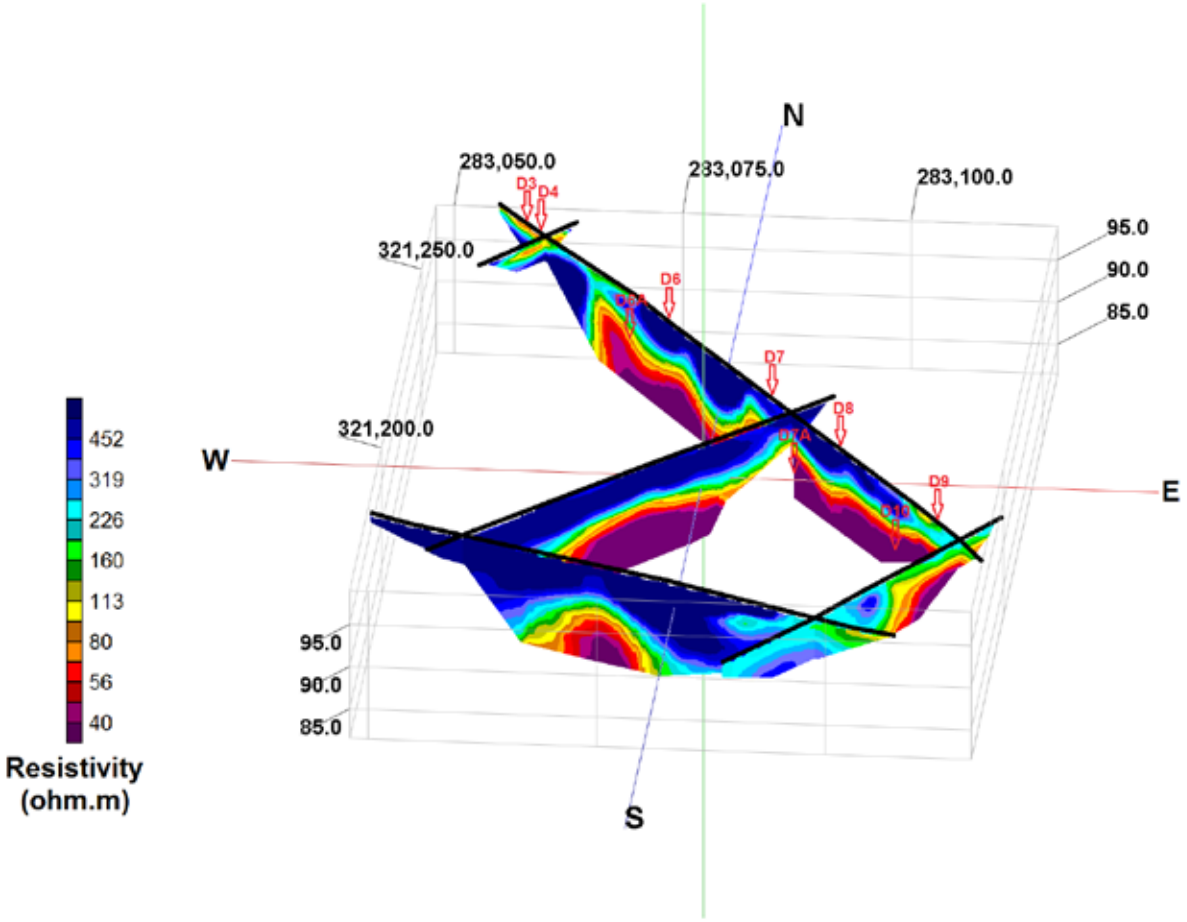

Figure 3.18. Fence diagram of Electrical Resistivity Tomography (ERT) profiles, with piezometer locations indicated by red arrows.

Although there is not enough piezometer data in the vicinity of the plume to compare the resistivity measurements with the direct contaminant measures statistically, it does appear that in this instance the ERT method is sensitive to the Cl^- plume at a concentration greater than approximately 30–40 mgL^{-1}. Chloride concentrations less than this, as measured at D6, D7 and D8, appear to have had little or no effect on the resistivity measurements.

Although in this instance it appears that the plume has been detected quite clearly, it should be pointed out that the measured plume resistivity values are not particularly low, and that the measured range of 40–110 Ωm is not dissimilar from a number of geological materials, including glacial till, where resistivities in the range 50–150 Ωm are usually observed in Ireland.

3.2.1.3 Seismic refraction

The purpose of carrying out seismic refraction at this site was to both improve understanding of the geological stratigraphy and to determine the location of possible contaminant pathways in the subsurface. Interpreted seismic refraction layered models for profiles S1, S2, S3, S4 and S5 are overlain on the relevant 2D ERT profiles in Fig. 3.19 for comparison.

Three layers were detected in all profiles. The shallowest layer (Layer 1) represents an upper topsoil layer between 0.75 and 1 m thick with a highly variable measured P-wave velocity of between 90 and 400 m/s. The resistivity values measured for this layer are high, usually in excess of 200 Ωm (except for the contaminated area near the treatment system and close to the stream near piezometer D9). When the two geophysical datasets are jointly interpreted, the low velocities and high resistivities suggest that this layer is unsaturated.

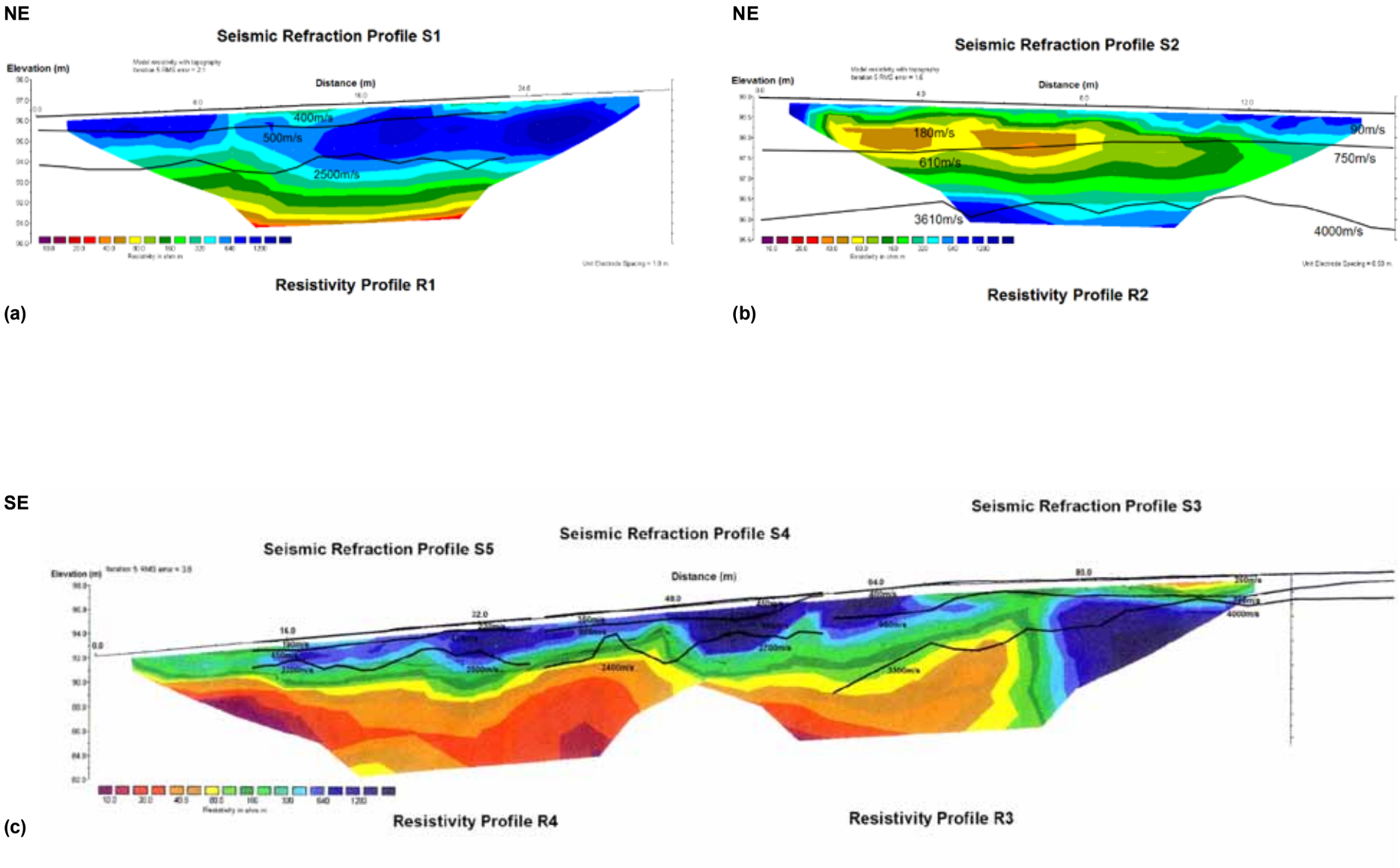

Figure 3.19. Seismic refraction profiles overlain on Electrical Resistivity Tomography (ERT) T profiles.

The underlying Layer 2 represents the subsoil, which appears to be 1.5–2.5m thick. The P-wave velocity of this layer varies between 450 and 950 m/s, again suggesting that this material was largely unsaturated when tested. This layer appears to be thinner in both the north-west and the south-east areas of the site (Fig. 3.19c) and thicker (up to 6 m) in the central portion of the site, at the south-eastern part of seismic refraction profile S3. This layer for the most part appears to correspond to the high-resistivity zone, observed to a depth of around 3 m.

Although the low velocities could possibly indicate that this material is firm glacial till (Long et al., 2012), the high resistivities measured would suggest that this is not the case. Joint interpretation of the ERT and seismic refraction datasets suggest that this material corresponds to the highly weathered bedrock that was observed during trial pitting at the site. This interpretation is supported by the observation made during the initial site characterisation, where the overall site was observed to be dominated by bedrock within 3 m of the surface and is, therefore, be considered to be of 'extreme' groundwater vulnerability. Infiltration to the groundwater table and lateral flow across and through a relatively permeable uppermost bedrock surface dominates over overland flow at this site (McCarthy et al., 2010). This layer represents a potential pathway for wastewater to travel, possibly at the interface between Layers 2 and 3 (i.e. between the weathered and competent material), which may have been too deep for detecting significant contaminants in the piezometers water samples.

Although the P-wave velocities of the upper two layers do not vary consistently across the site, the velocity of Layer 3 is considerably higher in the north-west (Fig. 3.19c). The velocities measured in this area are up to 4000 m/s, indicating highly competent bedrock, compared to the velocities to the south-east which vary between 2200 and 2500 m/s. The lower velocities measured in this area are typical of shale, and correlate well to the region of very low resistivity, observed above. By contrast, the high velocities measured in the north-west, which correspond to high resistivity values, are typical of greywacke, as indicated on the geological map of the region.

3.2.2 Site F

3.2.2.1 Subsurface contaminant concentrations at Site F

As with site D, high concentrations of both EC and Cl^- were recorded at Site F in monitoring wells nearest to the treatment system (Figs 3.16 and 3.20). In this case, as no percolation area was present measurements were acquired much closer to the septic tank and associated soakaway system. As shown in Fig. 3.16, a gradual decline in EC and Cl^- with distance from the tank was measured at this site.

Solute flux calculations for Cl^- again suggest a loss of Cl^- from the plume with increasing distance from the source, suggesting that this loss of contamination occurs to the underlying bedrock (McCarthy et al., 2010). Consistent concentrations observed from subsurface water samples extracted from piezometers down-gradient of the system at these sites suggest that effluent has also been entering groundwater at a constant rate over the duration of the monitoring period and has reached an invariant or steady-state configuration (McCarthy et al., 2010).

As was pointed out above, at this site an outhouse used to house animals and a slatted tank were located up-gradient of the tank on its western side. In addition, a portion of the greywater at this site (perhaps arising from the washing machine or relatively recently installed dishwasher) was being piped separately to a nearby ditch running along the eastern side of the site. As such, this site had potential alternative sources of contamination that may have confused data relating to the effluent plume.

3.2.2.2 Electromagnetics (EM-31)

Figure 3.21 presents EM survey results using a horizontal magnetic dipole for the quadrature component of the EM field. This approach normally provides a measurement of conductivity within 3 m of the surface. Although both vertical and horizontal orientations were trialled, this orientation was preferred as it was thought that any contamination relating to the septic tank in the glacial till would lie within this depth range. As shown on Fig. 3.21, measurements acquired within 10 m of the farm buildings in the north of the site generated high conductivity anomalies. High conductivities were also measured in the eastern part of the site, and not in the vicinity of the septic tank. This high conductivity anomaly is possibly related to contamination from a slatted

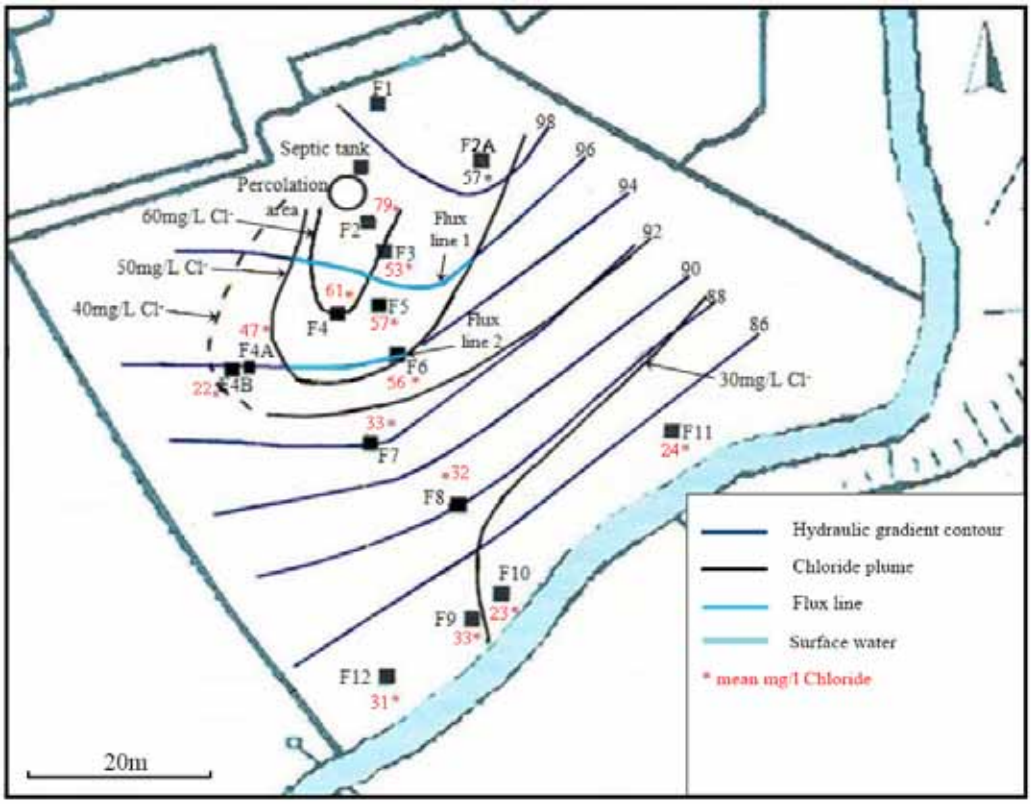

Figure 3.20. Site F chloride (Cl-) concentration distribution map showing the Cl- plume in subsurface water in glacial till and subsoil and flux lines. Mean Cl- concentrations calculated from the sampling period August 2008–August 2009 (from McCarthy et al., 2010).

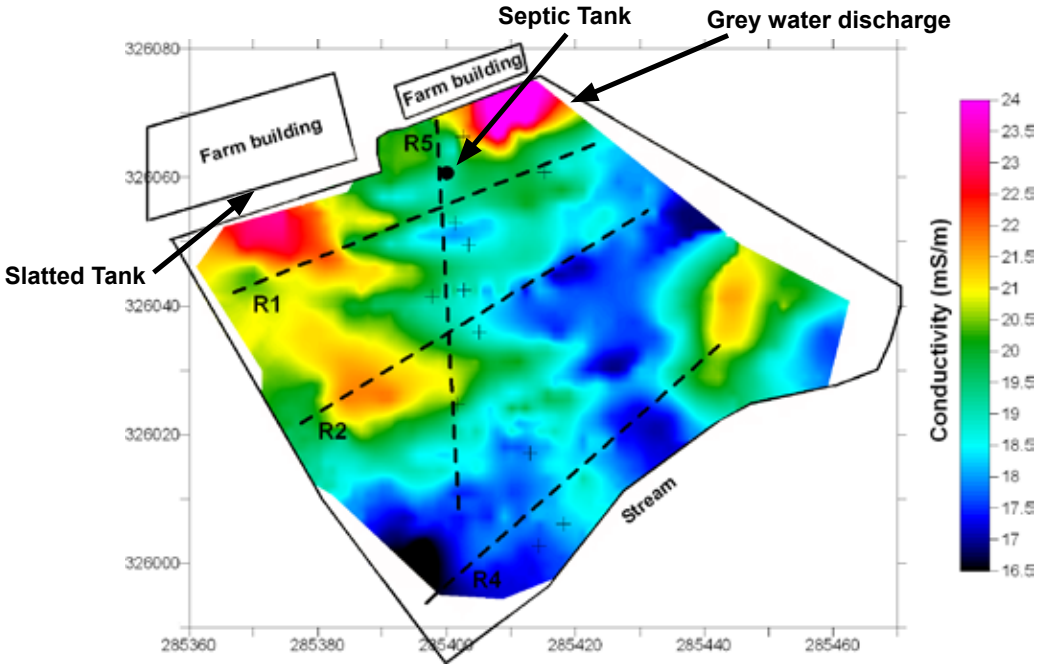

Figure 3.21. EM-31 survey results along with the corresponding locations of Electrical Resistivity Tomography (ERT) profile lines for Site F.

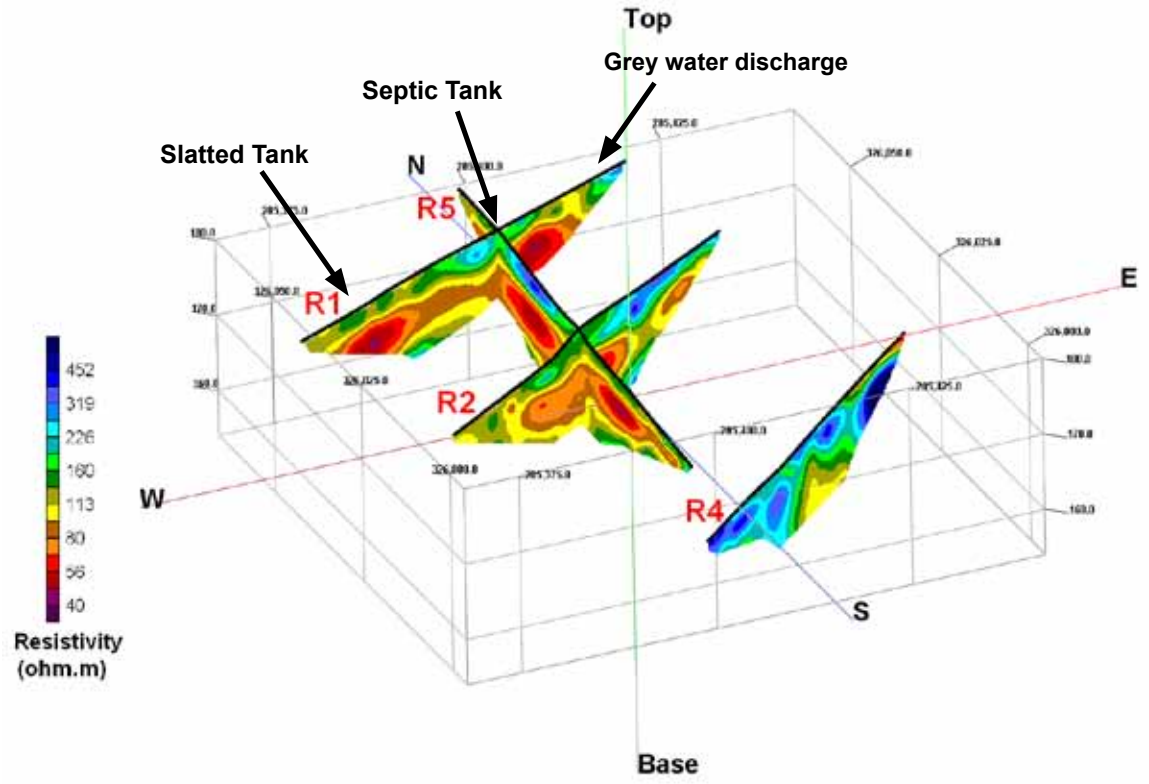

Figure 3.22. Fence diagram, combining Electrical Resistivity Tomography (ERT) Profiles R1, R2, R4 and R5.

tank, located as illustrated on Fig. 3.21. This anomaly exhibits considerably higher conductivity values than that measured in the vicinity of the septic tank. Although the values measured are above background levels, the lack of a high conductivity anomaly relating to the septic tank was surprising as the intensive water-quality monitoring had suggested that septic tank effluent had affected groundwater.

3.2.2.3 Electrical Resistivity Tomography

The 2D ERT profiles were combined using into a quasi-3D fence diagram in Fig. 3.22, in order to provide an indication of the 3D distribution of resistivity for the site. These profiles identified a number of distinctive low resistivity (20–50 Ωm) anomalies at depths of between 3 and 7 m (Fig. 3.22), which are likely to be due to contamination. As discussed above, the resistivity of Irish glacial till is usually greater than this and generally exceeds 50 Ωm (Long et al., 2012). The two distinctive low-resistivity features observed in the east and west of ERT Profile R1 are likely caused by contamination from the septic tank and the slatted tank respectively. The grey water pipe discharge to a ditch to the north-east of the site could also be having an effect on the measured resistivity values. The low resistivity anomalies appear to extend down slope towards the stream, following the septic tank effluent contaminant plume profile generated by Orr (2009). This latter study also demonstrated the hydraulic conductivity of the glacial till deposits to range from $1.1x10^{-3}$ cm/s to $1.1x10^{-6}$ cm/s. The hydraulic conductivity data, when considered with the age of the OSWTS (20–30 years old), and the prevailing hydraulic gradient suggest that the septic tank plume should be less extensive than that measured by both the water-quality monitoring and the ERT profiles.

3.2.2.4 Seismic refraction

Interpreted seismic refraction layered models for profiles S1 and S2 are overlain on ERT Profile R5 in Fig. 3.23 for comparison. The P-wave velocity and layer thickness data indicated in this figure is very consistent across all seismic profiles acquired at the site. As shown, three layers were detected. The shallowest layer (Layer 1) represents an upper topsoil layer between 0.75 and 1.1 m thick with a variable P-wave velocity of between 100 and 500 m/s measured across the site. The resistivity values measured for this layer are relatively high, usually in excess of 110 Ωm (except for the contaminated area near the treatment system, Fig. 3.23). When the two geophysical datasets are jointly interpreted, the low-velocity and high-resistivity values measured suggest that this layer is unsaturated.

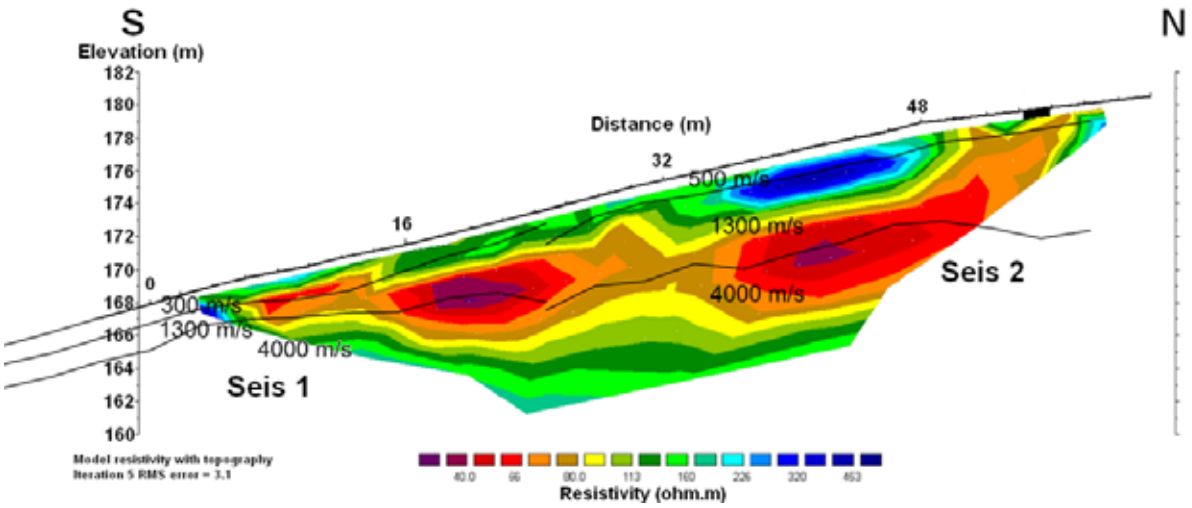

Figure 3.23. Interpreted P-wave velocity refraction models overlain on Electrical Resistivity Tomography (ERT) Profile R5.

The underlying Layer 2 represents the subsoil, which in this case appears to be 2–5 m thick. The P-wave velocity of this layer varies between 1200 and 1500 m/s. This layer varies in thickness from the north to the south of the site, being up to 6 m thick in the upgradient northern area of the site, near the septic tank and reducing to less than 2 m thick in the southern area. Trial pitting at the site confirmed this material to be glacial till. Although the measured P-wave velocities are in the low range for glacial till, values such as these are not uncommon in drumlinised areas of Ireland.

The velocity of the deepest layer (Layer 3) varies between 3500 m/s and 4100 m/s across the site, indicating competent bedrock. These values are consistent with the bedrock type revealed in the geological maps, which indicates that bedrock in the area is dominated by sandstone and microconglomerate. The resistivity values measured for this material are lower than would be expected for this rock type, which may indicate weathering of the bedrock surface and/or contamination of this layer resulting from effluent discharging from the potential sources outlined in this project.

Joint interpretation of the geophysical and piezometric data suggests that although the hydraulic conductivity of the glacial till layer was low, the upper bedrock surface was weathered/fractured; falling head piezometer tests suggested a higher hydraulic conductivity in this unit than the subsoil. This is corroborated by steep downward vertical hydraulic gradients observed in piezometer nests screened at the water table and at the base of the till, indicative of a more hydraulically conductive unit at depth. The combined geophysical and hydrogeological datasets suggest that a significant proportion of the septic tank effluent is being drawn downwards through the glacial till into the upper, more fractured zone of bedrock. This is consistent with the higher conductivities/lower resistivities observed on the ERT profiles, down-gradient of the septic tank system, close to the glacial till/rock interface (Figs 3.22 and 3.23). Given the suspected higher hydraulic conductivity of the deeper (top of bedrock) unit, and an anticipated lower effective porosity, this finding suggests that septic tank effluent may be transported more rapidly to surface water receptors through the subsurface than originally anticipated.

3.2.3 Site S

3.2.3.1 Subsurface contaminant concentrations at Site S

As previously noted, contaminant distribution at this site may have been complicated by the presence of high levels of a salt tracer (NaCl), injected prior to the start of the current project. Elevated levels were detected down-gradient of piezometer S5 to which the NaCl was added (Fig. 3.24). Significantly lower concentrations of all contaminants were measured on samples from the majority of other piezometers at this site (McCarthy et al., 2010), including those adjacent to the OSWTS: it is therefore probable that the plume shown here is related to the NaCl injection rather than because of any effluent emanating from the OSWTS.

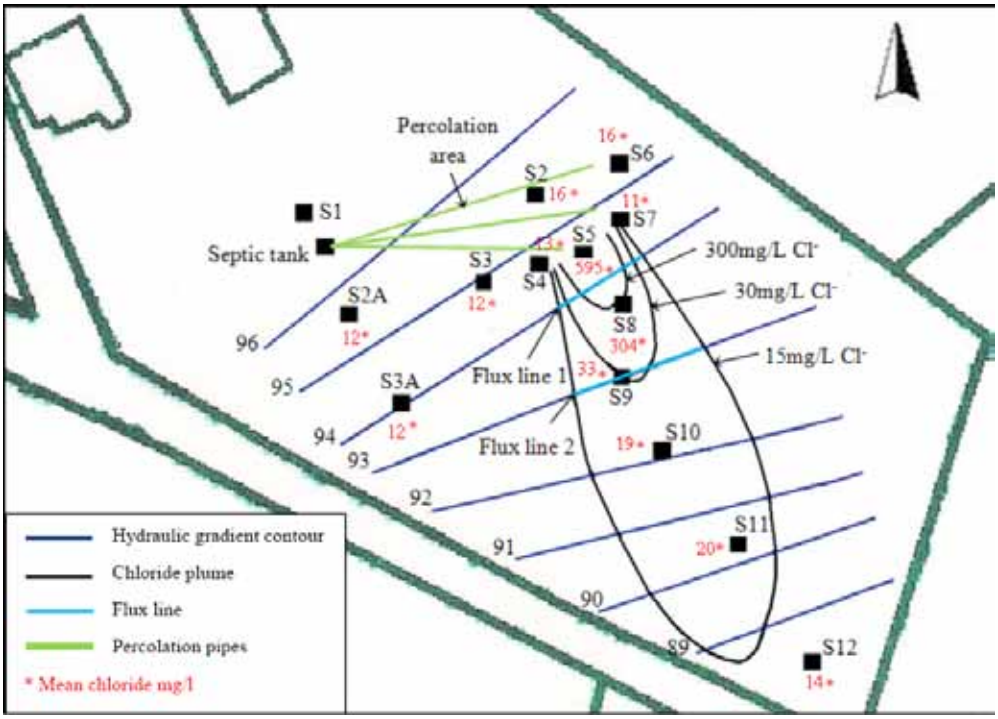

Figure 3.24. Site S chloride (Cl-) concentration distribution map showing the Cl- plume in subsurface water in glacial subsoil and flux lines (from McCarthy et al., 2010).

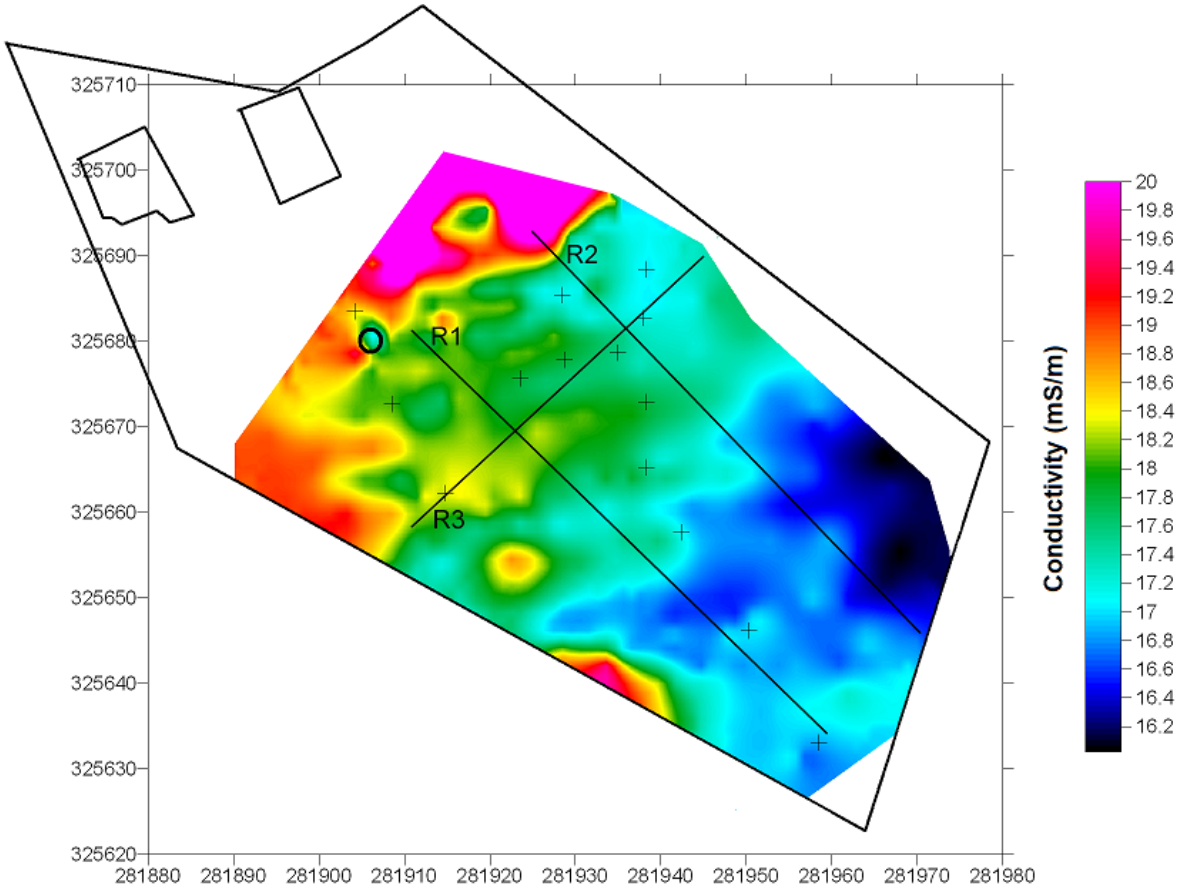

Figure 3.25. EM-31 survey results along with the corresponding locations of Electrical Resistivity Tomography (ERT) profile lines for Site S. Note the treatment system is indicated as a black circle.

3.2.3.2 Geophysical measurements at Site S

Significant issues were encountered at this site regarding the acquisition of geo-electrical and EM data. A considerable amount of electrical noise was observed on all three ERT datasets as well as on the EM ground conductivity profile. Electrical Resistivity Tomography profiles are not included here as the results were not considered reliable. Even after data despiking and filtering, inversion RMS errors were in excess of 25%. The presence of grounded wire fencing surrounding the site could have resulted in the electrical noise observed in the datasets.

Figure 3.25 presents EM survey results using a horizontal magnetic dipole for the quadrature component of the EM field. As shown, measurements acquired close to grounded wire fences in the north-west and south-east of the site resulted in high conductivity anomalies.

Although there is some indication of slightly elevated conductivity values in the vicinity of the treatment system and percolation area, particularly when compared to the relatively low conductivity area observed to the east, the dataset is not considered reliable enough to distinguish between such small conductivity variations. These slightly elevated conductivities are also not supported by any consistent evidence from the piezometer sampling. The lack of a high conductivity anomaly close to piezometers S5 and S8, where very high concentrations of Cl^- were measured, also suggests the data in this instance may not be fully reliable.

3.3 Failures in Irish Raised Bogs

3.3.1 Peat Thickness and Surface Morphology

The main objective of the Ground Penetrating Radar (GPR) work was to profile the sub-peat base and to relate this to the surface topography. The GPR trace may also show other structures within the peat mass, which may correspond to changes in degrees of humification, pockets of coarse fibres or wood fragments. At Carn Park, data was collected from across the southern

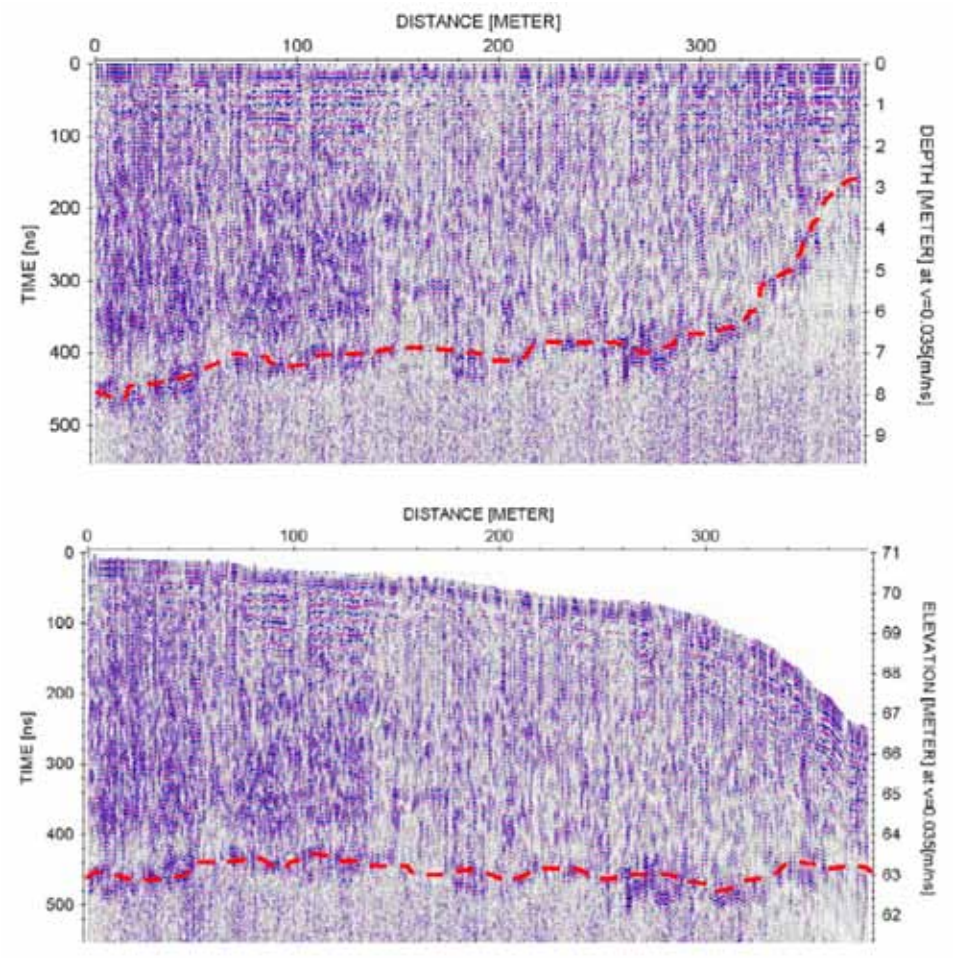

Figure 3.26. Ground Penetrating Radar (GPR) data following processing: (a) uncorrected for topography and (b) corrected for topography.

failed area as well as around its perimeter in order to assess the distribution of peat across the survey area. Figure 3.26 illustrates an example of processed GPR data from Carn Park before and after a topographic correction is applied. The base of the peat layer is highlighted by a dashed red line.

The data highlights the importance of applying a topographic correction as, following the correction, it appears the base of peat is relatively flat at around +63 mOD. The surface topography of the peat surface varies between +66 mOD and +72 mOD with the lowest point at the edge of the cut to the south-west of the survey area (Fig. 3.27). As discussed above, due to a problem with the RTK-DGS it was not possible to record data from the central area of the profile shown on Fig. 3.27. The slope of the bog surface behind the southern failed area is about 0.7°. Overall peat thickness was found to vary from approximately 2.5 m to 8 m.

Similarly, for the Aghnamona site the base of the peat was shown to be relatively flat, with a base elevation between +40 mOD and +41 mOD (Fig. 3.28b). The surface topography shows a pronounced lower level area, near to +44.5 mOD, in the failed zone. Behind the failed area the surface of the bog rises gradually to an elevation of +48 mOD at a slope of about 1°. These two sets of data can be combined to produce the plot of peat thickness shown on Fig. 3.28a and the 3D plot of surface and peat base topography on Fig. 3.28b. Peat thickness varies between about 4 m close to the edge of the bog and 7 m towards the centre. The relatively low thickness of peat layer closer to the margins of the bog has been observed on other feasibility study sites during this work, such as at Clara bog, Co. Offaly, and it likely a legacy of drainage of the bog and volume reduction resulting from peat-cutting activities at the margins which have now ceased. For both sites the GPR data shows a clear thinning of the peat in the area of the failures. In both cases the peat base topography is relatively flat and does not follow the much more pronounced variation in topography, mapped at the surface. This indicates that the observed surface movement has come from within the peat, rather than from the underlying material.

In addition to indicating peat thickness, the ERT data also provides information on the underlying materials. Figures 3.29a and 3.29b show the ERT profiles running perpendicular to the failures for both Carn Park and Aghnamona respectively. The relatively flat peat base profile is clear for both sites. For Carn Park the peat appears to be underlain by low-resistivity material which is consistent with the presence of limestone till indicated on the GSI soils maps (www.gsi.ie). Argillaceous limestone bedrock is also resolved below the till again as expected from the geological maps of the area. At Aghnamona, beneath the peat is a till

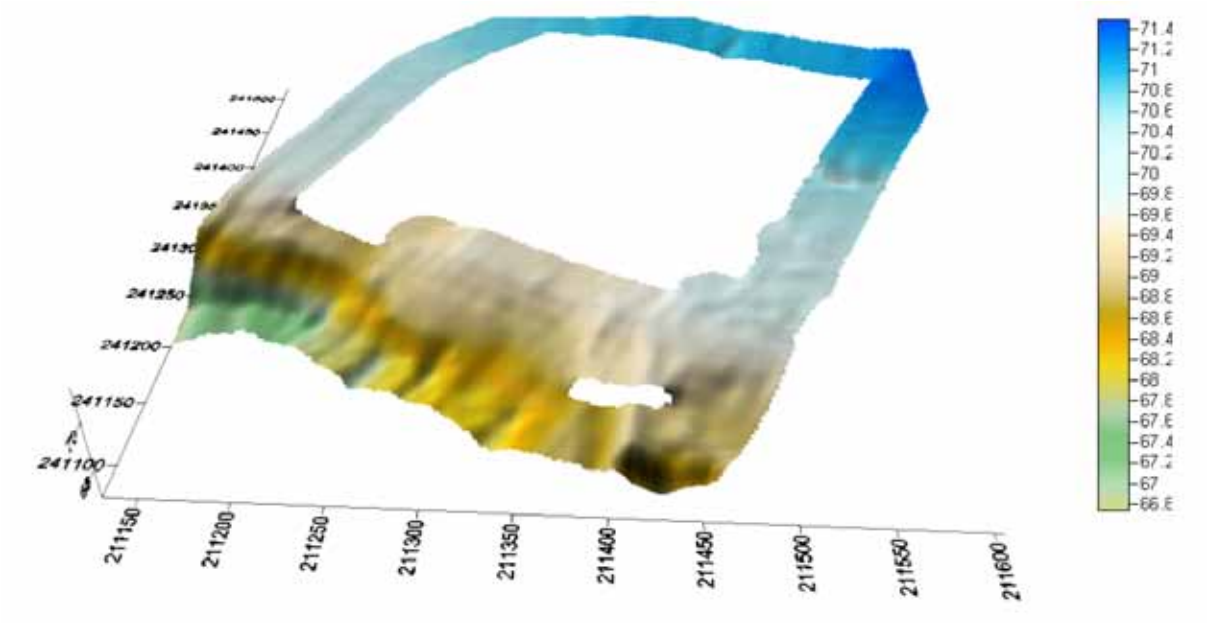

Figure 3.27. Surface topography for Carn Park, around the failed area.

mostly derived from sandstone bedrock which in turn overlies Waulsortian reef limestone, as expected from the geological records. For both sites, the resistivity is seen to increase with distance into the bog. This finding will be explored in conjunction with a study of the water content of the peat below.

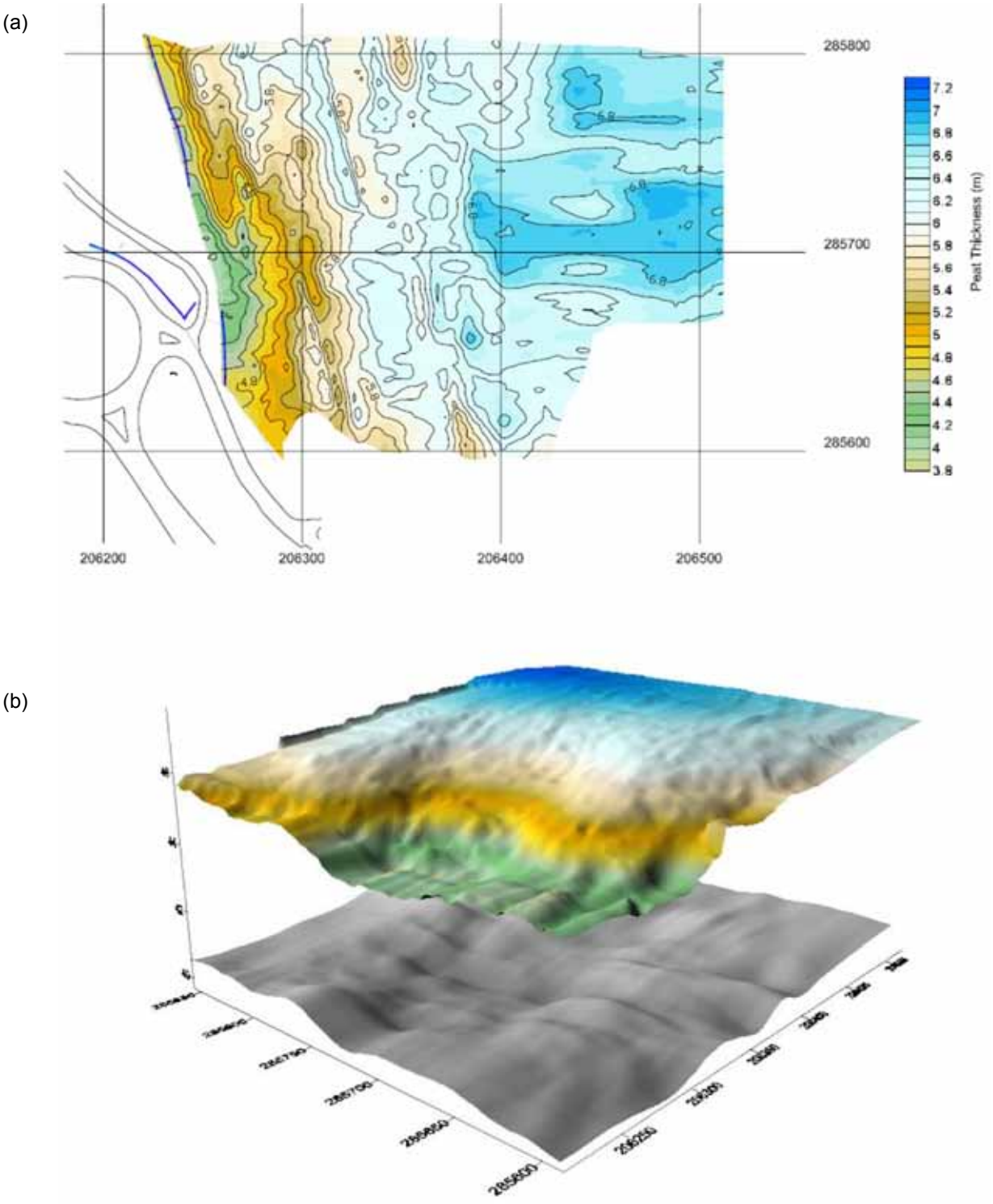

Figure 3.28. (a) Peat thickness and (b) 3D plot of surface and peat base topography for Aghnamona bog, Roosky. (East and north co-ordinates and elevation are given in m.)

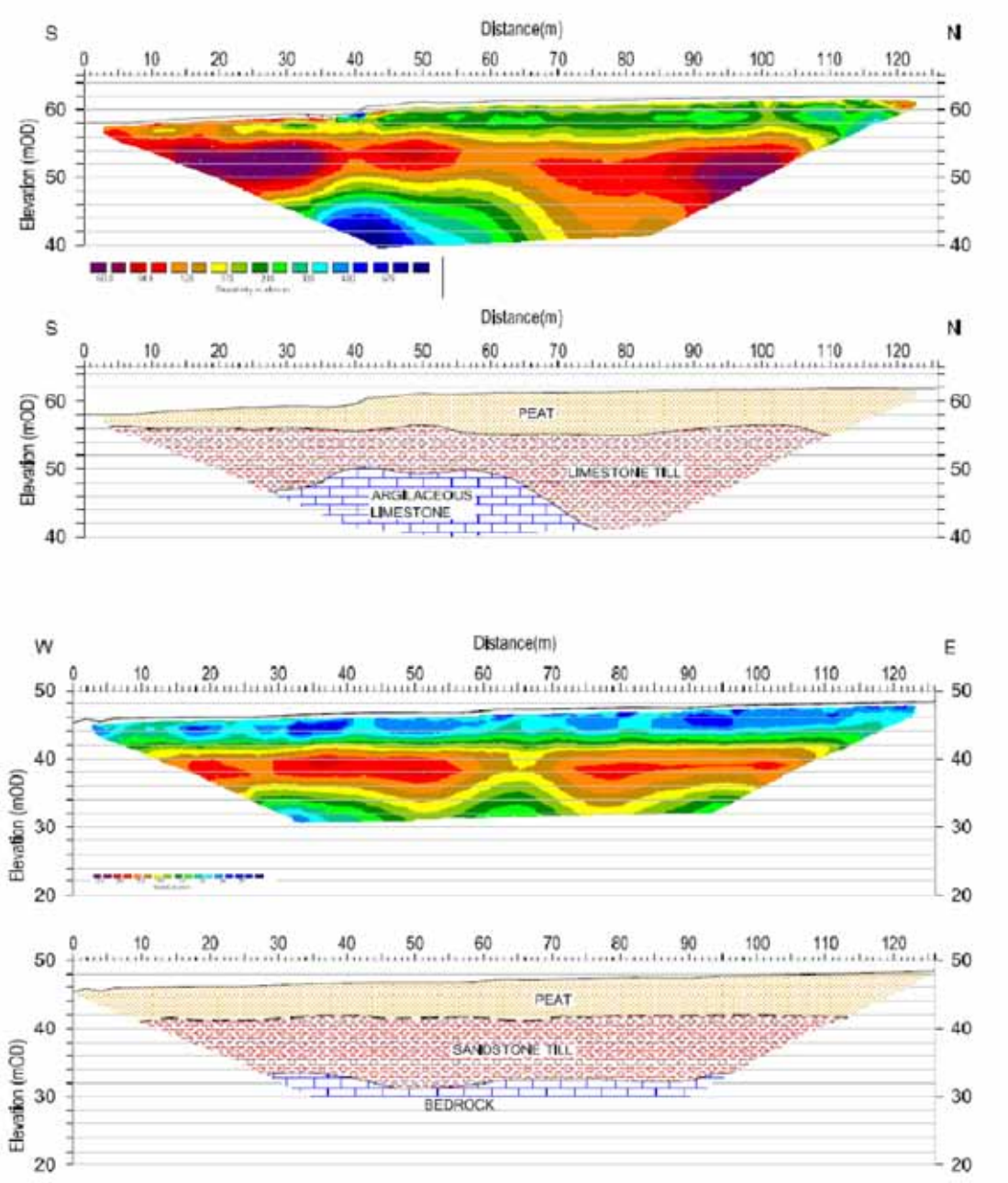

Figure 3.29. Electrical resistivity tomography (ERT) profiles through the failed areas; (a) Carn Park – Profile R2 and (b) Rooskey – Profile R2.

3.3.2 Description and Classification of Peat

A comparison between the von Post and Granlund (1926) peat probe logs from both sites from location P1 is shown on Fig. 3.30. From an engineering point of view, the peat at both sites can be described as a relatively uniform, very soft, light brown fibrous peat (BSI, 2006). The Aghnamona peat appears to be slightly more decomposed with H = 6 near the surface compared to H = 4 for Carn Park. At both sites the degree of decomposition decreases slightly with depth. The Carn Park peat has a greater portion of fine fibres and wood fragments but the coarse fibre content is greater for Aghnamona.

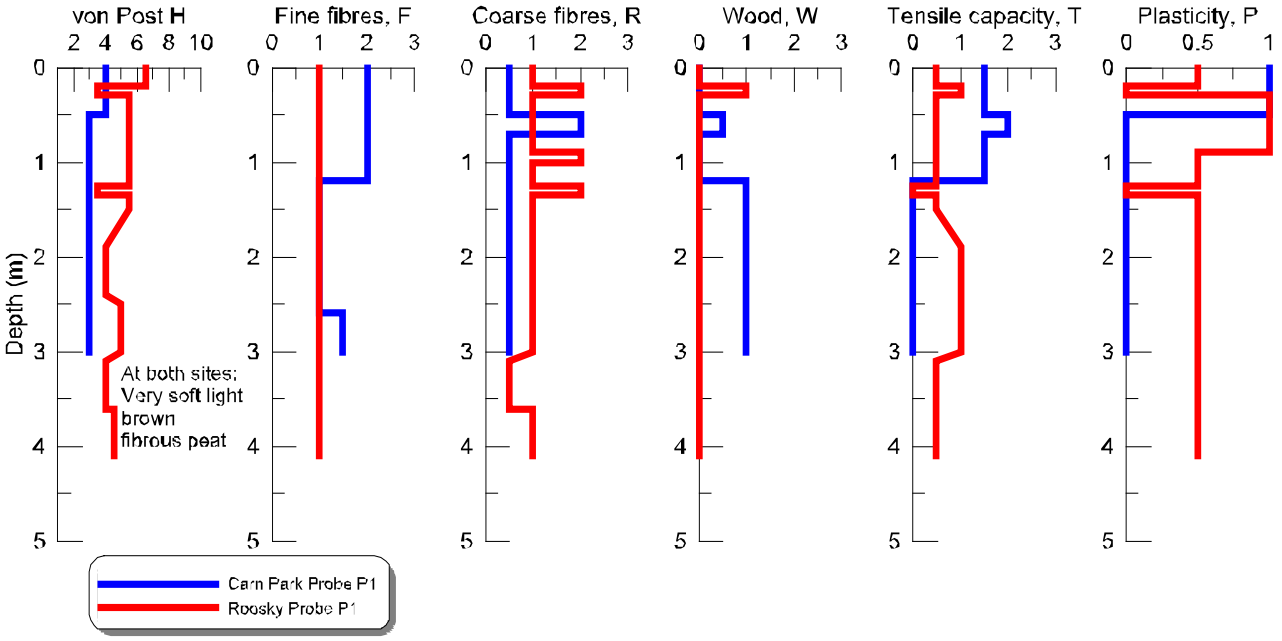

Figure 3.30. Von Post and Granlund (1926) peat logs (H=degree of humification: 1–10; F = fines fibres: 0–3; R = coarse fibres: 0–3; W = wood: 0–3; T = tensile strength: 0–3; P = plastic: 0 or 1).

3.3.3 Basic Index Data

A summary of water content, bulk density and loss on ignition values against depth for both sites are given in Fig. 3.31. In general, the water content of the Aghnamona peat is greater than that of Carn Park, corresponding to the greater degree of decomposition of the Aghnamona peat. At Carn Park water content decreases from about 1200% at 0.5 m towards 750% at 3 m. There is no difference between values taken from the southern and northern failed areas. For Aghnamona the values are relatively constant, with an average of about 1250%. For both sites, most of the data corresponds to tests taken near the failure edge or scarp. It can be seen that tests from Probes P1 at both sites show higher water contents than the rest of the data. These probes were located away from the failed face. This finding is explored in more detail below.

For both sites, bulk density values are similar and average about 1.05 Mg/m^3, which is typical for Irish peat. Loss on ignition values are high and are on average about 98%, confirming the almost complete organic nature of the material.

A series of additional samples were taken using the Russian sampler within the failure zone running perpendicular to the face along the line of ERT profile R2, at both sites. These samples were taken at depths of approximately 1.0 m and 1.5 m at Carn Park and at 0.75 m and 1.5 m at Aghnamona (see Fig. 3.32a and 3.32b), respectively. A very significant reduction in water content of the peat toward the face of the failure for both sites and for both test depths is very evident. At Carn Park the reduction in water content towards the face is more significant than that at Aghnamona, due to the older age of the failure. The greater degree of drainage and consolidation that has occurred has meant that the water content values do not become uniform until about 100 m from the face. At Aghnamona, the reduction in water content towards the face is clear but less substantial, and values appear to become uniform about 50 m from the front edge of the failure.

It is clear from Fig. 3.32 that the peat in the failed area has been drained and has suffered a reduction in water content. This reduction in water content has led to loss of volume and resulted in surface settlement of the peat, and is consistent with the findings of the GPR and ERT surveys described above.

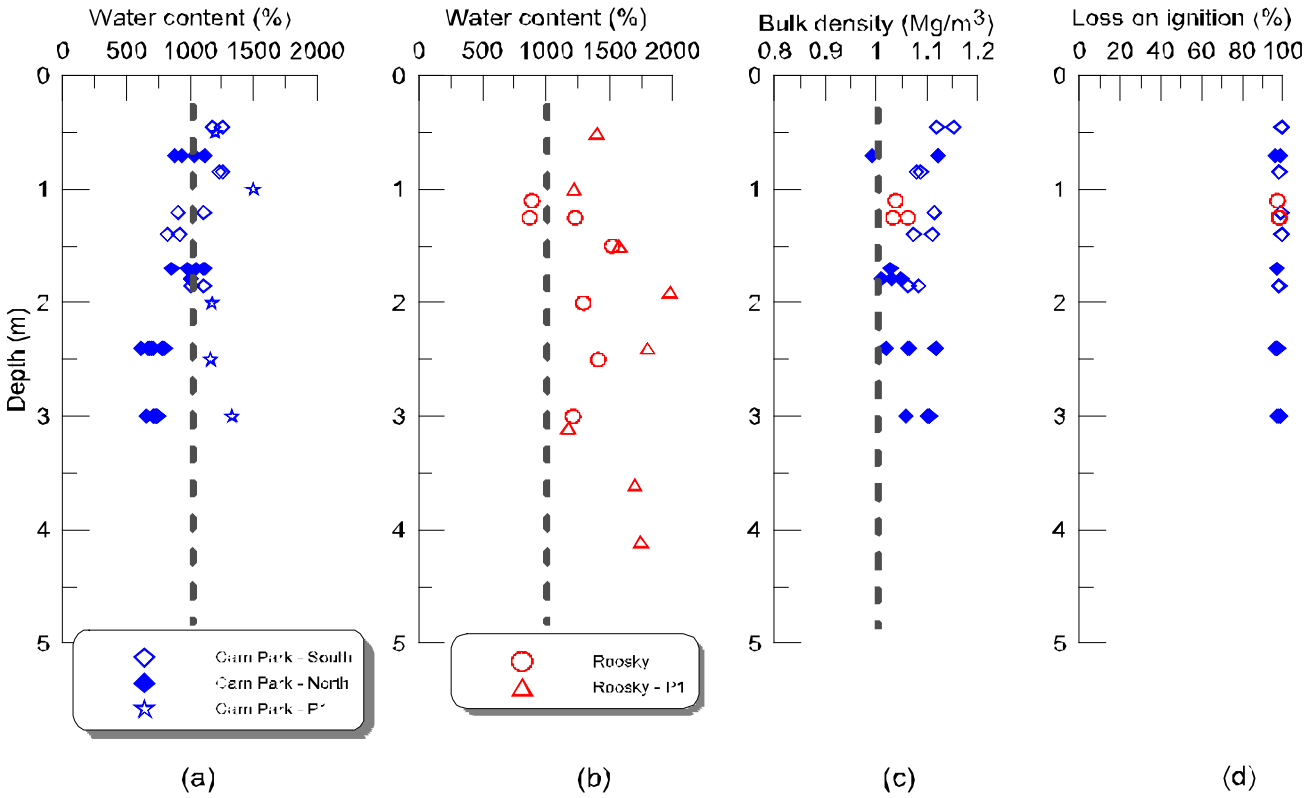

Figure 3.31. Basic characteristics of Carn Park and Aghnamona peat: (a) Carn Park water content, (b) Aghnamona water content, (c) bulk density both sites and (c) loss on ignition at 440°C both sites.

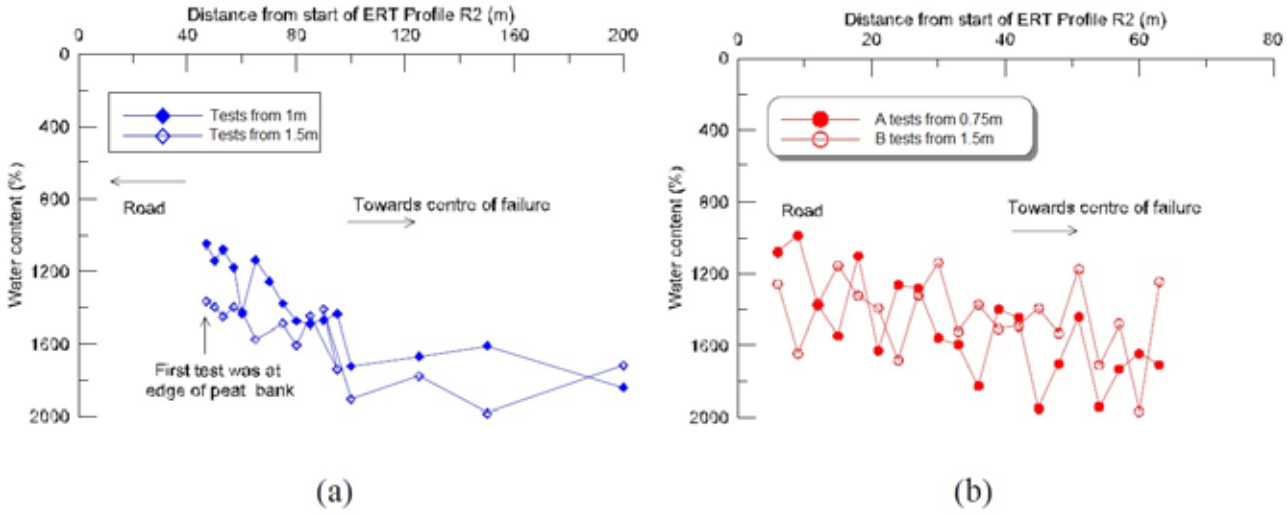

Figure 3.32. Longitudinal profiles of water content (a) Carn Park and (b) Aghnamona.

3.3.4 *Resistivity and Water Content*

The decreasing water content of the peat towards the edge of the failure corresponds to a very similar reduction in resistivity, as can be seen on Fig. 3.33, for the Aghnamona site. Water within the peat is relatively resistive, and reducing its content reduces the measured resistivity of the peat. This finding is similar to that of other researchers. For example, Ponziani et al. (2011) suggested that the water content of the peat may be estimated from the electrical conductivity, provided the electrical conductivity of the pore fluid is known.

3.3.5 *Compression and Consolidation Parameters*

A summary of oedometer tests carried out on three samples from the southern failure area at Carn Park is given on Fig. 3.34. The specimens, which were 37.5 mm high, were all obtained from the same block and were cut so that consolidation was (a) in the vertical plane, (b) in the horizontal plane, perpendicular to the cracks and (c) in the horizontal plane, parallel to the cracks respectively. All three specimens show similar consolidation behaviour, as exhibited on the classical log σ_v' versus stain plot (Figure 3.34a), and indicate a highly compressible material. A feature of the behaviour is the relatively high permeability measured at, or around, the in-situ vertical effective stress (σ_{v0}') and the significant reduction in permeability observed with increasing stress. There is no clear anisotropy of permeability evident in the test results.

3.3.6 *Undrained Shear Strength of Peat*

Direct simple shear test (DSS) results are summarised in Fig. 3.35. Results are presented in the form of undrained shear strength (s_u) versus depth and normalised undrained shear strength (s_u/σ_v') versus depth. It can be seen that the results are similar for both sites with s_u increasing from about 6 kPa at the surface to 10 kPa towards the base of the peat. The normalised s_u/σ_v' values for Aghnamona and Carn Park south show a gradual reduction from about 0.8 at the surface to 0.4 with depth.

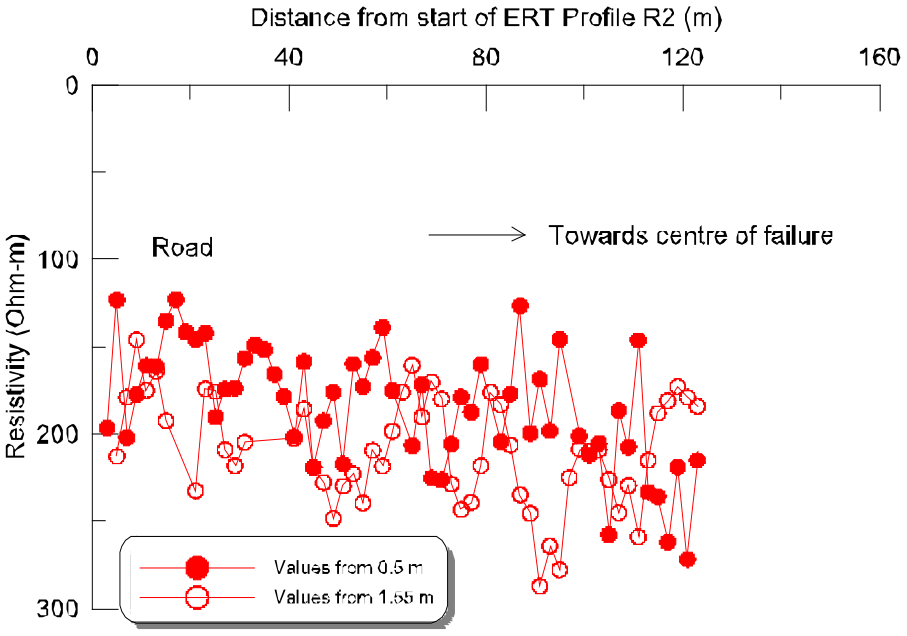

Figure 3.33. Longitudinal profile of resistivity for Aghnamona.

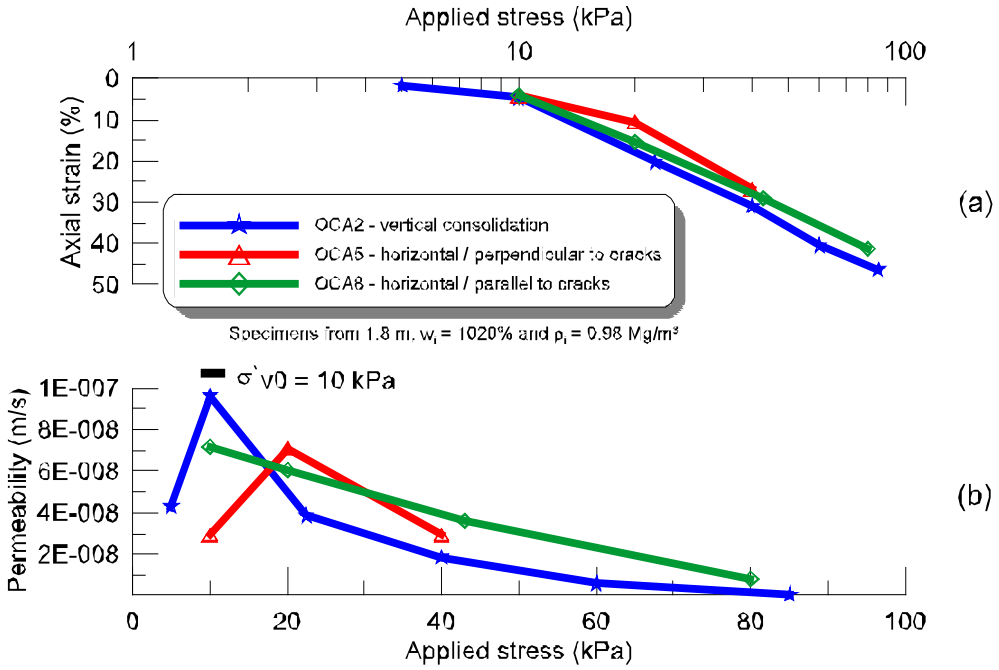

Figure 3.34. Summary of oedometer tests from Carn Park Southern area at 1.8 m (a) stress versus strain and (b) permeability versus strain.

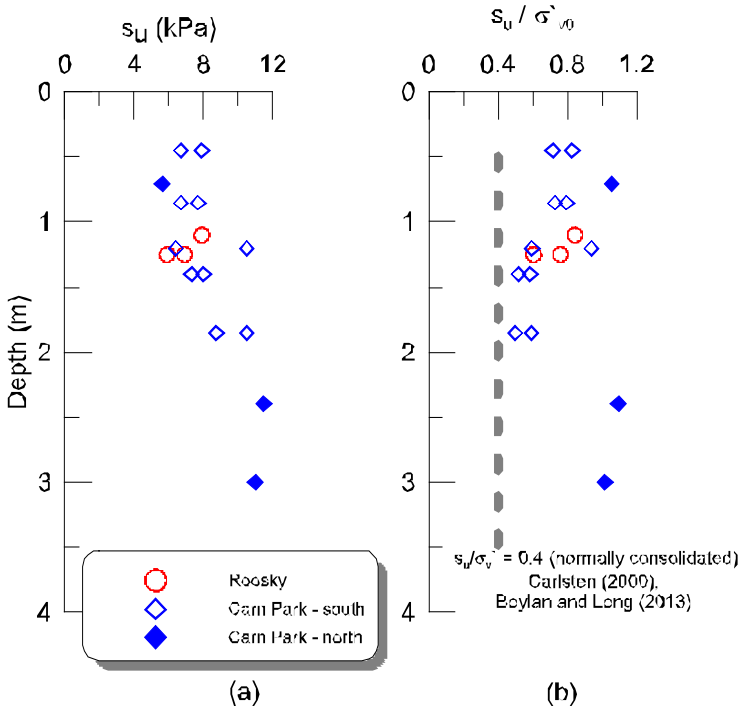

Figure 3.35. Undrained shear strength (s_u) from direct simple shear (DSS) tests (a) s_u with depth and (b) s_u/s'_{v0} with depth.

An s_u/σ_{v0}' value of 0.4 is consistent with the strength of peat in the normally consolidated condition as was shown by Carlsten (2000) for Swedish peat and Boylan and Long (2013) for Irish peat. The normally consolidated state of the Carn Park Southern peat below about 1.5 m is consistent with the data for the oedometer tests at

1.8 m, shown on Fig. 3.34. The peat at Carn Park north seems to be overconsolidated throughout its depth. This is likely to be due to the older age of the failure here and the greater amount of drainage and consolidation that has taken place.

3.3.7 Slope Stability Analyses

Three possible failure mechanisms could be considered to explain the observed phenomena as follows:

- Failure caused by applied shear stress exceeding the shear strength of the soils in the slope;
- Failure caused by water seepage;
- Failure caused by the influence of gas pressure.

3.3.7.1 Conventional slope stability analysis

In these analyses the disturbing force due to the weight of the soil mass are compared to the resistance provided by the shear strength of the soils in the slope using the principle of limit equilibrium. These conventional slope stability analyses were undertaken using the software OASYS – SLOPE (Version 19.0.1.5). SLOPE uses the generalised procedure of slices first introduced by Janbu (1957).

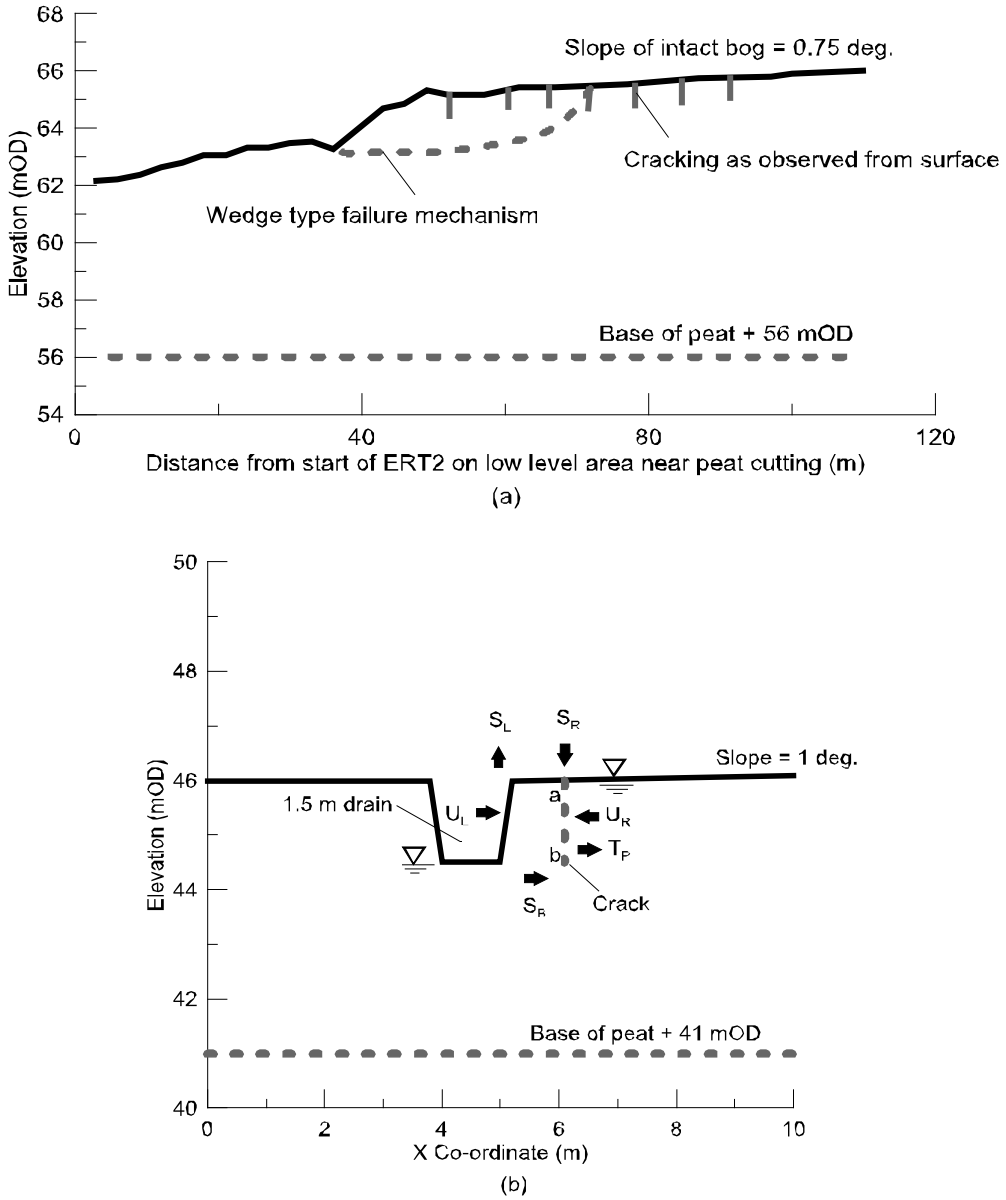

Figure 3.36. Stability analyses: (a) conventional slope stability analysis for Carn Park and (b) seepage analysis for Aghnamona.

ab respectively.

Figure 3.37. Failure of peat cliffs in Escuminac peat at Miramichi Bay, New Brunswick, Canada (Landva, 2009).

Various analyses were carried out, specifically using Janbu's method of variably inclined inter-slice forces, with the failed mass being sub-divided into 10 slices (Janbu, 1957). The example shown on Fig. 3.36a is for the southern failed area at Carn Park, where the surface slope is about 0.75° and the peat is some 9 m in thickness. Groundwater is assumed to be at the surface of the peat. The analyses assumed undrained conditions and that the unit weight and undrained shear strength of peat were taken as 10 kN/m^3 and 7 kPa respectively. Although various shapes of the failed mass were assumed in the calculations, including shallow and deep circular failures, the minimum factor of safety was obtained for the non-linear 'wedge' type failure shown on Fig. 3.36a. The calculated factor of safety for Carn Park was of the order of 8.0. (A similar result was obtained for Aghnamona.) If the undrained shear strength is reduced to 5 kPa the corresponding factor of safety reduces to about 6.0. These high calculated factors of safety for a conventional slope failure are not surprising given the very low slopes involved and the relatively high shear strength of the peat.

3.3.7.2 Seepage analysis

The observed water flow at the face of the failed areas together with the measured reduction in the water content of the peat towards the face suggest that seepage is occurring from the main body of the raised bog towards the edge. It is possible then that the seepage forces exerted by the flowing water are the cause of the observed cracks. The failures observed at Carn Park and Aghnamona are very similar in nature to those reported by Landva (1980) and Landva (2007) concerning the instability of some peat cliffs in Escuminac peat at Miramichi Bay in New Brunswick, Canada (see Fig. 3.37, Landva, 2009). These peat cliffs are about 6 km in length and up to 4.2 m high (Robichaud and Bégin, 2009). Similar to the observations at Carn Park and Aghnamona cracks were found to form a concentric semicircular pattern and existed at a distance of up to 40 m from the cliff face with the largest semicircles approaching 100 m in diameter. Landva (2007) suggested that an examination of the consistent crack pattern proved the key to understanding the failure. He pointed out that all of the cracks either extend to the shoreline or connect with other cracks which themselves eventually extend to the shoreline. He was then able to conclude that the fractures are tension cracks which develop progressively as a result of seepage forces within the peat mass. Landva (2007) then used conventional soil mechanics seepage analysis to study the failure. He assumed that the driving force for the failure was the differential water head between that in the main body of the peat and that at the cliff face.

The method used by Landva (2007) is applied to the Aghnamona site on Fig. 3.36b. The relevant forces on the potential failure block are shown on Fig. 3.36b and are:

- T_P = the tensile resisting force in the peat;
- U_R = the activating force due seepage pressure;
- U_L = the resisting force due water pressure in the drain;
- S_B = the shear force along the base of the block;
- S_L/S_R shear forces along the drain face and surface

For a crack to form along ab, 1 m behind the existing drain face, the peat would have to fail in tension along ab. This is possible if the available resistance provided by the peat is exceeded by the horizontal force acting in the direction of the drain. In this case:

- $T_P = 1.5 \times s_u = 1.5 \times 7 = 10.5$ kN/m;
- $U_R = 0.5 \times 1.5 \times 1.5 \times 9.81 = 11$ kN/m;
- $U_L = 0$ when drain is dry (frequently the case);
- $S_R = S_L = S_B = 0$ given the very low stiffness of the peat in bending and in shear.

It is found then that the activating force will exceed the resisting force when the differential water head exceeds about 1.4 m. As the drains at the edge of the failure at Carn Park and Aghnamona are some 3.8 m and 1.5 m deep respectively, this suggests that failure due to seepage pressures is very likely at both sites. The greater extent of the failure at Carn Park is probably at least partly due to the deeper drain at this site. As suggested by Landva (2007), the seepage forces are caused by drainage in the network of cracks extending to the cut faces. Seepage along the network of cracks is probably supported by the fact that the peat mass has relatively high permeability at in situ stress.

3.3.7.3 Failure due to gas pressure

Feehan and O'Donovan (1996) suggest that the gas emanating from peat is largely nitrogen (54% or so), methane (about 43%) with some some carbon dioxide (3%). A pale light is often seen to hover over bogs and this has been attributed to the spontaneous combustion of escaping methane. As detailed above there have been several failures of raised bogs in Ireland which have been attributed to 'bursts' caused by the build-up of water and gas pressures. However, the nature of these failures is very different to those observed here. Feehan and O'Donovan (1996) refer to one case of a bog being 'torn up and scattered as if by an explosion'. Although it is possible that the build-up of gas pressure contributed to the failures observed at the two sites under study, it is likely that the effect of seepage pressures dominated the processes observed.

4 Conclusions and Recommendations

This project has applied a number of recent geophysical developments, in addition to a range of traditional approaches, to a number of the areas of Irish concern to the proposed Soil Framework Directive (COM 2006, 232). Specifically, the areas that were investigated as part of this project included: (i) agricultural soil compaction, (ii) wastewater contamination and (iii) landslides in peatlands. In each of these areas, a range of geophysical and conventional field and laboratory testing methods were performed in order to establish the effectiveness of these geophysical techniques for investigating these threats, or in the case of peat landslides, for establishing the failure mechanisms. Conclusions, recommendations and proposals for future work resulting from these investigations are discussed below.

4.1 Agricultural Compaction

This study has explored the possibility of using geophysical measurements as alternatives to conventional methods for detecting agricultural compaction in a field environment. The investigation at the Lyons site involved comparisons between an uncompacted control and a trafficked treatment, whereas the investigation at the Oakpark site involved comparisons between compacted headland and an uncompacted area with almost identical soil properties. At both test sites, the two geophysical methods tested, MASW and ERT detected significant differences between compacted and uncompacted ground. The results using both approaches compared favourably with those obtained from conventional measurements of bulk density, cone penetrometers and shear vanes.

Both methods have a number of advantages over conventional field measures of compaction, such as their non-intrusive nature and the ability to measure a large amount of data, relatively quickly, particularly if portable systems incorporating land streamers are employed. The use of surface wave seismic methods, such as MASW, have not previously been reported in the agricultural literature, and as such the application to agricultural compaction is completely novel. Moreover, because of their large amplitude relative to other types of seismic waves, surface waves are less affected by noise than methods incorporating other types of seismic wave. The MASW approach has the ability to identify and separate fundamental and higher mode surface waves, which is an advantage over other surface wave techniques. The main limitation of the surface wave approach for the detection of compaction is the resolution of the technique at very shallow depths. In order to accurately detect the velocity of the upper 10 cm (approx.) a suitably high frequency source will have to be used. The small carpentry hammer source used in this study does not generate sufficiently high frequencies to sample this shallow material. Overall, the results show that the MASW approach can distinguish between the extreme states of heavily compacted and uncompacted soil. Further work will need to be completed, however, before this tool can be utilised practically for quantifying compaction. In particular, the sensitivity of the method for measuring smaller changes in compaction than those tested here should be explored. Although a significant variation in the inverted resistivity data close to the surface was observed using galvanic measurements of resistivity, this approach does not suffer from the same limitations as MASW with regard to near-surface resolution, if an appropriate electrode spacing and input current is selected.

Finally, the use of high-speed geophysical measurements, although extremely desirable from a practical and economic perspective, has not been entirely successful in this instance. Although the approaches tested in this study may be very suitable for engineering applications, where the depth of interest may be up to 30 m below ground level, the transfer of these methods to shallow-soils applications presents different challenges. The use of plate-coupled geophones on rough agricultural terrain appears to reduce the ability of the MASW method significantly – for example, for providing sufficient high-frequency data in order to account for the upper 25–30 cm (approx.). Further work is necessary in this regard to explore the possibility of using an alternative array of receivers. In addition, resistivity values using the capacitively

coupled Ohmmapper system are in general greater than those measured for the galvanically coupled data. It is thought that this difference is due to the large variation in the measured apparent resistivity measured close to the surface, which may have introduced artefact high- and low-resistivity zones into the inverted CR models, particularly at higher iterations. Despite the computation issues involved in processing the CR datasets, however, they clearly detected the reduction in resistivity of the compacted headland.

4.2 Wastewater Contamination

This study has explored the possibility of using geophysical measurements for detecting and mapping effluent plumes resulting from discharge of OSWTS. Safe disposal of effluent arising from OSWTS is essential for the protection of soil, ground and surface water. The catchment selected for this study is dominated by fine-grained glacial tills that have low permeability and are, therefore, expected to act as a barrier to vertical movement of contaminants and to substantially limit infiltration. Three sites within the Lough Muckno catchment were investigated, by designing a number of geophysical surveys with three different techniques, EM ground conductivity mapping, ERT and seismic refraction. Although a number of problems were encountered, the geophysical data significantly improved the research team's understanding of the extent of the wastewater plume and assisted in the identification of potential effluent pathways. Although there is not enough piezometer data in the vicinity of the plume to compare the resistivity measurements with the direct contaminant measures statistically, it does appear that in this instance the ERT method is sensitive to a number of contaminant tracers sampled. In particular, the Cl^- plume appears to be detectable with surface resistivity measurements at a concentration greater than approximately 30–40 mgL^{-1}. Jointly interpreting the seismic refraction and ERT data, in particular, provided invaluable data for characterising the plume. It should be pointed out that the measured resistivity values of the effluent plumes are not particularly low, and that the measured range of 20–110 Ωm may overlapa with a number of geological materials, including glacial till, where resistivities in the range 50–150 Ωm are commonly observed in Ireland. This may prove a limitation when characterising effluent plumes in more conductive, saturated clay-rich soils and subsoils.

The use of pipes directly discharging to surface water was also observed. These may act to divert effluent away from the soil-treatment area, and facilitate direct transportation of contaminants to surface waters. The use of discharge pipes, to provide additional drainage, is common throughout the catchment (McCarthy et al., 2010) and, based on anecdotal evidence, often used as a 'back-up' for percolation areas located in poorly draining land. This is likely due to the low permeability soils found in the area, where there is a high risk that the system will fail as a result of wastewater breaking to the surface or backing up into household plumbing.

In a catchment such as this, with a large population of grazing animals, it may be difficult using geophysical techniques to distinguish between contamination originating from OSWTS and that arising from other agricultural sources. Correct identification of the source of contamination is therefore crucial in order to manage water quality more cost effectively. In addition, when combined with this study the DKIT/QUB study highlights the need to put in place an appropriate inspection system that is capable of detecting pollution arising from malfunctioning systems and assessing whether the soil in the location is capable of adequate treatment. There is limited information available in Ireland concerning failure rates and required remediation of OSWTS. As noted above, this deficit will need to be addressed if Ireland is to meet its obligations under the WFD, which aims to restore all surface waters to good ecological status. Further, following a European Court of Justice ruling in 2009, Ireland has come under pressure to implement appropriate inspection procedures for OSWTS, in order to ensure that they do not present an environmental risk and that they comply with EU regulations. As shown here, geophysics has the potential to assist assessment of malfunctioning OSWTS in this regard.

Given the extent of comparable glacial deposits hosting significant numbers of similar wastewater treatment systems nationally, the data from these projects, when viewed with more detailed hydrogeological characterisations, has the potential to provide critical information to river basin district managers on the potential impact on water quality over large areas of Ireland.

4.3 Failures in Irish Raised Bogs

The purpose and motivation of this work was to explore the nature and thickness of the peat in order to attempt to explain failures observed in Irish raised bogs, in particular at the relatively flat Aghnamona and Carn Park sites. The following points can be concluded from this work:

- Geotechnical field and laboratory testing confirmed that the peat is typical of Irish raised bogs, to be up to 8 m thick and to be characterised by very high water content, low density, low undrained shear strength and high compressibility. The peat has relatively high permeability under in situ stress conditions;
- Drainage along the edge of both bogs has caused dewatering of the peat. This has manifested itself in a reduced water content of the peat towards the edge of the failure zone and clear thinning and compression of the peat which has led to surface settlement of the bog. The degree of consolidation is greater for Carn Park compared to Aghnamona because of the age of the failure;
- Geophysical surveys (GPR and ERT) have shown that the peat base is relatively flat and does not follow the pronounced variation in surface topography. This suggests that the observed surface movement has come from within the peat rather than from the material below the peat;
- The decreasing water content of the peat towards the edge of the failure corresponds to a very similar reduction in resistivity. Water within the peat is relatively resistive, and reducing its content reduces the measured resistivity of the peat. The relationship between water content and resistivity may provide an innovative way in which to monitor the relative fluctuations in water content of peat soils on sensitive sites where access is not readily available;
- GPR was found to be by far the most valuable geotechnical or geophysical site investigation method for use on peatlands for the following reasons:
  - The relative speed of data acquisition;
  - Its suitability for use on difficult terrain, such as peatlands;
  - The high-resolution resultant data, if an appropriate antenna is used;
  - The valuable peat thickness, peat base and surface morphological information it provides if used in conjunction with RTK dGPS.

  It should be pointed out that in order to provide highly accurate GPR data a number of peat probes should be carried out in order to calibrate the data. Rosa et al. (2009) statistically assessed the minimum number of calibration points (using peat coring) required to produce a representative estimate of EM velocity, and therefore depth. They observed that, depending on the variability of the site under investigation, more than six cores per kilometre may be required to provide accurate GPR peat-thickness information;
- Slope stability and seepage analyses have shown that seepage-induced forces were the most likely cause of the failures observed at the sites. Release of built-up gas cannot be ruled out as a minor contributing factor;
- Owing to the presence of drains/cut faces at the edges of the failed areas, these forces will continue to exist. The existing cracks on the bogs will continue to open and new cracks will develop towards the centre of the bogs, causing further damage, unless remedial measures are taken;
- It is recommended that, where infrastructural development is planned in close proximity to peatlands, a significant effort should be made to ensure than drainage of the peat does not occur.

Raised bogs are a rare habitat in the EU, and a large number of Irish raised bogs have received protection, through designations under European legislation via the EU Habitats Directive (92/43/EEC) and national legislation via the Wildlife Amendment Act (2000). The protection of these rare and important habitats from damage, such as that caused by raised bog landslides, is essential if Ireland is to comply with its EU obligations.

4.4 Overall Assessment of Geophysical Techniques

This study has made an effort to compare the results obtained from a range of geophysical techniques with those obtained from more conventional approaches. In almost all of the cases studied it was found that the geophysical techniques provided useful data that should be viewed as being complementary to the more traditional techniques rather than being viewed as direct replacements. It was observed during this study that some conventional geotechnical, agricultural and hydrological approaches, which are usually carried out at discrete locations, can be significantly enhanced by using geophysical techniques to link together information between conventional test locations – perhaps significantly reducing the need for large numbers of discrete investigations. When calibrated to geotechnical or hydrological parameters, geophysical techniques can potentially act as powerful tools, enabling a rapid, non-intrusive, cost-effective and large-scale assessment of the application being investigated. The recent development of high-speed continuously measuring systems has further contributed to the potential usefulness of geophysical techniques, enabling large, dense datasets to be acquired efficiently. Further work is necessary, however, to explore the application of these high-speed techniques for determining accurate, high-resolution data close to the surface, as is required for assessments of agricultural compaction.

4.5 Key Recommendations

- Currently, no comprehensive data is available on the severity or extent of soil compaction in Ireland. This would be a valuable resource;
- Further assessment of the sensitivity of the geophysical techniques used in this project for compaction assessments is recommended on a range of soils, other than those tested in this project;
- The DKIT/QUB OSWTS study, when combined with this study, highlights the need for an appropriate inspection system to be put in place that is capable of detecting pollution arising from malfunctioning wastewater systems and assessing whether the soil in the location is capable of adequate treatment;
- There is limited information available in Ireland concerning failure rates and required remediation of OSWTS. This deficit will need to be addressed if Ireland is to meet its EU obligations. As shown here, geophysics has the potential to assist assessment of malfunctioning OSWTS in this regard;
- Regarding failures in raised bogs, it is recommended that where infrastructural development is planned in close proximity to peatlands, a significant effort should be made to ensure that drainage of the peat does not occur. The protection of these rare and important habitats from damage, such as that caused by raised bog landslides, is essential if Ireland is to comply with its EU obligations.

References

Aki, K. and Richards, P.G. (1980). Quantitative seismology, W.H. Freeman and Co.

Alexander, R., Coxon, P. and Thorn, R.T. (1985). *Bog Flows in South-east Sligo and South-west Leitrim.* IQUA Field Guide, 8.

Allred, B.J., Groom, D., Ehsani, M.R., Daniels, J.J. (2008). Resistivity methods. In: Allred, B.J., Daniels, J.J., and Ehsani, M.R. (Eds), Handbook of Agricultural Geophysics, CRC Press, Taylor and Francis Group, 86–108.

Andresen A., Berre T., Kleven A., Lunne T. (1979). Procedures used to obtain soil parameters for foundation engineering in the North Sea. Marine Geotechnology 3 (3): 201–66.

Aristodemou, E. and Thomas-Betts, A. (2000). DC resistivity and induced polarisation investigations at a waste disposal site and its environments. *Journal of Applied Geophysics*, 44, 275–302.

Arman A. (1971). Discussion on Skempton and Petley (1970). *Geotechnique,* 21 (4): 418–21.

Besson, A., Cousin, I., Samouëlian, A., Boizard, H. and Richard, G. (2004). Structural heterogeneity of the soil tilled layer as characterized by 2D electrical resistivity surveying. *Soil and Tillage Research*, 79, 239–49.

Bjerrum, L., Landva, A.O. (1966). Direct simple-shear tests on a Norwegian quick clay. *Geotechnique,* 16 (1): 1–20.

Boylan, N. (2008). The shear strength of peat. PhD Thesis, University College Dublin.

Boylan, N. and Long, M. (2013). Evaluation of peat strength for stability assessments. Institution of Civil Engineers Journal of Geotechnical Engineering, Accepted for publication, November 2012.

British Standards Institution (BSI) (1990). BS 1377–5:1990—Methods of test for soils for civil engineering purposes. Compressibility, permeability and durability tests ISBN 0 580 18030 1. British Standards Institution, London.

BSI (2006). BS EN ISO 14688–2 (2004): Geotechnical investigation and testing. Identification and classification of soil. Principles for a classification, British Standards Institution.

Buselli, G., Davis, G.B., Barber, C., Height, M.I. and Howard, S.H.D. (1992). The application of electromagnetic and electrical methods to groundwater problems in urban environments, *Exploration Geophysics*, 23, 543–55.

Buselli, G., and Lu, K. (2001). Groundwater contamination monitoring with multichannel electrical and electromagnetics methods, *Journal of Applied Geophysics*, 48, 11–23.

Canter, L. and Knox, R. (1985). Septic Tank System Effects on Groundwater Quality. Lewis Publishers, Chelsea, MI, USA.

Carlsten, P. (2000). Geotechnical properties of some Swedish peats, 13th NGM 2000, Nordiska Geoteknikermötet, Helsinki, 51–60.

CEC (1992). Council Directive 92/43/EEC on the conservation of natural habitats and of wild fauna and flora. Council of the European Communities.

Central Statistics Office (2012). Profile 4: The Roof over our Heads. Stationery Office, Dublin, Ireland.

Cercato, M. (2009). Addressing non-uniqueness in linearized multichannel surface wave inversion. *Geophysical Prospecting*, 57, 27–47.

Cole, G.A.J. (1897). The bog slide at Knocknageeha, in the County of Kerry, *Nature*, 55, 254–6.

Colhoun, E.A., Common, R. and Cruickshank, M.M. (1965). Recent bog flows and debris slides in the north of Ireland. *Scientific Proceedings, Royal Dublin Society,* A (2), 163–74.

Comas, X., Slater, L., Reeve, A. (2004). Geophysical evidence for peat basin morphology and stratigraphic control on vegetation observed in a Northern peatland, *Journal of Hydrology*, 295, 173–84.

Conaghan, J. (2003). Raised bog ecological report, Coillte.

Creighton, R. (Editor), (2006). Landslides in Ireland. Geological Survey of Ireland.

Dabas, M., Hesse, A., Tabbagh, J., (2000). Experimental resistivity survey at Wroxeter archaeological site with a fast and light recording device. *Archaeological Prospection*, 7, 107–18.

Daly, D. (2003) Editorial. *In* Geological Survey Ireland Groundwater Newsletter. No.42. GSI Dublin, Ireland

Derwin, J. (2006). Bog flow at Carn Park bog cSAC (2336), Coillte.

Derwin, J. (2008). Restoring raised bogs in Ireland – A report on the restoration of Project Site No. 11 – Carn Park Bog Co. Westmeath. Report: LIFE04 NAT/IE/000121, Coillte.

Donohue, S. and Long, M. (2008a). Ground improvement assessment of glacial till using shear wave velocity. *Proceedings of the 3rd International Conference on Site Characterization ICS'3: Geotechnical and Geophysical Site Characterization*, Taipei, 825–30.

Donohue, S. and Long, M. (2008b). Assessment of an MASW approach incorporating discrete particle modeling. *Journal of Environmental and Engineering Geophysics*, 13 (2), 57–68.

Donohue, S., Forristal, D. and Donohue, L.A. (2013). Detection of soil compaction using seismic surface waves. *Soil and Tillage Research*, 128, 54–60.

Dykes, A.P. and Kirk, K.J. (2001). Initiation of a multiple peat slide on Cuilcagh Mountain, Northern Ireland. *Earth Surface Processes and Landforms*, 26, 395–408.

Dykes, A.P. and Warburton, J. (2007). Significance of geomorphological and subsurface drainage controls on failures of peat-covered hillslopes triggered by extreme rainfall. *Earth Surface Processes and Landforms*, 32 (12), 1841–62.

Eigenberg, R.A., Korthals, R.L. and Nienaber, J.A. (1998). Geophysical electromagnetic survey methods applied to agricultural waste sites. *J. Environ. Qual.* 27, 215–19.

EPA (2010). Code of Practice: Wastewater Treatment and Disposal Systems Severing Single Houses. Environmental Protection Agency. Available at: http://www.epa.ie/pubs/advice/water/wastewater/code of practice for single houses/#d.en.27964 [accessed 5 June 2013].

European Commission (EC) (2000). European Parliament and Council Directive 2000/60/EC of the European Parliament and of the Council establishing a Framework for Community Action in the Field of Water Policy.

European Commission (EC) (2002). Communication from the Commission to the Council, the European Parliament, the Economic and Social Committee and the Committee of the regions towards a Thematic Strategy for Soil Protection.

European Commission (EC) (2006a). Communication from the Commission to the Council, the European Parliament, the European Economic and Social Committee and the Committee of the regions. Thematic Strategy for Soil Protection. COM 2006, 231.

European Commission (EC) (2006b). Directive of the European Parliament and of the Council establishing a Framework for the Protection of Soil and Amending Directive 2004/35/EC. COM 2006, 232.

Feehan, J. and O'Donovan, G. (1996). The bogs of Ireland – An Introduction to the Natural, Cultural and Industrial Heritage of Irish Peatands. UCD Environmental Institute.

Fetter, C.W. (2001). Applied Hydrogeology (4th edn), Prentice Hall, New Jersey.

Foti, S., Parolai, S., Albarello, D. and Picozzi, M. (2011). Application of Surface-Wave Methods for Seismic Site Characterization. *Surveys in Geophysics*, 32 (6) 777–825.

Freeland, R.S., Yoder, R.E, and Ammons, J.T. (1998). Mapping shallow underground features that influence site-specific agricultural production. *Journal of Applied Geophysics*, 40, 19–27.

Geonics, Ltd. (1984). Operating manual for EM-31-D non-contacting terrain conductivity meter, Geonics, Ltd., Toronto, Ontario, Canada.

deGroot-Hedlin, C. and Constable, S. (1990). Occam's inversion to generate smooth, two-dimensional models form magnetotelluric data. *Geophysics*, 55, 1613–24.

Hagedoorn, J.G. (1959). The plus-minus method of interpreting seismic refraction sections. *Geophysical Prospecting*, 7, 158–82.

Hanninen, P. (1992). Application of ground penetrating radar to peatland investigations, *Proc. Fourth Int. Conf. on Ground Penetrating Radar*, Rovaniemi, Finland. Geological Survey of Finland, Special Paper 16, 217–21.

Hobbs, N.B. (1986). Mire morphology and the properties and behaviour of some British and foreign peats. *Quarterly Journal of Engineering Geology and Hydrogeology*, 19, 7–80.

Hoefer, G. and Hartge, K.H. (2010). Subsoil compaction: cause, impact and prevention, in Soil Engineering, Dedousis, A.P., Bartzanas (Eds), Chapter 9, 121–42.

Janbu, N. (1957). Earth pressure and bearing capacity calculations by generalised procedure of slices, Proceedings 4th International Conference on Soil Mechanics and Foundation Engineering, London, pp. 207–12.

Jenssen, P.D. and Siegrist, R.L. (1990). Technology assessment of wastewater treatment by soil infiltration systems. *Water Science and. Technology.* 22 (3/4), 83–92

Jones R.B. (1958). In-situ measurement of the dynamic properties of soil by vibration methods. *Geotechnique*, 8 (1), 1–21.

Kaplan, O.B. (1991). Septic Systems Handbook. Lewis Publishers, Inc., Chelsea, MI, USA.

Kuras, O., Beamish, D., Meldrum, P.I. and Ogilvy, R.D. (2006). Fundamentals of the capacitive resistivity technique. *Geophysics*, 71, G135–G152.

Kuras, O., Meldrum, P.I., Beamish, D., Ogilvy, R.D. and Lala, D. (2007). Capacitive Resistivity Imaging with Towed Arrays, *Journal of Environmental and Engineering Geophysics*, 12 (3), 267–79.

Lalor, S.T.J. (2004). Soils of UCD Research Farm, Lyons Estate, Celbridge, Co. Kildare. Masters Thesis, University College Dublin.

Landva, A.O. (1980). Erosion and instability of the peat cliff at Escuminac, New Brunswick, National Research Council of Canada Technical Memorandum, 128, 93–102.

Landva, A.O. (2007). Characterisation of Escuminac peat and construction on peatland. In: T.S. Tan, K.K. Phoon, D.W. Hight and S. Leroueil (Eds), *Proceedings of Characterisation and Engineering Properties of Natural Soils*, Singapore, 2135–91.

Landva, A.O. (2009). Characteristics of organic soils and construction on organic terrain, Cross Canadian Lecture Tour – Spring 2009. Canadian Geotechnical Society. Available on www.terratlantic.nb.ca

Lapen, D.R., Moorman, B.J. and Price, J.S. (1996). Using ground-penetrating radar to delineate subsurface features along a wetland catena. *Soil Science Society of America Journal*, 60, 923–31.

Lee, B.D., Jenkinson, B.J., Doolittle, J.A., Taylor, R.S., and Tuttle, J.W. (2006). Electrical Conductivity of a Failed Septic System Soil Absorption Field. *Vadose Zone Journal*, 5, 757–63.

Loke, M.H. and Barker, R.D. (1996). Rapid least-squares inversion of apparent resistivity pseudosections by a quasi-Newton method. *Geophysical Prospecting*, 44, 131–52.

Loke, M.H. and Dahlin, T. (2002). A comparison of the Gauss-Newton and quasi-Newton methods in resistivity imaging inversion. *Journal of Applied Geophysics*, 49, 149–62.

Loke, M.H. (2004). Res2DInv ver. 3.54. Geoelectrical Imaging 2D and 3D. Instruction Manual. Geotomo Software.

Long, M. and Rogers, M. (1995). Geotechnical behaviour of very soft calcareous soils in Ireland, Proceedings XIth European Conference on Soil Mechanics and Foundation Engineering. Danish Geotechnical Society (DGF), Copenhagen, 8.103–8.108.

Long, M. and Jennings, P. (2006). Analysis of the peat slide at Pollatomish, Co. Mayo, Ireland. *Landslides*, 3 (1), 51–61.

Long, M. and Donohue, S. (2010). Characterisation of Norwegian marine clays with combined shear wave velocity and CPTU data. *Canadian Geotechnical Journal*, 47 (5), 709–718.

Long, M., Jennings, P. and Carroll, R. (2011). Irish peat slides 2006–2010. *Landslides*, 8 (3), 391–401.

Long, M., Daynes, P., Donohue, S. and Looby, M. (2012). Retaining wall behaviour in Dublin's fluvio-glacial gravel. *Proceeding of the Institution of Civil Engineers, Geotechnical Engineering*, 165, 289–307.

Long, M. Trafford, A. and Donohue, S. (2014). Investigation of failures in Irish raised bogs. *Landslides,* DOI: 10.1007/s10346-013-0440-2

Lu, Z., Hickey, C.J. and Sabatier, J.M. (2004). Effects of compaction on the acoustic velocity in soils. *Soil Science Society of America Journal,* 69, 7–16.

Luke, B. and Calderón-Macías, C. (2007). Inversion of seismic surface wave data to resolve complex profiles. *Journal of Geotechnical and Geoenvironmental Engineering*, 133 (2), 155–65.

Martínez-Pagán, P., Faz, A. and Aracil, E. (2009). The use of 2D electrical tomography to assess pollution in slurry ponds of the Murcia region, SE Spain. *Near Surface Geophysics*, 7 (1), 49–61.

Martinho, E. and Almeida, F. (2006). 3D behaviour of contamination in landfill sites using 2D resistivity/IP imaging: case studies in Portugal. *Environmental Geology*, 49, 1071–8.

Materechera, S.A. (2009). Tillage and tractor traffic effects on soil compaction in horticultural fields used for peri-urban agriculture in a semi-arid environment of the North West Province, South Africa. *Soil and Tillage Research*, 103, 11–15.

Mayne, P.W. and Rix, G.J. (1993). G_{max}-q_c relationships for clays. *Geotechnical Testing Journal, ASTM*, 16 (1), 54–60.

Mayne, P.W. and Rix, G.J. (1995). Correlations between cone tip resistance and shear wave velocity in natural clay. *Soils and Foundations*, 35 (2),: 107–10.

McCarthy, V., Flynn, R., Orr, A., Rafferty, P, Minet, E., Meehan, R., Archbold, M. and Linnane, S. (2010). A field study assessing the impact of on-site wastewater treatment systems (OSWTS) on surface water in a Co. Monaghan catchment, Dundalk Institute of Technology (DKIT) Report.

McMechan, G.A. and Yedlin, M.J. (1981). Analysis of dispersive waves by wave field transformation. *Geophysics*, 46, 869–74.

Minerex Environmental Ltd (MEL) (2004). Leitrim County Council – Hydrogeological Impact Assessment of the Proposed N4 Dromod – Roosky Bypass, MEL 1614-084 (Rev. 7), Dublin, Ireland.

Møller, I. (2001). OhmMapper field tests at sandy and clay till sites in Denmark, *7th Annual Meeting of the Environmental and Engineering Geophysical Society*-European Section, Proceedings, 4p.

O'Flynn, M. (2013). The influence of harvest traffic before and after shoot emergence in wet and dry soil conditions on soil compaction and crop response in an establishing miscanthus crop. PhD Thesis, In Preparation.

Orlando, L. and Marchesi, E. (2001). Georadar as a tool to identify and characterise solid waste dump deposits. *Journal of Applied Geophysics*, 48, 163–74.

Orr, A. (2009). The impact of septic tanks on surface and groundwater quality in a poorly drained catchment. MSc. Thesis, Queen's University Belfast.

Palmer, D. (1980). The generalized reciprocal method of seismic refraction interpretation. *Society of Exploration Geophysicists*, Tulsa, OK, 104 p.

Park, C.B., Xia, J. and Miller, R.D. (1998). Imaging dispersion curves of surface waves on multichannel record, *SEG, 68th Annual Meeting*, New Orleans, Louisiana, 1377–380.

Park, C.B., Miller, D.M. and Xia, J. (1999). Multichannel Analysis of surface waves. *Geophysics*, 64 (3), 800–8.

Park, C.B., Miller, R.D. and Miura, H., (2002). Optimum field parameters of an MASW survey. 6th International Symposium, Society of Exploration Geophysicists-Japan.

Parsekian, A., Slater, L. and Glaser, P. (2008). Geophysical Characterization of the Red Lake Peatland Complex, Northern Minnesota, 21st Symposium on the Application of Geophysics to Engineering and Environmental Problems (SAGEEP), Philadelphia, 858–61.

Pellerin, L., Groom, D., and Johnston, J. (2003). Characterizaion of an old diesel fuel spill? Results of a multi-receiver OhmMapper survey, Society of Exploration Geophysicists (SEG) 73rd Annual Meeting, Dallas, TX, 5008–11.

Perozzi, L. and Holliger, K. (2008). Detection and Characterization of Preferential Flow Paths in the Downstream Area of a Hazardous Landfill. *Journal of Environmental and Engineering Geophysics*, 13 (4), 343–50.

Petersen, H., Fleige, H., Rabbel, W. and Horn, R. (2005). Applicability of geophysical prospecting methods for mapping of soil compaction and variability of soil texture on farm land. *Journal of Plant Nutrition and Soil Science*, 168, 68–79.

Ponziani, M., Slob, E.C., Ngan-Tillard, D.J.M. and Vanhala, H. (2011). Influence of water content on the electrical conductivity of peat. *International Water Technology Journal (IWTJ)*, 1 (1), 14–21.

Ranjan, R.S., and Karthigesu, T. (1995). Evaluation of an electromagnetic method for detecting lateral seepage around manure storage lagoons. American Society of Agricultural Engineering (ASAE) Paper. no. 952440.

Raper, R.L., Asmussen, L.E. and Powell, J.B. (1990). Sensing hard pan with ground penetrating radar, *Transactions* American Society of Agricultural Engineering *(ASAE)*, 33, 41–6.

Robichaud, A. and Bégin, Y. (2009). Development of a raised bog over 9000 years in Atlantic Canada. Mires and Peat. *International Mire Conservation Group and International Peat Society*, 5 (4), 1–19.

Rosa, E., Larocque, M., Pellerin, S., Gagné, S. and Fournier, B. (2009). Determining the number of manual measurements required to improve peat thickness estimations by ground penetrating radar. *Earth Surface Processes and Landforms*, 34 (3), 377–83.

Santos, F.A.M., Mateus, A., Figueiras, J. and Gonçalves, M.A. (2006). Mapping groundwater contamination around a landfill facility using the VLF-EM method – A case study. *Journal of Applied Geophysics*, 60, 115–25.

Sasaki, Y. (1989). Two-dimensional joint inversion of magnetotelluric and dipole–dipole resistivity data. *Geophysics*, 54, 254–62.

Schnaid F, Lehane B.M. and Fahey M. (2004). In-situ test characterisation of unusual geomaterials. In *Proceedings of the 2nd International Conference of Site Characterisation* (*ISC2)*, Porto, 1, 49–74.

Schouten, M.G.C. (2002). Conservation and Restoration of Raised Bogs; Geological, Hydrological and Ecological Studies. Department of the Environment and Local Government/Staatsbosbeheer.

Seladji, S., Cosenza, P., Tabbagh, A., Rangerd, J. and Richard, G. (2010). The effect of compaction on soil electrical resistivity: A laboratory investigation. European Journal of Soil Science, 61: 1043–55.

Sidhu, D. and Duiker, S.W. (2006). Soil compaction in conservation tillage: crop impacts. *Agronomy Journal*, 98, 1257–64.

Slater, L. and Reeve, A. (2002). Understanding peatland hydrology and stratigraphy using integrated electrical geophysics. *Geophysics*, 67, 365–78.

Soane, B.D. and Van Ouwerkerk. C. (1998). Soil compaction: A global threat to sustainable land use. *Advances in GeoEcology*, 31, 517–25.

Socco, L.V., Foti, S. and Boiero, D. (2010). Surface-wave analysis for building near-surface velocity models – Established approaches and new perspectives. *Geophysics*, 75 (5), 75A83–75A102.

Sørensen, K. (1996). Pulled array continuous electrical profiling. *First Break*, 14, 85–90.

Stevens, R.J., O'Bric, C.J. and Carton, O.T. (1995). Estimating nutrient content of animal slurries using electrical conductivity. *Journal of Agricultural Science,* 125, 233–8.

Stokoe, K. H., II, Wright, G. W., James, A. B. and Jose, M.R. (1994). Characterisation of geotechnical sites by SASW method. In Woods, R.D. (Ed) *Geophysical characterization of sites*, Oxford Publishers, New Dehli.

Theimer, B.D., Nobes, D.C., Warner, B.G. (1994). A study of the geoelectrical properties of peatlands and their influence on ground-penetrating radar surveying. *Geophysical Prospecting*, 42, 179–209.

Trafford, A. (2009). Mapping thickness of raised peat bog deposits using GRP. In *Proceedings EAGE Near Surface 2009, 15th Annual Meeting of Environmental and Engineering Geophysics*. EAGE, Dublin.

van Cuyk, S., Siegrist, R., Logan, A., Masson, S., Fischer, E. and Figueroa, L. (2001) Hydraulic and purification behaviours and their interactions during wastewater treatment in soil infiltrations systems. *Water Resources*, 35, 953–64.

Vinten, A.J.A., Mingelgrin, U. and Yaron, B. (1983). The effect of suspended solids in wastewater on soil hydraulic conductivity: Vertical distribution of suspended solids. *Soil Science Society of America Journal*, 47, 408–12.

von Post, L. and Granlund, E. (1926). Peat resources in southern Sweden. *Sveriges geologiska undersökning*, Yearbook, 335 (19.2 Series C): 1–127, Stockholm.

Voorhees, W.B., Nelson, W.W and Randall, G.W. (1986). Extent and persistence of subsoil compaction caused by heavy axle loads. *Soil Science Society of America Journal*, 50, 428–33.

Warburton, J., Holden, J. and Mills, A.J. (2004). Hydrological controls of surficial mass movements in peat. *Earth Science Reviews*, 67, 139–56.

Warner, B.G., Nobes, D. and Theimer, B.D. (1990). An application of ground penetrating radar to peat stratigraphy of Ellice Swamp, southwestern Ontario. *Canadian Journal of Earth Sciences*, 27, 932–8.

Wildlife (Amendment) Act (2000). An Act to amend and extend the Wildlife Act, 1976, and to provide for connected matters. Irish Statute Book.

Wyrobek, S.M. (1956). Application of delay and intercept times in the interpretation of multi-layer refraction time distance curves. *Geophysical Prospecting*, 4 (2), 112–30.

Xia, J., Miller, R.D., Park, C.B. (1999). Estimation of near surface shear wave velocity by inversion of Rayleigh waves. *Geophysics*, 64 (3), 691–700.

Yates, M.V. (1985) Septic tank density and ground-water contamination. *Ground Water*, 23: 586–91.

Acronyms

ANOVA	Analysis of variance
CPT	Cone penetration test
CR	Coupled resistivity
cSAC	candidate Special Area of Conservation
DD	Dipole Dipole
DKIT	Dundalk Institute of Technology
DSS	Direct simple shear tests
EC	Electrical conductivity
EM	Electromagnetic
ERT	Electrical Resistivity Tomography
EU	European Union
GPR	Ground Penetrating Radar
GRM	Generalized reciprocal method
GSI	Geological Survey of Ireland
GWS	Group water scheme
HMD	Horizontal magnetic dipole
IP	Induced Polarisation
MASW	Multichannel Analysis of Surface Waves
NHAs	Natural Heritage Areas
NGI	Norwegian Geotechnical Institute
NPWS	National Parks and Wildlife Service
OSWTS	On-site wastewater treatment systems
QUB	Queen's University Belfast
RMS	Root Mean Square
SACs	Special Areas of Conservation
SDs	Standard deviations
UCD	University College Dublin
VMD	Vertical magnetic dipole

Appendix 1: Project Outputs

End of project report and all paper abstracts are available for download at:
http://erc.epa.ie/safer/reports

Published Papers

- **Donohue, S.**, Forristal, D. and Donohue, L.A. (2013). Detection of soil compaction using seismic surface waves. *Soil and Tillage Research*, 128, 54–60.
- Long, M. Trafford, A. and **Donohue, S.** (2014). Investigation of failures in Irish raised bogs. *Landslides,* DOI: 10.1007/s10346-013-0440-2.
- **Donohue, S.**, Flynn, R., McCarthy, V., Orr, A., Rafferty, P. and Galvin, K. (2010). Geophysical assessment of contamination from a wastewater treatment system in the Milltown lake catchment, Ireland. *EAGE Near Surface 2010, 16th Annual Meeting of Environmental and Engineering Geophysics*, Zurich, September.
- **Donohue, S.**, Gavin, K., Long, M., Tolooiyan, A. and Trafford, A. (2011). Understanding Irish landslides using geophysics. *Proceedings of the Geophysical Association of Ireland Seminar on Engineering Geophysics*, 17–22.

Papers in Preparation

- **Donohue, S.**, McCarthy, V., Orr, A., Rafferty, P., Galvin, K. and Flynn, R. The effectiveness of geophysical measurements for detecting and mapping contamination from wastewater treatment systems in a catchment dominated by low permeability soils. To be submitted to the *Journal of Applied Geophysics.*

Presentations Relating to Project

- **Donohue, S.**, Gavin, K., Long, M., Tolooiyan, A. and Trafford, A. (2011). Understanding Irish landslides using geophysics. Presented to the *Geophysical Association of Ireland Seminar on Engineering Geophysics*. February 2011.
- **Donohue, S.**, Flynn, R., McCarthy, V., Orr, A., Rafferty, P. and Galvin, K. (2010). Geophysical assessment of contamination from a wastewater treatment system in the Milltown lake catchment, Ireland. Presented to the *EAGE Near Surface 2010, 16th Annual Meeting of Environmental and Engineering Geophysics*, Zurich. September 2010.
- **Donohue, S**. (2009) Characterisation of physical properties of soils using geophysics. Presented to the *Environmental Protection Agency STRIVE Research Seminar*, Dublin, November 2009.

Appendix 2: Paper Abstracts

Reference

Donohue, S., Forristal, D. and Donohue, L.A. (2013). Detection of soil compaction using seismic surface waves. *Soil and Tillage Research*, 128, 54–60.

Abstract

Seismic geophysical methods have rarely been used in precision agriculture, predominantly due to the perception that they are slow and results require a complex evaluation. This paper explores the possibility of using a recently developed surface wave seismic geophysical approach, the multichannel analysis of surface waves (MASW) method, for assessment of agricultural compaction. This approach has the advantage of being non-intrusive, rapid and is able to produce 2D ground models with a relatively high density of spatial sampling points. The method, which was tested on a research site in Oakpark, Ireland, detected a significant difference in shear wave velocity between a heavily compacted headland and an uncompacted location. The results from this approach compared favourably with those obtained from measurements of bulk density and penetrometer resistance and demonstrate that the MASW approach can distinguish between the extreme states of heavily compacted and uncompacted soil.

Reference

Long, M. Trafford, A. and Donohue, S. Investigation of failures in Irish Raised Bogs. *Landslides,* DOI: 10.1007/s10346-013-0440-2.

Abstract

This paper presents the results of field geophysical testing and laboratory testing of peat from Carn Park and Roosky raised bogs in the Irish Midlands. The motivation for the work was to investigate the reasons for the failure of the bogs despite them having surface slopes of some 1°. It was found that the peat is typical of that of Irish raised bogs being up to 8 m thick towards the ‘high’ dome of the bogs. The peat is characterised by low density, high water content, high organic content, low undrained shear strength and high compressibility. The peat is also relatively permeable at in situ stress. Geophysical ERT and GPR data shows a clear thinning of the peat in the area of the failures corresponding to a reduction in volume from dewatering by edge drains / peat harvesting. This finding is supported by detailed water content measurements. It was also shown that the peat base topography is relatively flat and indicates that the observed surface movement has come from within the peat rather than from the material below the peat. Slope stability and seepage analyses confirm the reason for the failure was seepage induced forces on the peat mass. These forces will continue to operate, causing the exiting cracks to widen and creating new cracks unless remedial work is undertaken.

Reference

Donohue, S., Flynn, R., McCarthy, V., Orr, A., Rafferty, P. and Galvin, K. (2010). Geophysical assessment of contamination from a wastewater treatment system in the Milltown lake catchment, Ireland. *EAGE Near Surface 2010, 16th Annual Meeting of Environmental and Engineering Geophysics*, Zurich, September.

Abstract

Residential on-site wastewater treatment systems (OSWTS), where contaminated wastewater discharges to the subsurface, act as the dominant means of domestic wastewater disposal in rural Ireland; septic tanks constitute the most common technology employed. The objective of this study was to determine the effectiveness of a number of non-invasive geophysical techniques, employed in conjunction with hydrogeological data, for characterising the three dimensional extent of a contaminant plume generated by septic tank effluent discharging to glacial-till subsoils at a test site within the Milltown Lake Catchment, Co. Monaghan, Republic of Ireland. The findings of this study will feed into a larger project which aims to develop an improved understanding of the risk posed by OSWTS to natural water quality, as part of the Irish national response to the EU Water Framework Directive (WFD, 2000/60/EC). Information gathered in this programme will be integrated with existing knowledge to develop more sustainable solutions for minimizing the impacts of wastewater disposal on natural water quality in rural settings. Moreover, given the extent of comparable glacial deposits hosting significant numbers of similar wastewater treatment systems nationally, the data from these projects, when viewed with more detailed hydrogeological characterisation, have the potential to provide critical information to river basin district managers on the potential impact on water quality over large areas of Ireland.

Reference

Donohue, S., Gavin, K., Long, M., Tolooiyan, A. and Trafford, A. (2011). Understanding Irish landslides using geophysics. *Proceedings of the Geophysical Association of Ireland Seminar on Engineering Geophysics*, 17–22.

Introduction (No abstract required)

Until recently, Ireland has been regarded as a relatively benign environment in terms of landslide hazard. Following the major Pollatomish and Derrybrien slides of 2003 the Geological Survey of Ireland (GSI), established the Irish Landslides Working Group who prepared a nationwide database of landslide events (Creighton et al., 2006). The majority (54 %) of the events reported in the database involved peat as the principal material followed by debris related slides (26 %). It is likely that in the future there will be increased landslide activity as development in Ireland increases and expands into potentially hazardous areas. Increasing rainfall related to climate change may also increase landslide hazard. This paper will discuss the role of geophysics in improving our understanding of two different types of Irish landslide, infrastructural embankment failures and peat slides.

Since the early work of Bogoslovsky and Ogilvy (1977) and McCann and Forster (1990), geophysical techniques have been used increasingly in landslide and slope stability investigations (e.g. Hack, 2000; Cosentino et al., 2003; Jongmans and Garambois, 2007; Donohue et al., 2011). Geophysical techniques are well-suited for these studies as they may provide information on subsurface geology and hydrogeology. Furthermore, a number of these techniques are non-invasive and cost-effective, which make them ideal for studying the spatial and temporal variations

of the subsurface that cannot be captured using discrete boreholes or other forms of geotechnical investigation. Geophysical methods are therefore ideally used as a complimentary tool, which, together with traditional geotechnical investigations, will typically provide a more complete understanding of the physical behaviour of the slope or landslide in question.

Reference

Donohue, S. (2009) Characterisation of physical properties of soils using geophysics. Presented to the *Environmental Protection Agency STRIVE Research Seminar*, Dublin, November 2009.

Abstract

This project will enhance our ability to rapidly and non-invasively determine soil physical properties, thereby enabling improved identification of threatened soils. A number of recent geophysical developments, in addition to a range of traditional approaches, will be applied to a number of areas of Irish concern to the proposed Soil Framework Directive (COM 2006, 232). A considerable amount of development to the testing methods is required in order to make them suitable and as such a number of feasibility studies have been proposed. Specifically, the areas that are being investigated as part of this project include agricultural compaction, contamination (by wastewater treatment systems) and peatlands (peat slides).

An Ghníomhaireacht um Chaomhnú Comhshaoil

Is í an Gníomhaireacht um Chaomhnú Comhshaoil (EPA) comhlachta reachtúil a chosnaíonn an comhshaol do mhuintir na tíre go léir. Rialaímid agus déanaimid maoirsiú ar ghníomhaíochtaí a d'fhéadfadh truailliú a chruthú murach sin. Cinntímid go bhfuil eolas cruinn ann ar threochtaí comhshaoil ionas go nglactar aon chéim is gá. Is iad na príomh-nithe a bhfuilimid gníomhach leo ná comhshaol na hÉireann a chosaint agus cinntiú go bhfuil forbairt inbhuanaithe.

Is comhlacht poiblí neamhspleách í an Ghníomhaireacht um Chaomhnú Comhshaoil (EPA) a bunaíodh i mí Iúil 1993 faoin Acht fán nGníomhaireacht um Chaomhnú Comhshaoil 1992. Ó thaobh an Rialtais, is í an Roinn Comhshaoil, Pobal agus Rialtais Áitiúil.

ÁR bhFREAGRACHTAÍ

CEADÚNÚ

Bíonn ceadúnais á n-eisiúint againn i gcomhair na nithe seo a leanas chun a chinntiú nach mbíonn astuithe uathu ag cur sláinte an phobail ná an comhshaol i mbaol:

- áiseanna dramhaíola (m.sh., líonadh talún, loisceoirí, stáisiúin aistrithe dramhaíola);
- gníomhaíochtaí tionsclaíocha ar scála mór (m.sh., déantúsaíocht cógaisíochta, déantúsaíocht stroighne, stáisiúin chumhachta);
- diantalmhaíocht;
- úsáid faoi shrian agus scaoileadh smachtaithe Orgánach Géinathraithe (GMO);
- mór-áiseanna stórais peitreail;
- scardadh dramhuisce;
- dumpáil mara.

FEIDHMIÚ COMHSHAOIL NÁISIÚNTA

- Stiúradh os cionn 2,000 iniúchadh agus cigireacht de áiseanna a fuair ceadúnas ón nGníomhaireacht gach bliain
- Maoirsiú freagrachtaí cosanta comhshaoil údarás áitiúla thar sé earnáil - aer, fuaim, dramhaíl, dramhuisce agus caighdeán uisce
- Obair le húdaráis áitiúla agus leis na Gardaí chun stop a chur le gníomhaíocht mhídhleathach dramhaíola trí comhordú a dhéanamh ar líonra forfheidhmithe náisiúnta, díriú isteach ar chiontóirí, stiúradh fiosrúcháin agus maoirsiú leigheas na bhfadhbanna.
- An dlí a chur orthu siúd a bhriseann dlí comhshaoil agus a dhéanann dochar don chomhshaol mar thoradh ar a ngníomhaíochtaí.

MONATÓIREACHT, ANAILÍS AGUS TUAIRISCIÚ AR AN GCOMHSHAOL

- Monatóireacht ar chaighdeán aeir agus caighdeáin aibhneacha, locha, uiscí taoide agus uiscí talaimh; leibhéil agus sruth aibhneacha a thomhas.
- Tuairisciú neamhspleách chun cabhrú le rialtais náisiúnta agus áitiúla cinntí a dhéanamh.

RIALÚ ASTUITHE GÁIS CEAPTHA TEASA NA HÉIREANN

- Cainníochtú astuithe gáis ceaptha teasa na hÉireann i gcomhthéacs ár dtiomantas Kyoto.
- Cur i bhfeidhm na Treorach um Thrádáil Astuithe, a bhfuil baint aige le hos cionn 100 cuideachta atá ina mór-ghineadóirí dé-ocsaíd charbóin in Éirinn.

TAIGHDE AGUS FORBAIRT COMHSHAOIL

- Taighde ar shaincheisteanna comhshaoil a chomhordú (cosúil le caighdéan aeir agus uisce, athrú aeráide, bithéagsúlacht, teicneolaíochtaí comhshaoil).

MEASÚNÚ STRAITÉISEACH COMHSHAOIL

- Ag déanamh measúnú ar thionchar phleananna agus chláracha ar chomhshaol na hÉireann (cosúil le pleananna bainistíochta dramhaíola agus forbartha).

PLEANÁIL, OIDEACHAS AGUS TREOIR CHOMHSHAOIL

- Treoir a thabhairt don phobal agus do thionscal ar cheisteanna comhshaoil éagsúla (m.sh., iarratais ar cheadúnais, seachaint dramhaíola agus rialacháin chomhshaoil).
- Eolas níos fearr ar an gcomhshaol a scaipeadh (trí cláracha teilifíse comhshaoil agus pacáistí acmhainne do bhunscoileanna agus do mheánscoileanna).

BAINISTÍOCHT DRAMHAÍOLA FHORGHNÍOMHACH

- Cur chun cinn seachaint agus laghdú dramhaíola trí chomhordú An Chláir Náisiúnta um Chosc Dramhaíola, lena n-áirítear cur i bhfeidhm na dTionscnamh Freagrachta Táirgeoirí.
- Cur i bhfeidhm Rialachán ar nós na treoracha maidir le Trealamh Leictreach agus Leictreonach Caite agus le Srianadh Substaintí Guaiseacha agus substaintí a dhéanann ídiú ar an gcrios ózóin.
- Plean Náisiúnta Bainistíochta um Dramhaíl Ghuaiseach a fhorbairt chun dramhaíl ghuaiseach a sheachaint agus a bhainistiú.

STRUCHTÚR NA GNÍOMHAIREACHTA

Bunaíodh an Ghníomhaireacht i 1993 chun comhshaol na hÉireann a chosaint. Tá an eagraíocht á bhainistiú ag Bord lánaimseartha, ar a bhfuil Príomhstiúrthóir agus ceithre Stiúrthóir.

Tá obair na Gníomhaireachta ar siúl trí ceithre Oifig:

- An Oifig Aeráide, Ceadúnaithe agus Úsáide Acmhainní
- An Oifig um Fhorfheidhmiúchán Comhshaoil
- An Oifig um Measúnacht Comhshaoil
- An Oifig Cumarsáide agus Seirbhísí Corparáide

Tá Coiste Comhairleach ag an nGníomhaireacht le cabhrú léi. Tá dáréag ball air agus tagann siad le chéile cúpla uair in aghaidh na bliana le plé a dhéanamh ar cheisteanna ar ábhar imní iad agus le comhairle a thabhairt don Bhord.

Science, Technology, Research and Innovation for the Environment (STRIVE) 2007-2013

The Science, Technology, Research and Innovation for the Environment (STRIVE) programme covers the period 2007 to 2013.

The programme comprises three key measures: Sustainable Development, Cleaner Production and Environmental Technologies, and A Healthy Environment; together with two supporting measures: EPA Environmental Research Centre (ERC) and Capacity & Capability Building. The seven principal thematic areas for the programme are Climate Change; Waste, Resource Management and Chemicals; Water Quality and the Aquatic Environment; Air Quality, Atmospheric Deposition and Noise; Impacts on Biodiversity; Soils and Land-use; and Socio-economic Considerations. In addition, other emerging issues will be addressed as the need arises.

The funding for the programme (approximately €100 million) comes from the Environmental Research Sub-Programme of the National Development Plan (NDP), the Inter-Departmental Committee for the Strategy for Science, Technology and Innovation (IDC-SSTI); and EPA core funding and co-funding by economic sectors.

The EPA has a statutory role to co-ordinate environmental research in Ireland and is organising and administering the STRIVE programme on behalf of the Department of the Environment, Heritage and Local Government.

Environmental Protection Agency
An Ghníomhaireacht um Chaomhnú Comhshaoil

ENVIRONMENTAL PROTECTION AGENCY
PO Box 3000, Johnstown Castle Estate, Co. Wexford, Ireland
t 053 916 0600 f 053 916 0699
LoCall 1890 33 55 99
e info@epa.ie w http://www.epa.ie

SSTI
Strategy for Science, Technology and Innovation

Comhshaol, Pobal agus Rialtas Áitiúil
Environment, Community and Local Government